NAS8-21385
NASA CR-102238
N69-37369

FINAL REPORT

PHASE I

STUDY OF AN ELECTROSTATIC ZERO-GRAVITY WORK BENCH PROTOTYPE

SPACE DIVISION CHRYSLER CORPORATION

STUDY ON

AN ELECTROSTATIC ZERO-GRAVITY

WORK BENCH PROTOTYPE

Prepared by: G. E. Hagen
Program Manager

Approved by: D. N. Buell, Manager
Advance Engineering Branch

Chrysler Corporation Space Division
New Orleans, Louisiana

FINAL REPORT

STUDY ON AN ELECTROSTATIC ZERO-GRAVITY WORK BENCH PROTOTYPE

Contract No. NAS8-21385

April 23, 1969

Prepared for

NATIONAL AERONAUTICS AND SPACE ADMINISTRATION
Marshall Space Flight Center, Alabama 35812

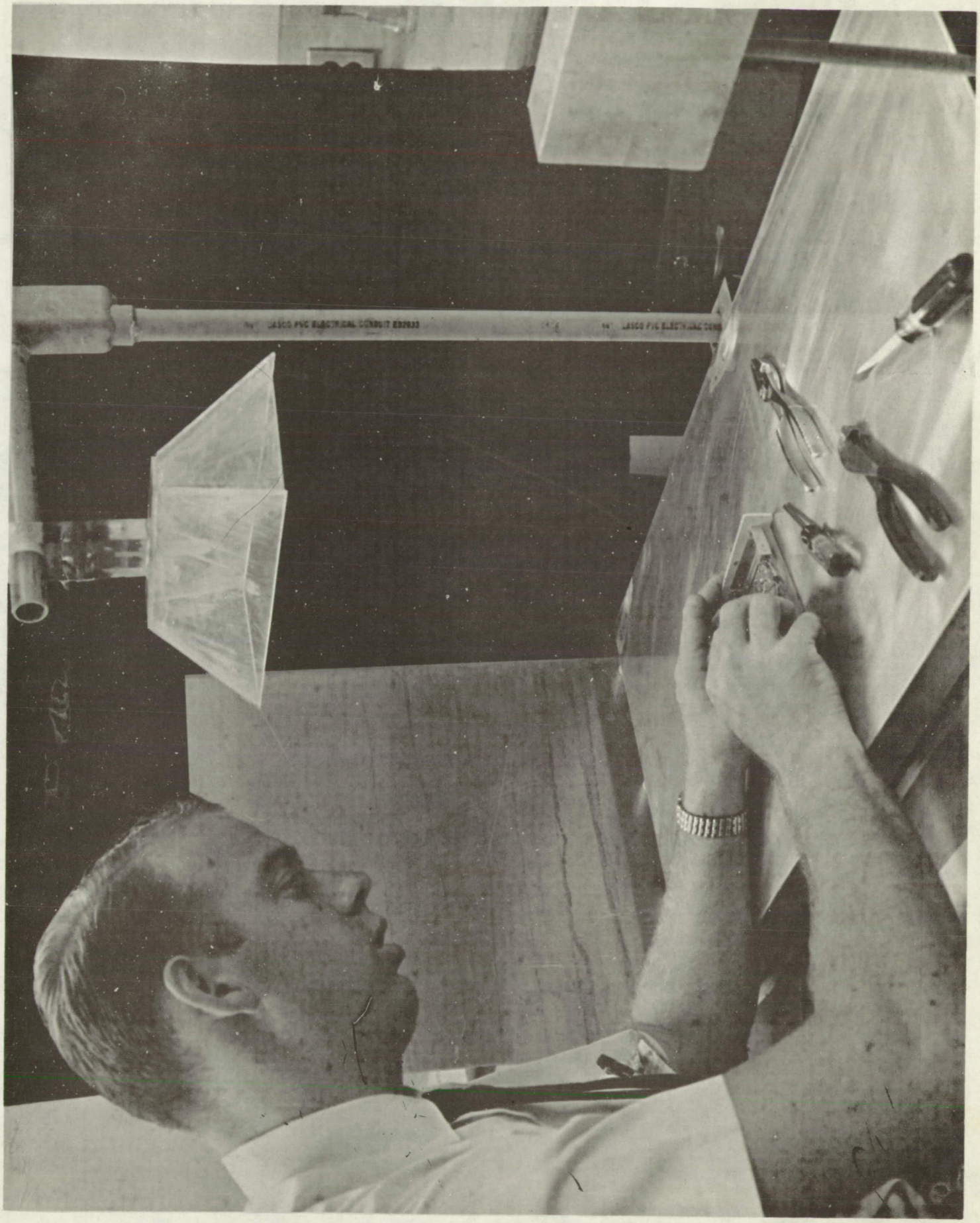

Frontispiece

TABLE OF CONTENTS

SUMMARY OF THIS REPORT 1

INTRODUCTION

The Problem 2
Solutions Available 2
The Electrostatic Worktable 3
Organization of this Report 3
Conclusions 4

EXPERIMENTAL RESULTS

Impedance Tests 5
Attractive Force Tests 8
Adhesion Tests 11

COMPARISON WITH COMPUTED RESULTS

Impedance of the System 17
Attractive Force 17

SAFETY

Electric Shock 20
Radio Interference 21
Ozone Production 21
Ultraviolet Light 24
X-Ray Production 24
Inflammability 25

CONCLUSIONS 26

APPENDIX I - POISSON'S EQUATION APPLIED TO AN ION BEAM

A General Solution of Poisson's Equation I-1
Solution for Ion Flow between Concentric Spheres I-3
Solution for Ion Flow between Parallel Planes I-5
Approximate Solution for the Table I-7

APPENDIX II - GRAPHS OF EXPERIMENTAL RESULTS

Impedance Tests with Wire Ion Source Figures 15-24
Impedance with Needle Point Source Figures 26-33
Attractive Force Tests Figures 34-51
Adhesion Tests Figures 52-68

ILLUSTRATIONS

The Electrostatic Worktable		Frontispiece
Figure		Page
1	Impedance Variation with Pressure	6
2	Force versus Height above Table	6
3	Adhesive Force versus Bias Voltage	6
4	Worktable Test Set-up	7
5	Needle Point Ion Source with Shield	9
6	Attractive Force Test Set-up	10
7	Paschen's Law	12
8	Distribution of Charges in Electroadhesion	12
9	Adhesion Test Set-up	14
10	Adhesion Test Set-up Diagram	15
11	Computed versus Experimental Impedance	18
12	Radio Interference Tests	22
13	Radio Interference Tests	23
14	Mathematical Model of the Table	I-6

SUMMARY OF THIS REPORT

A working prototype of the electrostatic worktable was constructed, consisting of an ion source, a power supply and a coated table. A number of types of ion sources were tested, and the best performance was obtained from a needle point surrounded by a perforated non-conducting box. Tests of the impedance of the ion beam were made at various cabin pressures; figure 1 shows the relationship found between impedance and pressure. The table was then turned on its side, and objects were suspended in front of it by threads to simulate weightlessness. Forces produced at various heights above the table were measured, a typical variation being shown in figure 2. Objects both conducting, non-conducting, grounded and ungrounded were suspended in contact with the table and the force necessary to pull them away was measured. Figure 3 shows the adhesive force obtained on a 1-inch metal disc as a function of bias voltage.

A series of tests pertaining to safety was made. Taking a worst case, consisting of a metal sheet as large as the table top, it was found impossible to receive an electric shock by handling it in the ion beam. It was also shown by computation that an object as large as a basketball could not store enough energy from the ion beam to cause a spark capable of causing ignition of flammable objects. A test for ozone showed that the accumulation after an hour was still below the danger point. A test for ultraviolet was negative, although it will be recommended that the ion source shield be opaque to ultraviolet. It was shown by computation that X-ray production is not possible with this apparatus. Finally, it was found that the worktable was space qualified from the standpoint of RFI interference.

During the course of the testing, two important advancements in the state-of-the-art were made. One was the use of a perforated box around the ion source, limiting the current of the ion beam and protecting the user from contact with the high voltage. The other was the use of porcelain as an electroadhesive coating for the table, this material being an improvement over all other known coatings in being both non-toxic and non-flammable.

From the results of these tests a set of design criteria was drawn up, specifying required current, voltages and the like. It was found that it is entirely feasible to design the final hardware such that it falls within the goals set forth in Contract NAS8-21385.

I. INTRODUCTION

A. THE PROBLEM

In zero-gravity construction or maintenance work the handling of tools and parts presents special problems, since they tend to float about the cabin and become lost. Many types of clamps, adhesives and the like have been successfully used, although all have their limitations. In all cases, the astronaut is forced to give a large part of his attention to securing each tool or part as he lays it down, and this detracts materially from his ability to concentrate on the job itself. This problem becomes more acute as the job becomes more intricate or as the need for speed increases. Needed was a means of freeing the astronaut from his preoccupation with zero-gravity mechanics and allowing him to devote his full attention to the task at hand.

B. SOLUTIONS AVAILABLE

A preferred solution to the above problem is a system in which some other force takes the place of gravity, and floating objects are attracted down to a table or work area and held there. Available forces to consider are: Centrifugal, aerodynamic, magnetic, electromagnetic and electrostatic.

1. Centrifugal

When observed from within a rotating system, a free object will be seen to drift outward away from the axis of rotation, like a marble placed on a phonograph record. A centrifugal force system consumes no power after the rotation has once been established. However, it would require that either the entire spacecraft or some large portion of it be rotated. If the entire ship were rotated, no zero-gravity experiments could be performed anywhere aboard, and experiments requiring a fixed telescope or antennae would be greatly complicated. If just a portion of the craft rotated, we would have the complexity of sliding contacts and seals between the two portions, and a wobble problem that would require delicate balancing.

2. Aerodynamic

If a fan is placed under a screen or perforated table and sucks air through the table, the air movement will tend to carry objects to the table and hold them there. This may be a practical solution and is currently under consideration. It has the unavoidable disadvantage of requiring a continuous and substantial power consumption, and may possibly be unduly vulnerable to eddy currents produced by any rapid movements of the astronaut's hands.

3. Magnetic

It is well known that a magnet will attract an object containing iron or other magnetically permeable material. However, the fact that only iron objects are attracted rules it out as a practical solution to the problem. It should also be noted that this attractive force falls off with the square of the distance from either pole; this makes it impractical to attempt to attract an object magnetically over any considerable distance such as the working area over a table.

4. Electromagnetic

An oscillating magnetic field such as a radio wave will induce electric currents to flow in any object of high electrical conductivity, and its reaction with these currents can produce usable force; this is the principle of the common alternating current motor. However, the fact that it reacts only with conductors is a serious disadvantage; it is also power-consuming and would interfere with radio reception and with many of the spacecraft's sensitive instruments.

5. Electrostatic

When two objects (called electrodes) have an opposite electric charge, the space between them is said to have an electric field; if the electrodes are properly shaped, this field can be made uniformly strong over a considerable area. Any electrically charged object placed in such a field will be attracted to one edge of the field; that is, toward one electrode. Furthermore, injecting ions (charged air molecules) into this area will cause any free objects to acquire an electric charge, regardless of their size, shape or material. Thus, the combination of an electric field and an ion beam can produce a force system which acts on all objects, is of useful magnitude, and which consumes only nominal power. It is the use of electrostatic forces in place of gravity that is the subject of this study.

C. THE ELECTROSTATIC WORKTABLE

A test prototype of the electrostatic worktable is shown in the frontispiece. It is a place where an astronaut can seat himself and perform tasks which involve a number of tools and parts. Everything he lays on the table stays put. Anything he lets go of drops to the table and stays there. The system leaves him free to concentrate on the task at hand, and momentarily forget about zero-gravity techniques. Yet only the area on and directly above the table is affected; in other parts of the spacecraft, zero-gravity conditions remain as the desired environment for other experiments.

D. ORGANIZATION OF THIS REPORT

The scope of work spelled out in Contract NAS8-21385 does not outline the tests to be made in the pre-design investigation, but merely lists a set of design goals which would apply to the completed design of the flight hardware. The

purpose of this research was to make the necessary experimental tests and analysis to determine the feasibility of designing a safe and useful piece of hardware which would fall within these specifications. The report is organized to display the results of these tests in their logical order. Appendix I contains a mathematical discussion of the principle of the electrostatic worktable, and Appendix II contains graphs of the actual experimental runs.

E. CONCLUSIONS

Our conclusions constitute a set of design criteria upon which a satisfactory design may be based. They are discussed in section VII.

II. EXPERIMENTAL RESULTS

A. IMPEDANCE TESTS

The strength of the electric field around a charged fine point decreases with the square of the radial distance from the point; this means that the field very close to a sharp needle point will be strong enough to exceed the dielectric strength of the air, and the point will break into corona discharge. The same will happen close to a fine wire, where the field is inversely proportional to the first power of the radius. Once corona starts, a flood of ions (charged air molecules) move away from the point or wire and drift toward grounded objects. In the case of the electrostatic worktable, the ion source (point, points or wire) must not only supply the ions for the ion beam, but also create the electric field which causes charged objects to be attracted to the table.

Another requirement of the ion source is that it forms a shaped beam of ions which will be concentrated on the table top rather than flow in all directions. This is possible by having a non-conducting shield surrounding the ion source; this shield will charge up and have a focusing effect on the ion beam. The theory behind this ability to focus the beam on the table is developed in the theoretical section, Appendix I.

1. Test Prototype

A prototype of the worktable was built as sketched in figure 4. First tests were done with a coating of alkyd resin on the table top, this being the best known electroadhesive material at that time. A mockup of a camera and a backdrop were included in order to accurately simulate the geometry of grounded objects later to be used on the flight version.

A strip alongside the table was brought out to a separate connection in order to determine the effectiveness of the beam focusing; current drawn by the strip indicates that the beam is wider than the table top. At the point where the strip just stops passing current, we can assume the beam is 18 inches wide and of a length determined by the shape of the focusing shield. The entire model was placed in an environmental chamber capable of producing spacecraft cabin pressures of 7.5 psia and 5 psia. It was not necessary to use an oxygen-rich atmosphere, since ionization potentials and ion drift velocities of oxygen and nitrogen are almost identical.

2. Fine Wire Ion Source

A fine wire was first tried. Graphs of actual data taken appear in Appendix II, figures 15 through 25. Various voltages were placed on the ion source. It was found that the current was excessive even at low voltages, which would lead to high power consumption. It was also found that the beam width was much wider

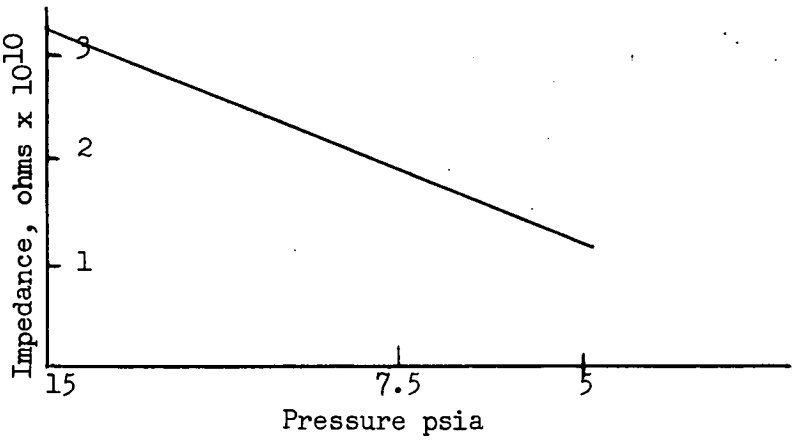

Figure 1.

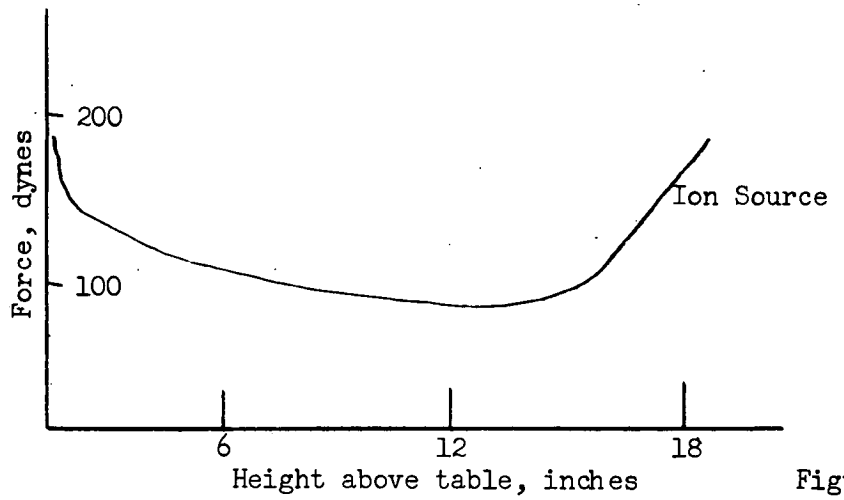

Figure 2.

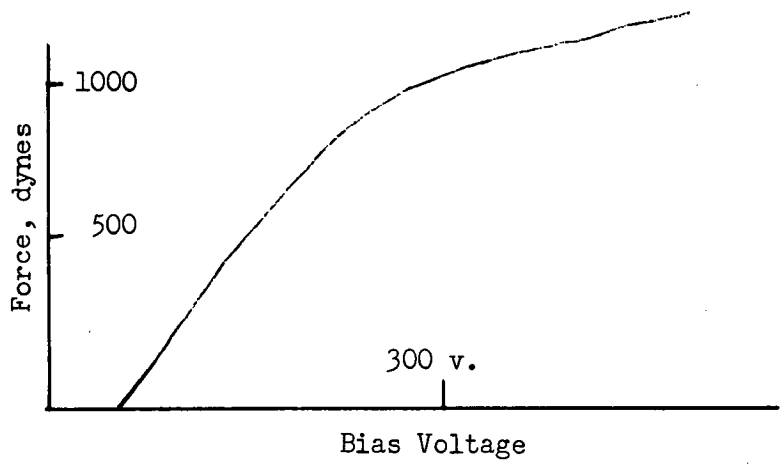

Figure 3.

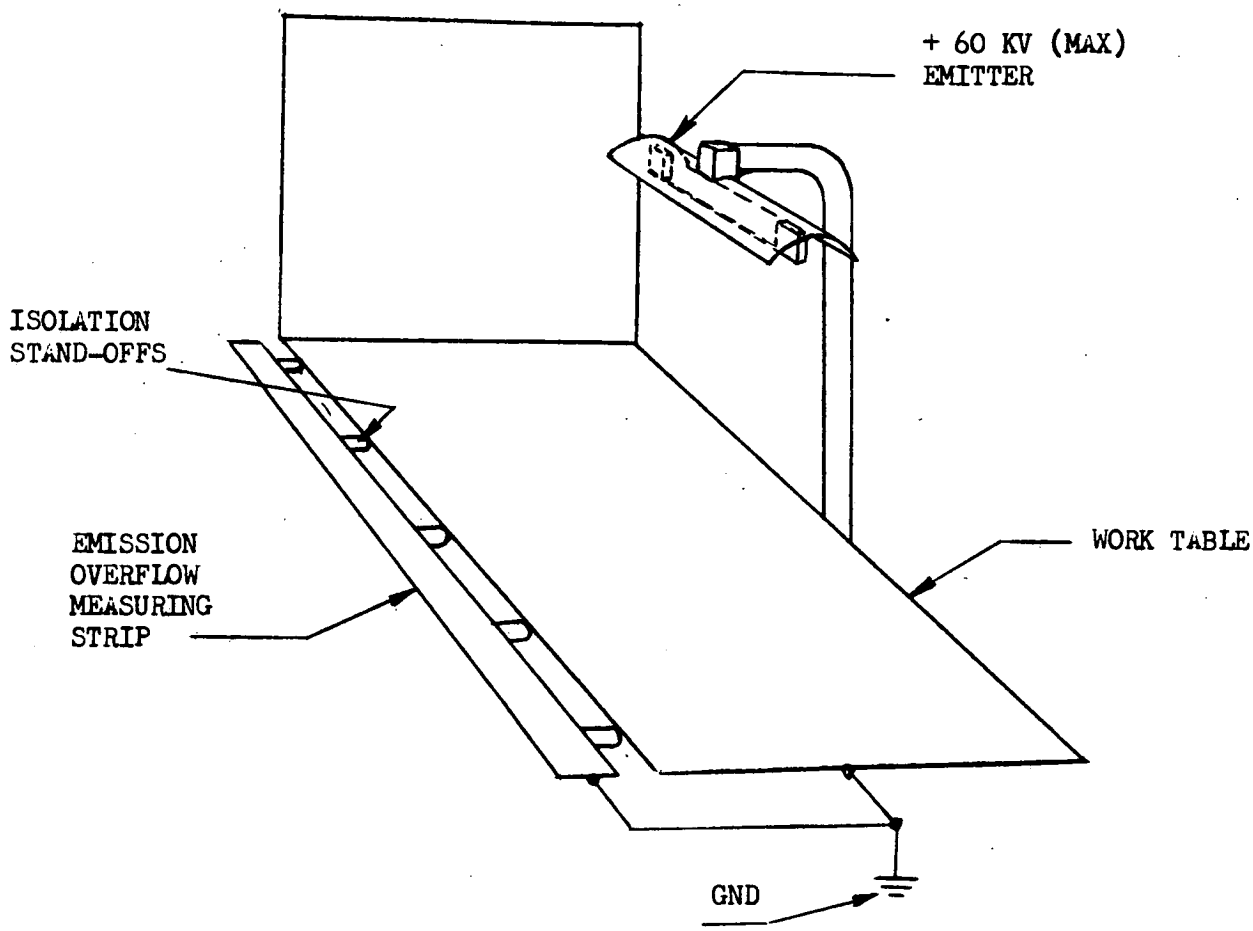

ELECTROSTATIC WORK TABLE
WORK TABLE TEST SET-UP

FIGURE 4

than the table top. The focusing shield was made progressively narrow to improve focusing, although current drawn by the strip could not be eliminated. It was concluded that wire source produced too high an ion current for this application.

3. Needle Point Source

We then went to a needle-point source, as sketched in figure 5. This dropped the current drastically at atmospheric pressure, but the current was still high at spacecraft cabin pressure. A number of designs of ion shields were tried. Making a deeper, narrower shield gave better focusing and lower current, as shown in graphs 26 through 33, Appendix II.

4. Other Source Configurations

Multiple points and hot wire sources were tried briefly, but extensive data runs were not made, since both of these configurations produced excessive current, even at atmospheric pressure. It was at this point concluded that a needle point source in a deep plastic box was the best solution, and we would proceed on to test attractive forces.

B. ATTRACTIVE FORCE TESTS

1. Experimental Set-Up

The prototype test table was now set up in the low-pressure chamber as shown in figure 6. A 3.85 gram ping-pong ball was selected as a standard object with which to compare the force produced by various voltages and geometric arrangements. With the table on its side, the ball was suspended from the ceiling of the chamber by two nylon threads which permitted it to swing toward or away from the table. A telescope was placed outside the window of the chamber such that the two threads could be lined up with a scale to show the exact displacement of the ball. The force on the ball at any time could then be computed from the observed angle at which it was hanging.

2. Force Tests, Alkyd Resin Table Top, Open Point Ion Source

A series of test runs was made first with the ball 12 inches from the table moving finally to 3 inches from the table (figures 34 through 46, Appendix II). Force was poor at 5 psia, and current was relatively high. We also had difficulty with the ball oscillating. It was later determined that the oscillation was due to air currents stirred up by the heavy ion current — a phenomenon known as "corona wind".

There followed a series of some 50 test runs which are not described here because they did not add any useful knowledge except to point out the need of drastically reducing the current flow while maintaining a high electric field.

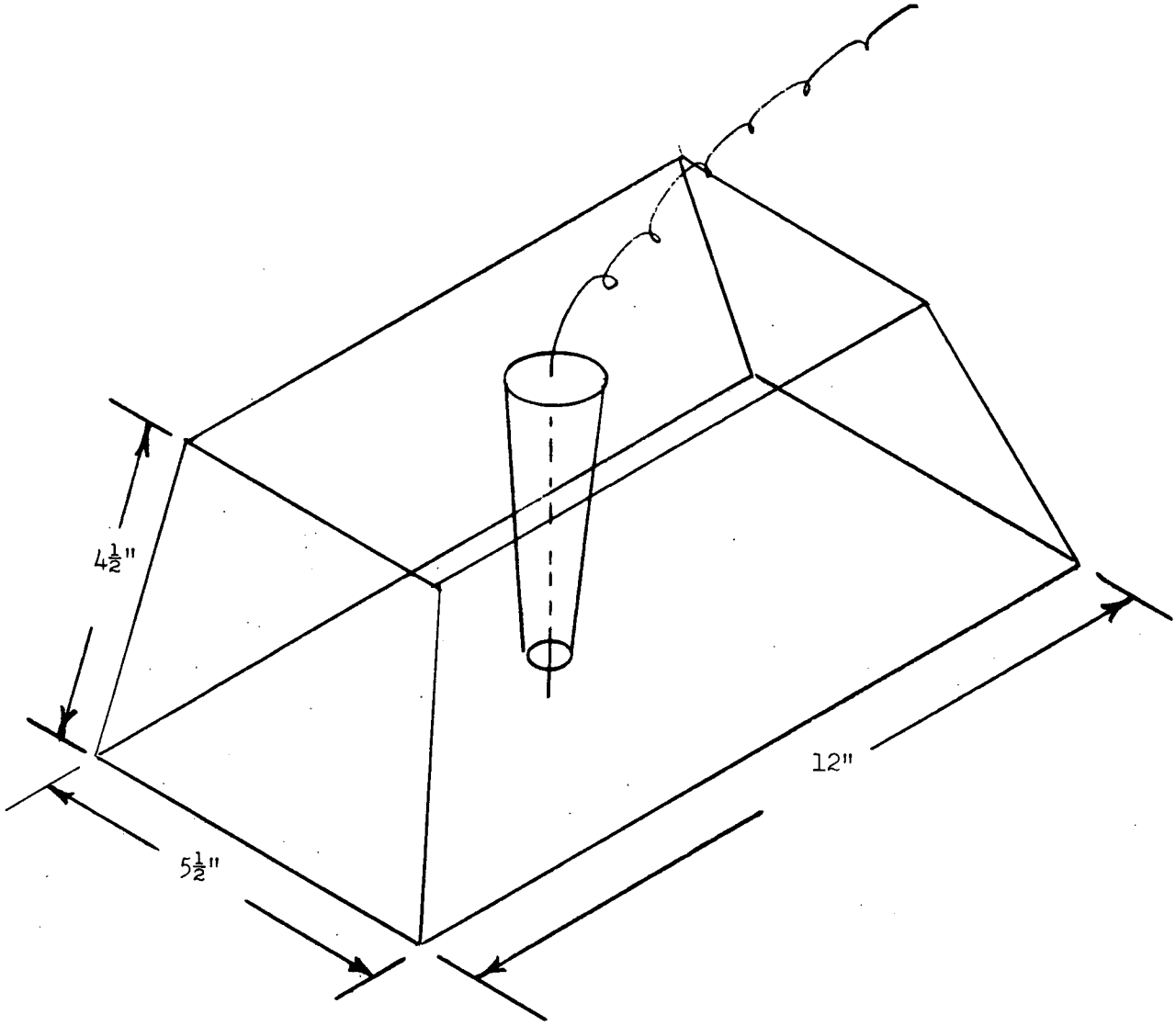

Figure 5. Single Point Ion Source with Shield.

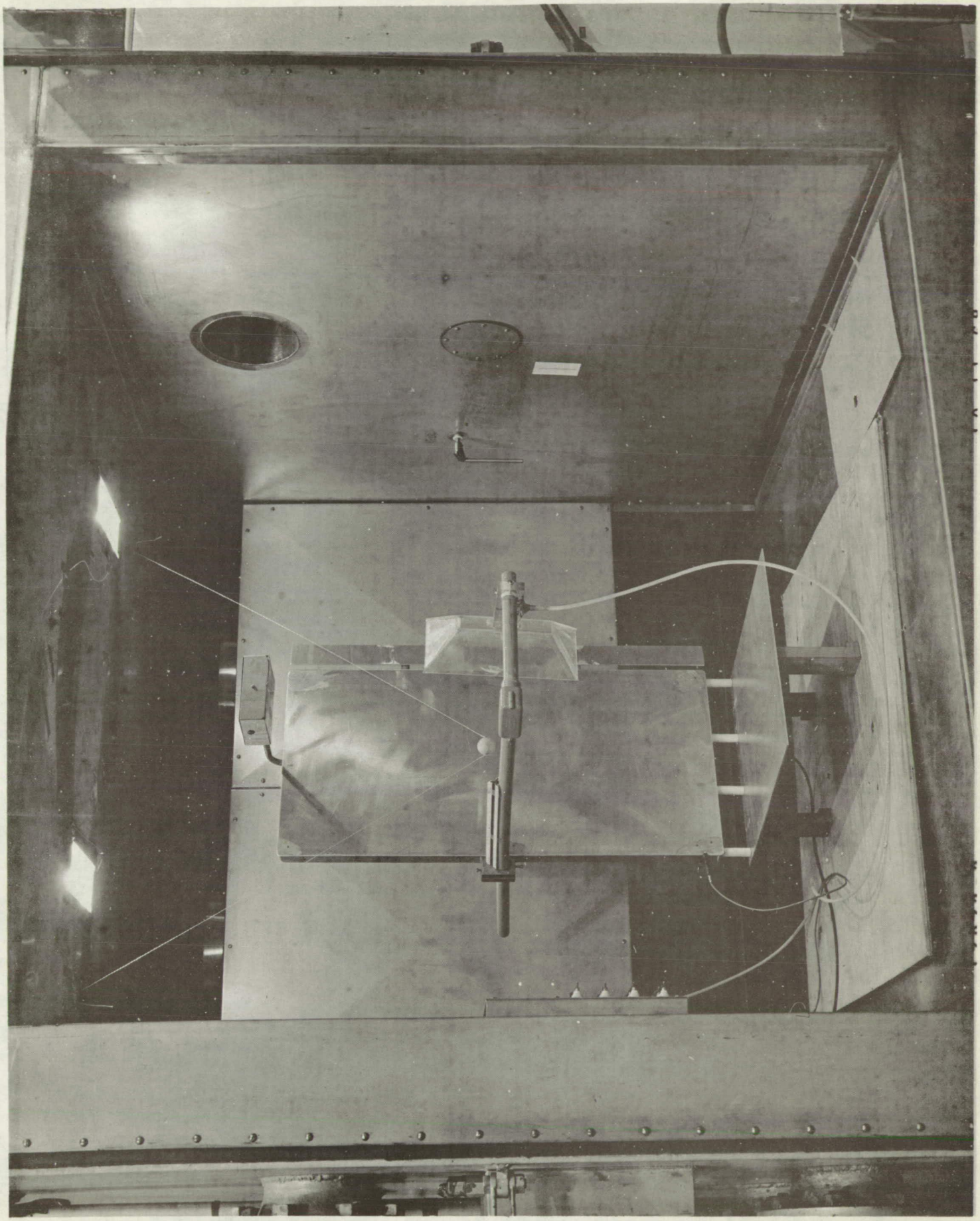

Figure 6

3. Force Tests, Covered Point Source

At this point it was discovered that a perforated cover could be placed over the point source, cutting the current to less than .002 microamperes but maintaining a strong electric field. A number of types of covers were tried. Figure 47, Appendix II, shows results with a bakelite cover, figure 48 with fiberglass strips and, finally, figure 49 shows the results with a perforated fiberglass cover. This was by far the best result to date, producing forces exceeding 0.1 grams at 5 psia and as high as 0.18 grams at 7.5 psia. This was one of the most important discoveries made during the course of the research, since it reduced the required power to a fraction of a watt and at the same time placed a protective cover over the point source to prevent accidental contact with the high voltage.

C. ADHESION TESTS

1. Background

The attractive force between two adjacent charged objects is proportional to the square of the strength of the electric field between them. Furthermore, with a given applied voltage, this field strength is inversely proportional to the distance between the objects. All this means that as two objects of opposite polarity are brought close to one another, the force between them increases very rapidly. Unforturnately, at ordinary distances, the electric field cannot be allowed to rise above about 30,000 volts per centimeter at atmospheric pressure (or even proportionately less at lower pressures) because the air breaks down and sparking occurs.

A phenomenon was discovered in 1966 in the Chrysler Space Division Laboratories which led to the invention of the "electroadhesor". The law which governs the voltage at which a spark will occur is known as Paschen's Law, and is shown graphically in figure 7. This shows that the breakdown voltage is a function of the product of the spacing between the objects and the ambient pressure. At ordinary distances and pressures, the breakdown voltage is directly proportional to this product; thus, if pressure is constant, the limiting voltage goes down directly as two objects of opposit polarity are allowed to come close. However, as can be seen from figure 7, the curve reaches a lower limit at about 300 volts and starts back up again sharply as the product is further reduced. At atmospheric pressure the minimum corresponds to a space of .01 centimeters (or .03 cm at 5 psia spacecraft cabin pressure) and if the spacing is made smaller than this, the allowable voltage again becomes great. Since the electric field strength is not only proportional to the voltage, but also inversely proportional to the spacing, the field strength increases even more rapidly, and the attractive force still more rapidly, being proportional to the square of the field strength. This means that forces comparable to those produced by magnetic means can be developed.

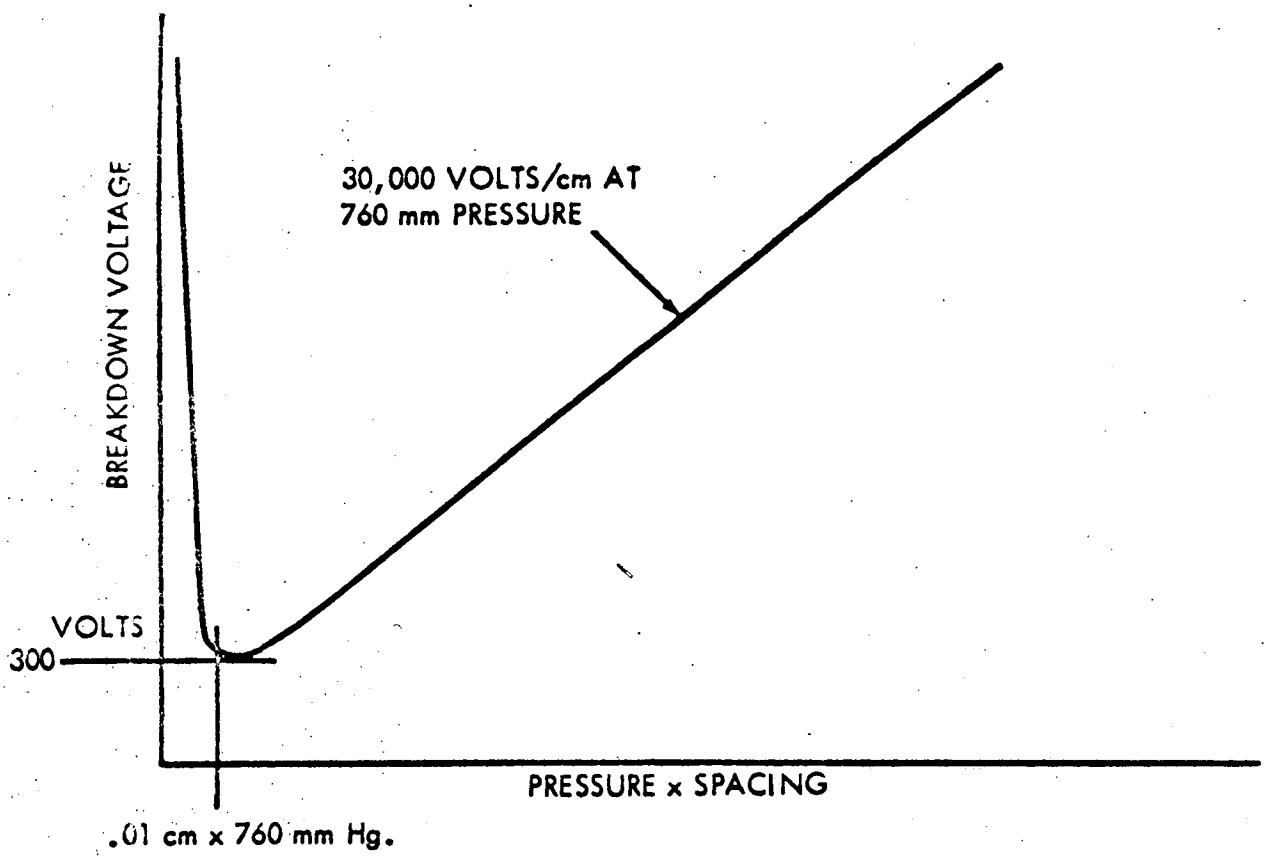

Figure 7. Paschen's Law

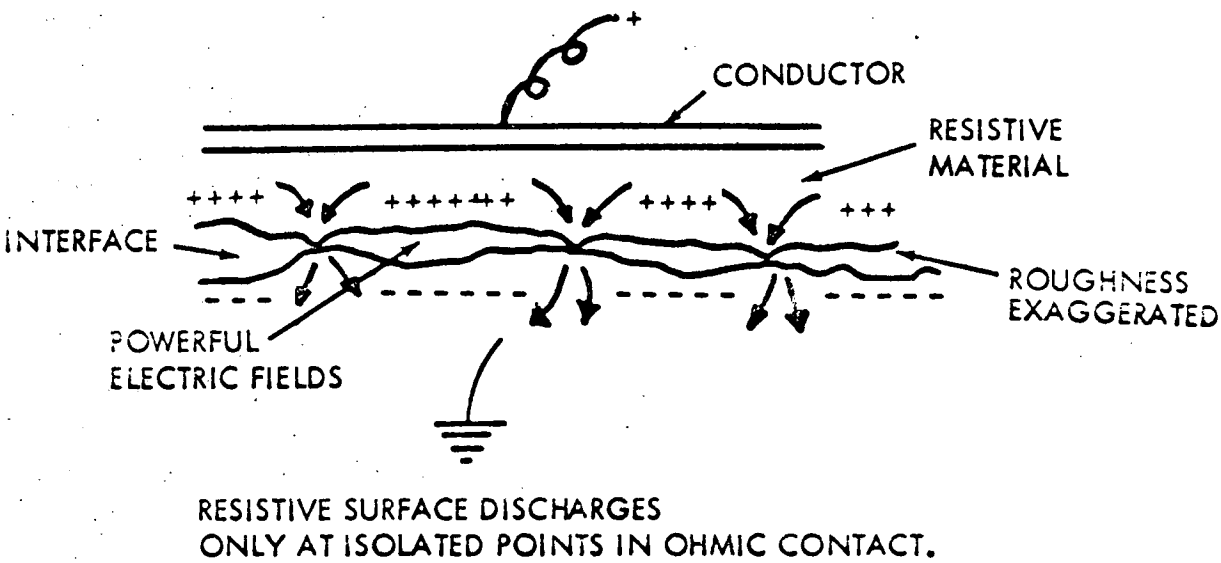

Figure 8. Distribution of Electric Charges

The principal requirement to produce this phenomenon is that one of the objects (in our case, the table top) must be coated with a substance of the proper resistivity — conductive enough to carry charges to the surface of the coating yet resistive enough to prevent points of ohmic contact from draining these charges (see figure 8). With this coating in place, any object reaching the table top is firmly held, the electroadhesive forces being much stronger than the attractive forces seen above the table.

There is a further complication that when the astronaut touches a metal object he drains the charges from it and there is no electroadhesion; this makes it difficult to lay something down without having it bounce. To overcome this, a second power supply is included which biases the metal back of the table about 300 volts below ground (hull) potential. This maintains the electroadhesion even when the object is grounded. The table coating has an amply high resistance to prevent the operator from getting a shock from the bias voltage, and the device is so constructed that he cannot reach the charged bottom side of the table.

2. Experimental Results

a. Ungrounded Object, Alkyd Resin Coating

The experimental set-up was now arranged as shown in figure 9 and sketched in figure 10. The standard ping-pong ball was placed against the table, high voltage turned on, then the attached weight backed off by remotely controlling the reversible motor unit until the ball broke away. A scale at upper left read motor travel before breakaway, and from the adhesive force was computed. Results with the ball in the center of the table are shown in figure 52 and at the edge in figure 53, Appendix II.

b. Grounded Object, Alkyd Resin Coating

We now replaced the ball with a flat disc 1 inch in diameter hung by a grounded metal chain. In these tests the high voltage was not used, but a bias voltage was applied between ground and the metal backing of the table. The very high forces shown in figure 54, Appendix II, were received.

c. Ungrounded Metal Object

The metal disc was then suspended by a thread and the high voltage was used, again showing high adhesive forces (figures 55-57, Appendix II).

d. Ungrounded Metal Object with Other Coatings

A number of other table coatings were now tried in a search for some material that was non-flammable and would not outgas toxic vapors. Among these were Enamel (figure 58), Teflon (figure 59), Waterglass (figure 62), and finally,

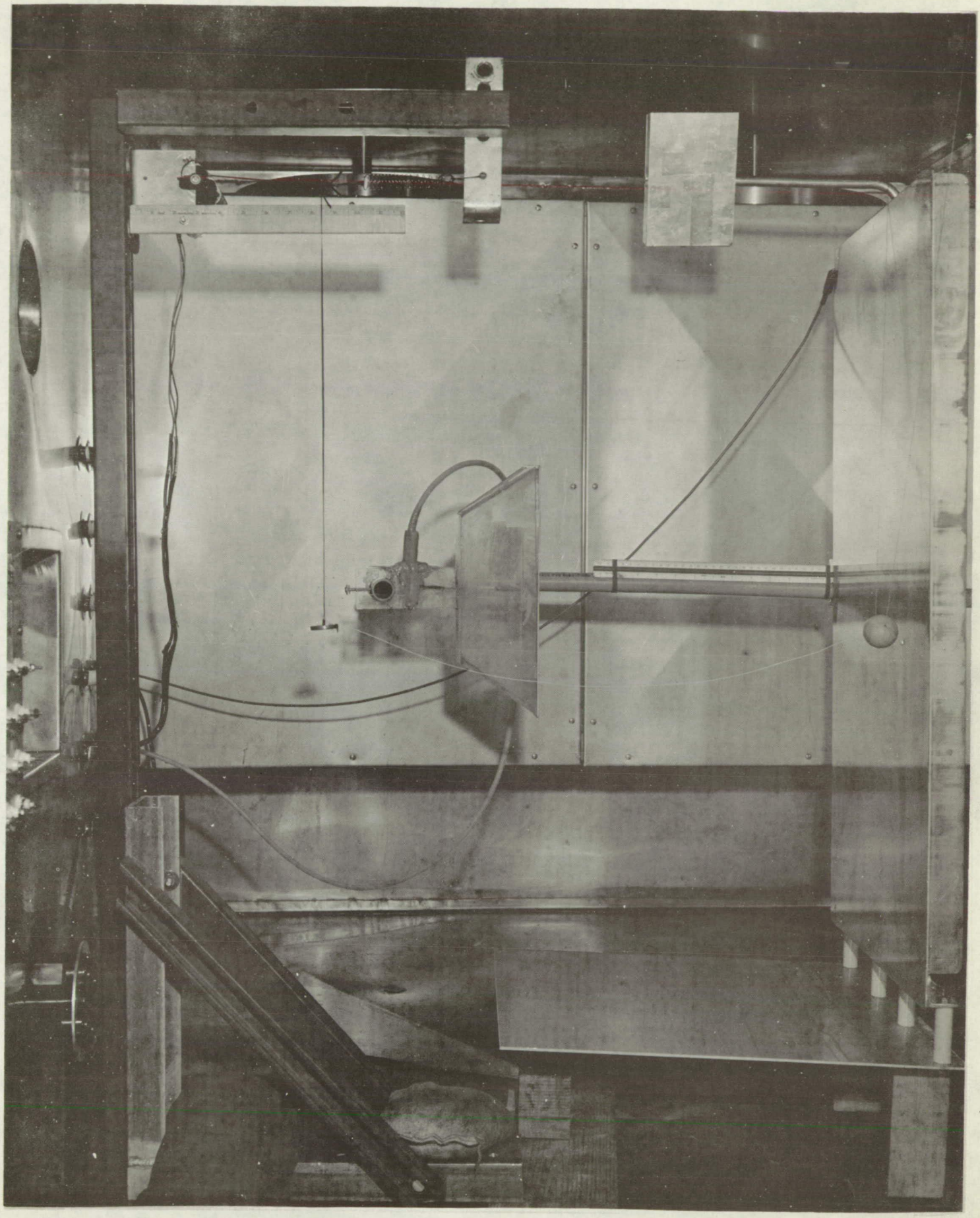

Figure 9

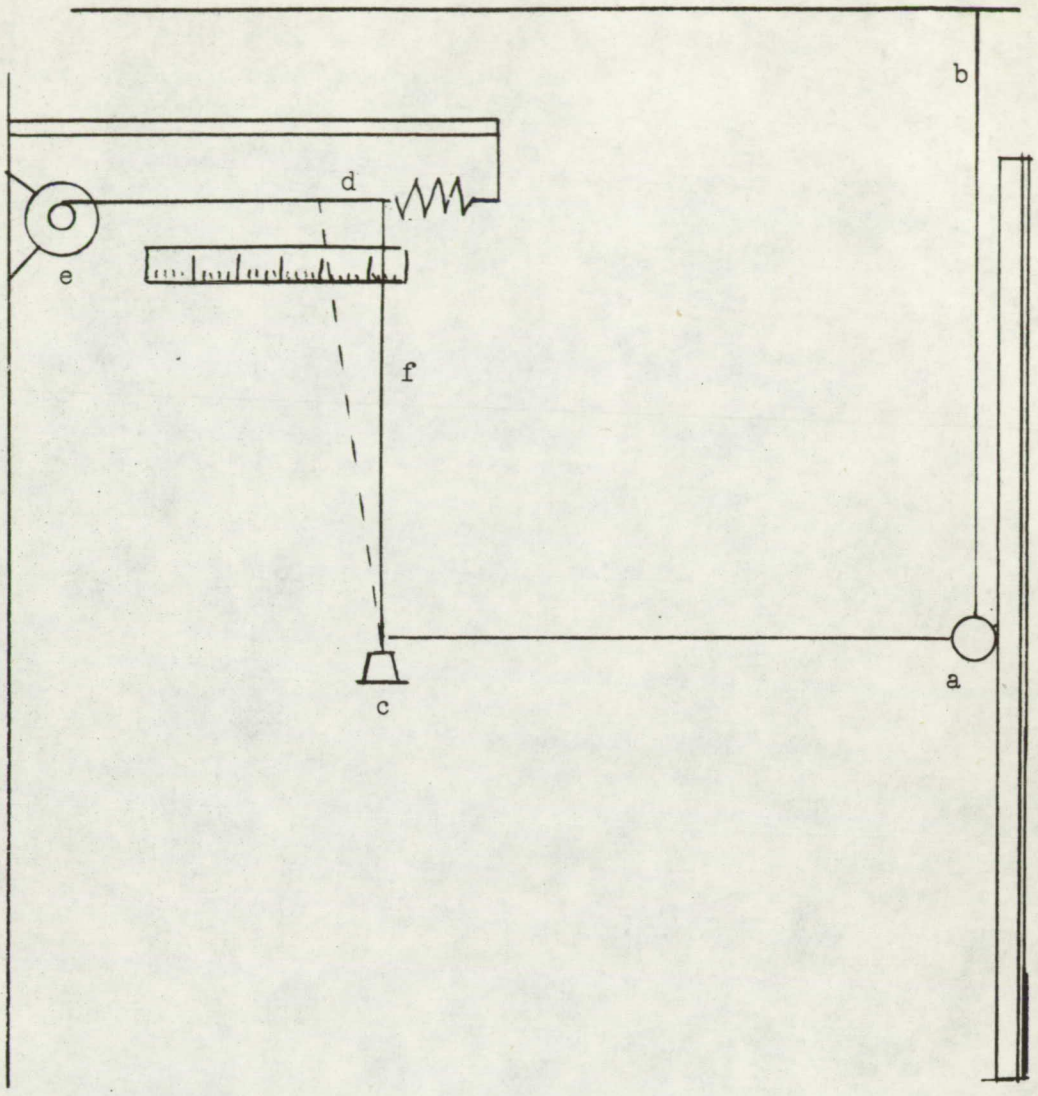

Adhesion Test Set-Up

Standard ball (a) is suspended vertically against table by string (b). Standard weight (c) is suspended by string (f) from movable, spring-loaded cord (d), which is operated by remote controlled motor (e). The angle of the string (f) at the moment the ball pulls away from the table is used to compute the pull-away force.

Figure 10.

fired-on Procelain (figure 63). Not only did the porcelain give the best results of any, but it is ideal from other standpoints, being non-toxic, non-flammable, readily cleanable, not effected by humidity and has good wear resistance.

III. COMPARISON WITH COMPUTED RESULTS

A. IMPEDANCE OF THE SYSTEM

In equation (31), Appendix I, if we set V = 0 at the table top, we can derive an expression for the measured current:

$$I_m = \frac{KMA}{32} \quad \frac{Vp^2}{(\sqrt{3}R^{3/2} + r^{3/2})}$$

M for oxygen at 7.5 psia will be 3.2 cm/sec per volt/cm, and our recommended voltage for this pressure is 30 kilovolts. The table area is 18" x 36" and a recommended height for the emitter is 18 inches. Arbitrarily choosing R = 25.4 cm, r = 45.7 cm at the table surface. The resulting I_m, in microamperes, is plotted in figure 11. To compare with this is plotted the current measured on a test run made October 9 with a choked-down ion shield but without the perforated plate that was later installed, if we assume that the effect of the ion shield is to reduce the applied voltage by 10 kilovolts, the curves are in exact agreement.

Later, when a perforated plate was added to cover the bottom of the shield, the current dropped to less than .01 microamperes. Our ability to measure such tiny currents in the face of leakages which might be in the same order of magnitude is doubtful.

B. ATTRACTIVE FORCE

Using the experimental values from the run of October 10, that is, using the measured currents and assuming that 10 kilovolts is lost because of the ion shield, the following values of E and V for a point 5 inches above the table are calculated using equations 31, 33 and 34, Appendix I, and the force on the ball compared with that measured:

V (Statvolts)	E (Statvolts/cm)	f (dynes) Computed	Measured
.56	6.58	28.5	6.9
1.27	5.66	148.	20.8
1.85	17.1	293.	41.6
2.16	29.7	427.	69.3
2.74	35.6	683.	110.9

This would indicate that on this test the ball was only getting charged a fraction of the maximum theoretical figure. Much higher forces were obtained after the perforated shield was installed, although our inability to get accurate current measurements prevents the above type of comparison from being made on the later data runs. Failure of the ball to receive full charge in the above

NO. 340-20 DIETZGEN GRAPH PAPER
20 X 20 PER INCH

EUGENE DIETZGEN CO.
MADE IN U. S. A.

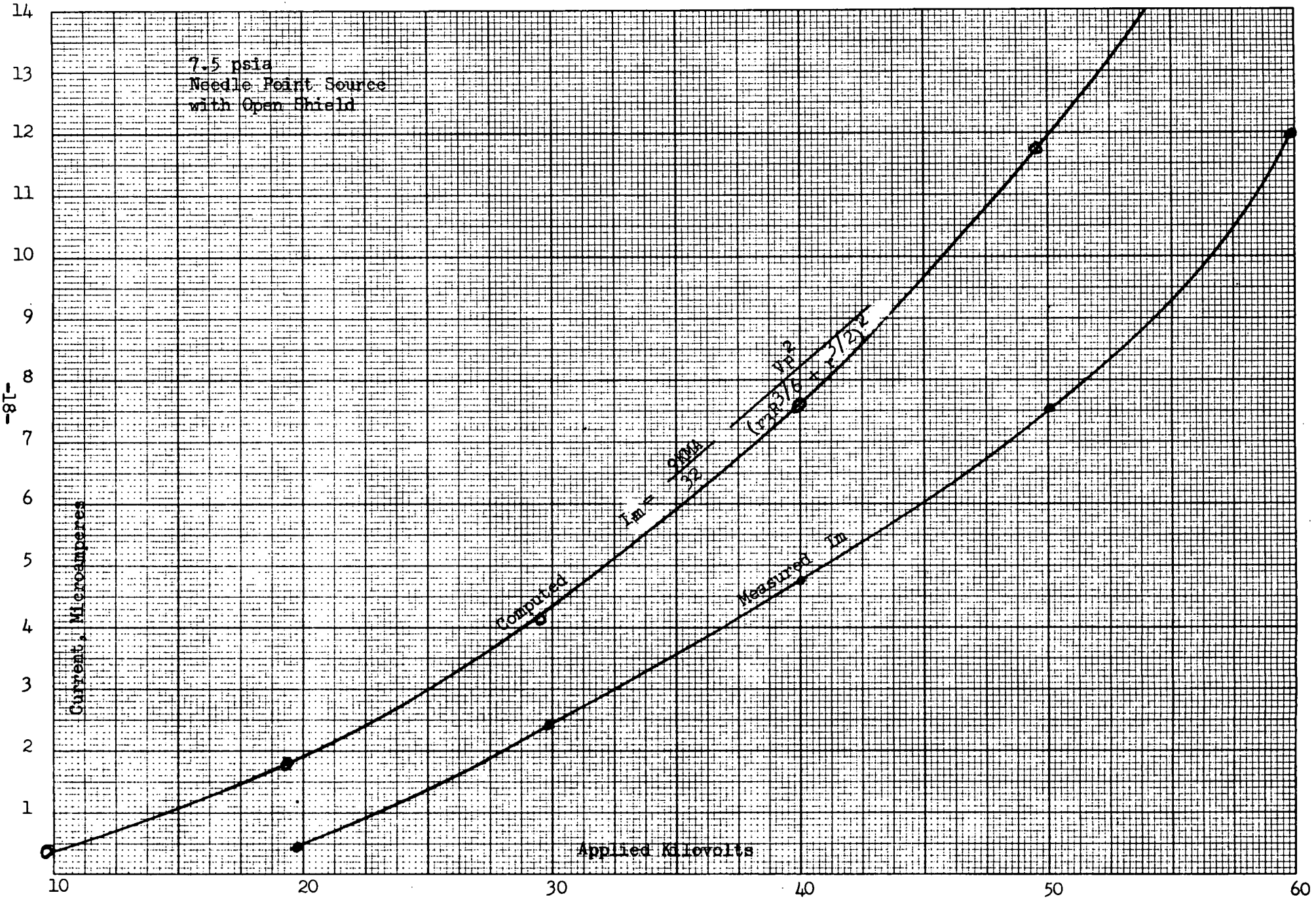

Figure 11

tests is attributed to secondary ionization at the table top; when high ion currents are run the ion drift velocities near the surface of the table are high enough to create new ion pairs, from which the negative members move upward and partially neutralize the positive charge on the ball.

IV. SAFETY

A. ELECTRIC SHOCK

1. Mathematical Analysis

Normally one associates electric shock with high voltages, and the higher the voltage the greater possibility of shock. In the case of the electrostatic workbench, however, although the voltages used are far in excess of those necessary to produce shock, it is not possible to actually contact the high voltage terminal because of the plastic box which surrounds it. The only possibility of shock would be through touching an ungrounded metal object which had been charged up to a high potential by the ion beams. Assuming the voltage was ample to overcome the body's resistance, the question of whether or not a detectable shock is received upon touching such an object will depend on how much energy is stored on the object. This, in turn, will depend on the capacitance of the object with respect to its surroundings. The stored energy in joules will be

$$E = \frac{1}{2} CV^2$$

where C is capacitance in farads and V is the potential in volts.

As an example, let us take a spherical object 20 centimeters in diameter, since this is probably as large as anything that will be handled. If the object is momentarily suspended half way up to the ion source and 30 kilovolts is applied, we might expect the object to be at a potential of 15 kilovolts. The capacitance of the sphere will be 10 cm in the electrostatic system or about 10^{-11} farads. At 15 kv this means it will store .00011 joules.

We have been unable to locate any reference which describes the threshold energy at which a shock can be felt. From the writer's experience, an electric current must be at least several milliamperes before it can be felt. If the resistance of the human skin is about one megohm, the time constant of the system would be in the region of about 10 microseconds. If the .00011 joules discharged over 10 microsecond interval, the current would be only 0.7 milliamperes. As a very rough estimate, then, we should not expect to receive any detectable shock.

2. Experimental Results

As an experimental check on the above, the prototype worktable was set up on its side and various sized metal objects were suspended by insulating threads about half way between the ion source and the table. Power was turned on and the objects were given time to charge. Then with one hand grounded, the experimenter touched the object and noted whether he could feel any shock. Cautious at first, a metal disc 1-1/8 inches in diameter was tried, slowly increasing the voltage

up to 60 kilovolts. Finding no detectable shock, larger and larger objects were tried. Finally, a circular metal sheet 17-1/2 inches in diameter was tried. This represents a worst possible case, since an object this size practically blocks off the ion beam and therefore tends to charge up to the full voltage of the ion source. No shock could be felt in any case. It was concluded that it is not possible for the operator to receive a perceptible shock through handling metal objects over the worktable.

3. Power Supply Safety

Although the plastic box surrounding the ion source is designed to prevent the astronaut from contacting the high voltage, there is the possibility that the box might be accidentally broken, or that some part of the insulation would break down. It should first be noted that there is no possibility of serious injury, since the power supply will be an oscillator type DC to DC converter which will not be capable of sustaining a current of more than a few tenths of a milliampere. A shock will be received, of course, if the astronaut does manage to contact the high voltage, because of the discharge of the energy stored in the filter condensers of the supply. As a final safety measure, therefore, a resistor of 300 megohms is placed in the high voltage line as close to the supply itself as possible. With this resistor in the line, at 30 kilovolts the maximum current, even on a dead short, could not exceed 0.1 milliamperes. To add further redundancy, an active current limiting device will be included in the power so that even without the protective resistor it could not deliver more than its normal current in event of a short circuit. It was one of the most useful results of the research done on this contract to discover that only a few microamperes of current is necessary to produce usable forces; it is this low current that makes it possible to insert the 300 megohm resistor mentioned above without serious loss of operating voltage.

B. RADIO INTERFERENCE

A standard RFI test was run in which the entire prototype worktable, including power supply was taken into a screened room. The page following is the report from the laboratory on this test. The worktable satisfied the requirements of MIL-I-6181D when operated at 30 kilovolts, which is as high a voltage as will be recommended for flight hardware. Failure to qualify at 60 kv was probably due to leaky insulators, rather than to anything inherent to the principle of the device. Photographs (figures 12 and 13) show the equipment used in the RFI tests.

C. OZONE PRODUCTION

In testing for ozone production, the table was placed in a chamber of approximately 125 cubic feet. Since this is much smaller than the S-IVB workshop, any accumulation of ozone is more quickly detected. The instrument used was a Mast Development Company direct reading ozone concentration meter model 724-2. The testing device ran continuously for ten minutes at intervals of 10 kilovolts.

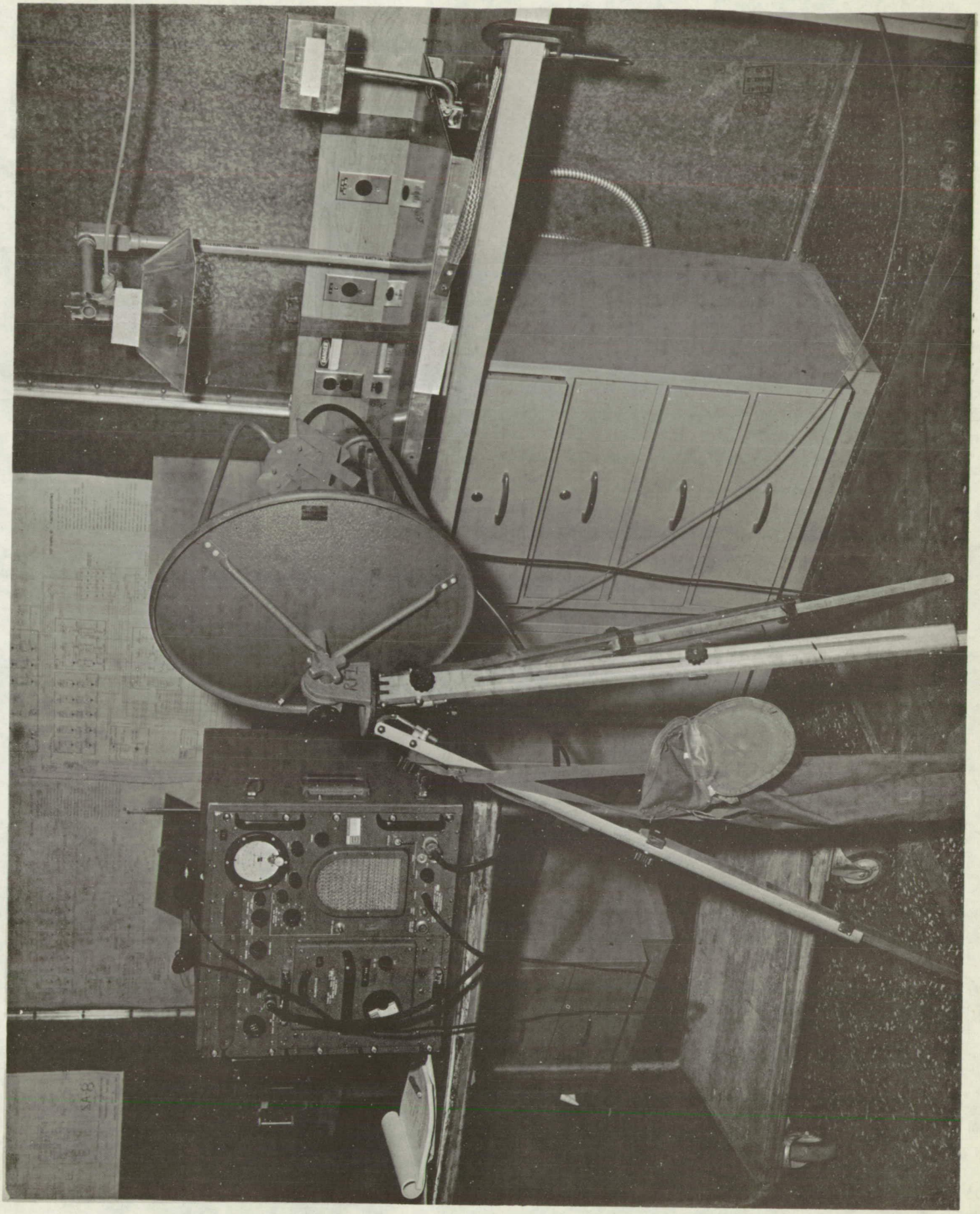

Figure 12

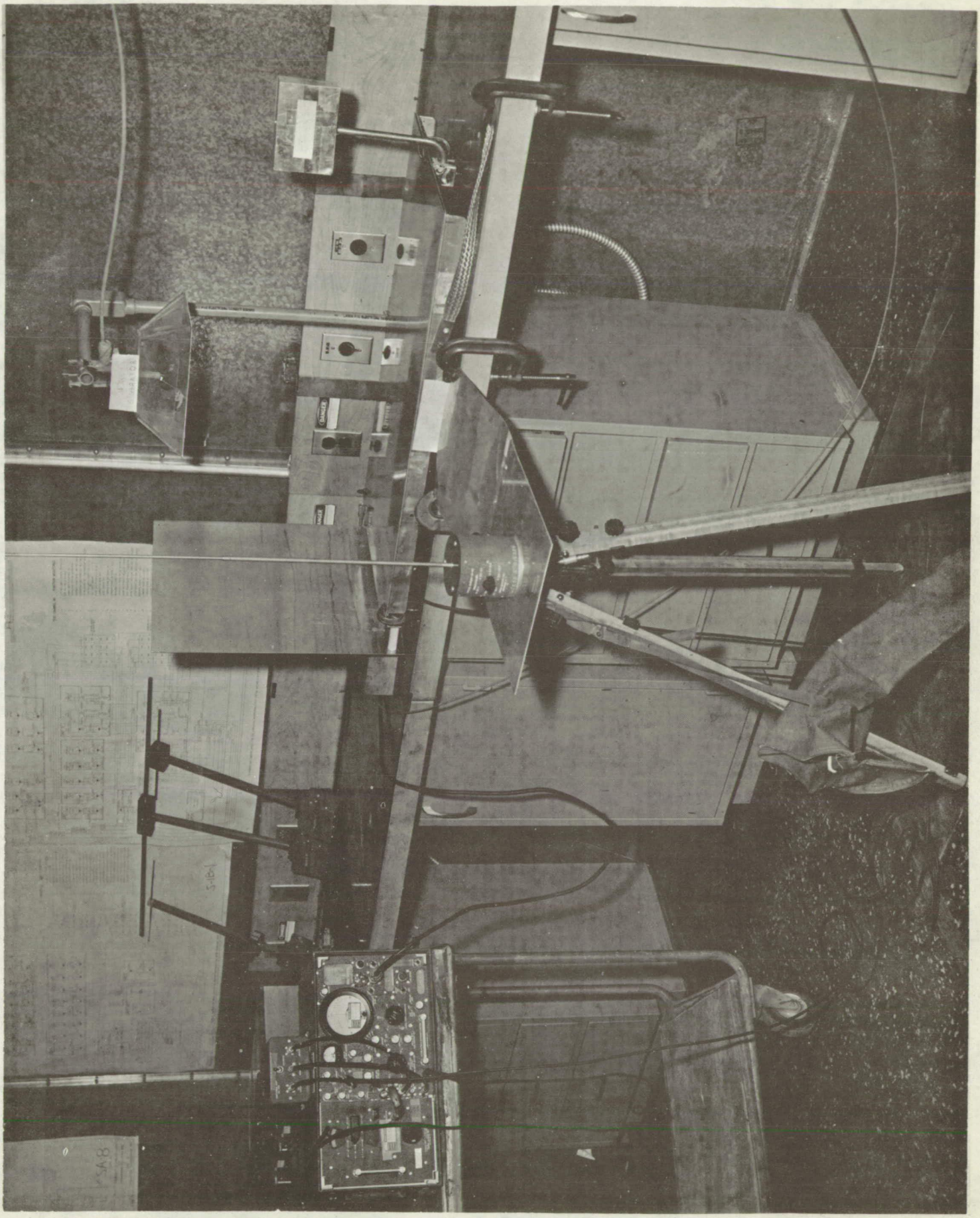

Figure 13

After the 50 kilovolt run, the table had been in operation within the chamber for a one-hour period. No ozone was detected. The sensitivity of the equipment was such that we know the ozone concentration to be less than five parts per hundred million.

Aerojet General Corporation of Asuza, California, recently completed a study entitled "Comparative Studies of 90-Day Continuous Exposure to O_3, NO_2 and CCl_4 at Reduced and Ambient Pressures". They concluded that a concentration of one part per hundred million of ozone was perfectly safe, since concentrations larger than that had produced no detectable symptoms. The volume of the S-IVB LH_2 tank is over 10,000 cubic feet, as compared to the 125 cubic feet of the test chamber. If, as we have shown, an hour's operation of the worktable did not accumulate a concentration of over 5 pphm in the test chamber, it would not reach a concentration of .06 pphm in the S-IVB. Thus, we are safe by a factor of 16, not including the fact that their study is based on continuous exposure.

It was necessary to make the ozone test at atmospheric pressure, since the ozone measuring device would not operate in a vacuum. However, the generation of ozone is a function of the kinetic energy which the ions can pick up in any one free path. If this energy is insufficient to decompose the oxygen molecule, then no ozone will be formed. The energy is proportional to the strength of the electric field (and therefore to the applied voltage), and inversely proportional to absolute pressure. We may, therefore, expect the same ozone production at 20 kv, 5 psia, and at 30 kv, 7.5 psia as we do at 60 kv, atmospheric. The above voltages are those which will be recommended at the corresponding pressures.

D. ULTRAVIOLET

Ultraviolet light can be produced in a corona discharge, and is the result of the energy released when positive and negative ions (or positive ions and electrons) recombine. In the case of the worktable, throughout the working area we have ions of all one sign (positive) and there is, therefore, no recombination going on. There will be a small amount of recombination within the plastic box very close to the needle point where secondary ionization is occurring, and it is possible that some ultraviolet light would be radiated. There is no danger from ultraviolet light because the shield surrounding the ion source will be of a material opaque to ultraviolet light.

E. X-RAYS

As oxygen ions drift toward the table they collide with oxygen molecules and either stop dead or bounce off in a new direction, because the ion and the molecule are about the same weight. This means that the maximum energy of the ions is limited to what they can pick up in one free path. At a spacecraft cabin pressure of 5 psia, a mean free path for an oxygen ion is of the order of 10^{-5} centimeters. If we use 20 kilovolts at this pressure, the electric field will be of the order of one kilovolt per centimeter. This means that

the average energy released on each collision will be around .01 electron volts. It is generally known that particles must acquire energies of at least 104 electron volts before any significant X-rays are produced. The situation is a little more complicated when more than one gas is used, but since we are safe by six orders of magnitude, we can forget about any danger of X-rays in the normal use of the table. One caution should be noted: vacuum tubes, electric discharge tubes having partial vacuums and the like should not be handled on the worktable without special precuation, especially when operating 30 kilovolts, because of the possibility of inadvertently creating an X-ray tube.

F. INFLAMMABILITY

1. Flammability of the Worktable

The recommended table top material is baked-on porcelain. This material is applied at a red heat (1500°F) and is therefore already thoroughly oxidized and nonflammable. The plastic box around the ion source and the supporting arm may be of any non-conducting material, and one such material will be later chosen from those recommended for spacecraft use. So far as the power supply is concerned, it is recommended that the equipment be designed to meet the requirements of MIL-E-8189, General Specification for Guided Missiles Electronic Equipment, modified to incorporate requirements for spacecraft environment as set forth in MSFC Astrionics Laboratory Design Guide Line Manuals and MSC Manned Spacecraft Criteria and Standards Manual.

2. Ignition of Other Objects

The ability of a spark discharge from an object being handled to cause ignition in an oxygen atmosphere is dependent on the energy of the discharge. Even though voltage may be high, it takes a certain minimum number of joules (ampere-seconds) of energy to cause ignition of even the most flammable materials. MSC report 66-3, now out of print, set the level at .06 joules. A more recent unpublished work at MSC described experiments in which ignition was caused at .03 joules, but at a pressure of 19 psia of pure oxygen. The energy stored on a basketball sized object held in the ion beam is of the order of .0001 joules. We are therefore safe, by about a factor of 600, in saying that it is not possible to start a fire by discharging an object in the ion beam.

V. CONCLUSIONS

It was the purpose of this research to arrive at a set of design criteria upon which a satisfactory design might be based. Therefore, the design criteria constitute our conclusions, and are described as follows.

A. TABLE TOP

1. Size and Shape

The size and shape of the table top will be such as to clamp to the aerodynamic bench, which is hard mounted. Final specifications on this size and shape are not available at this date. The table top must also fold or disassemble so as to fit in a specified shape in the Multiple Docking Adapter. Again, specifications are not yet a ailable, since a given volume must be shared by parts of the aerodynamic assembly which have not yet been specified.

2. Material

The table top will be porcelain-coated steel. There will be either a suitable radius or a plastic rim such as to prevent chipping of porcelain around the edge. A standard porcelain coating used by Rittiner Industrial Enameling, Inc. of New Orleans has been tested and found adequate. The panel will be reinforced on the back side sufficiently to meet all acceleration and vibration specifications for both static firing and flight. Clamping must be such that the table top is electrically insulated from the spacecraft hull. All materials will satisfy the requirements specified for the Apollo Telescope Mount, or some other spacecraft materials list agreeable to the customer.

B. ION SOURCE

The ion source will be a stainless steel needle point housed in an insulated box perforated on the bottom. Perforations shall be 1/8 inch in diameter spaced at 1/2 inch centers; perforated portion of the box shall be 1/8 inch thick. The material of the box may be any approved non-conducting material. It should be opaque to ultraviolet light. The shape of the box will depend on the shape of the table top; it will be such as to focus the ion beam exactly on the table. The needle point will be mounted on an insulated base and connected directly to the power supply.

C. POWER SUPPLY

Power supply will be adjustable from 10 to 40 kilovolts and be capable of supplying a d.c. current of 1.0 microamperes. There should be not less than 300 megohms of protective resistance in series with the high voltage lead.

There will also be a bias voltage output of 300 volts at 1.0 milliamperes, with 10 megohms of protective resistance in series with this output. The power supply should be close to the ion source box (or integral with it) and there will be an insulated cable within or attached to the support column containing 28 volt input leads, ground wire and bias voltage output to the back of the table. The power supply will be completely potted in an approved plastic and all insulation will be in accordance with accepted standards. Switch and voltage adjustments will be in a convenient position.

VI. RECOMMENDATIONS

In looking back over the research done on this contract, one can easily see that a more rigorous analysis of the principles involved as well as more elaborate research might turn up a great deal more knowledge on this use of electrostatic forces. Nevertheless, the goal of this particular contract was achieved; that is, enough was found out about the principles to enable us to design a working piece of hardware. In fact, a number of valuable discoveries were made, such as the use of porcelain and the perforated shield ion source.

Although our present design will produce a piece of hardware that will do the job required, it is recommended that at some future date further research be done toward optimizing the design, since it may well be that far stronger forces are achievable with further refinements.

APPENDIX I

MATHEMATICAL ANALYSIS

A. POISSON'S EQUATION APPLIED TO AN ION BEAM

1. A general solution of Poisson's equation

The ion source of the electrostatic workbench consists of a fine needle point connected to a high voltage power supply and housed in a perforated box to limit the discharge current and to protect the operator from the high voltage. The opposite (negative) terminal of the power supply is connected to the work-table surface, which is approximately 18 inches below the ion source. When the high voltage is turned on, the needle point undergoes a minute discharge (a few microamperes) and positive ions escape from the perforated box and inhabit the area directly above the table. Electric flux from the charged box as well as from the ions themselves gives rise to an electric field above the table. This field will, at any point, be the negative gradient of the potential at that point.

$$\bar{E} = -\bar{\nabla} V \tag{1}$$

Where $\bar{E}$ is the strength of the field, V is the potential and $\bar{\nabla}$ is the La Placian operator. Overbars are used to designate vector quantities. If we assume that all ions are positive, each ion becomes a source of electric flux, and from Gauss' law, the divergence of the electric field throughout the charged region is

$$\bar{\nabla} \cdot K\bar{E} = 4\pi\rho \tag{2}$$

where ρ is the charge density and K is the dielectric constant of the air. Substituting for $\bar{E}$ from (1) we derive Poisson's equation,

$$\nabla^2 KV = -4\pi\rho \tag{3}$$

which governs the potential throughout the region.

Now, if a steady state has been reached, we know from the nature of an electric current that there will be no closed loops; that is, the curl of the current will be zero:

$$\bar{\nabla} \times \bar{I} = 0 \tag{4}$$

where $\bar{I}$ is a vector representing current density; that is, current per unit area taken normal to the direction of the vector. This suggests that the

current vector $\bar{I}$ is mathematically derivable from some potential function. Let us define a "current potential" Φ (not to be confused with the electric potential V) such that

$$\bar{I} = -\bar{\nabla}\Phi \tag{5}$$

Now, the divergence of any electric current must be zero in any region not containing an electrode,

$$\bar{\nabla} \cdot \bar{I} = 0 \tag{6}$$

and substituting (5) into (6) we see that Φ must be a solution to La Place's equation:

$$\nabla^2\Phi = 0 \tag{7}$$

This provides us with a convenient starting point, since solutions to this familiar equation are well known for at least most simple boundary configurations. The task remains to relate the two potential functions.

If we assume that the region above the table is in an atmosphere of sufficient pressure that the mean free path is short compared to the physical dimensions of our boundaries, and this is certainly the case even at 5 psia, then it has been shown by Loeb and others that the drift velocity of the ions is directly proportional to the electric field:

$$\bar{v} = M\bar{E} \tag{8}$$

where $\bar{v}$ is the velocity with which the ions are moving and M is their mobility, a constant for a given type of ion and a given atmospheric pressure. Furthermore, if all electric current is being carried by these ions, the current density must be simply the product of ion velocity and charge density:

$$\bar{I} = \rho\,\bar{v} \tag{9}$$

and from (8) and (9) we derive

$$\bar{I} = \rho M\bar{E} \tag{10}$$

or

$$\bar{\nabla}\Phi = \rho M\bar{\nabla}V \tag{11}$$

We now have the relationship between the two potential functions. One can see by observation that in order for the two gradients to be everywhere parallel, surfaces of equal Φ must also be surfaces of equal V; although the two potential functions are not necessarily equal, they are at least the same family of surfaces. Furthermore, if we take the curl of both sides of (11) we have the somewhat surprising result

$$\bar{\nabla}\rho \times \bar{\nabla}V = 0 \tag{12}$$

which tells us, since the two gradients must be everywhere parallel to have a zero cross product, that surfaces of equal potential must be surfaces of equal ion density. This means that since the table top is certainly an equipotential surface, the ions will be just as dense near the edge as they are at the center. Note, however, that equation (11) ceases to hold in a region where the ion density ρ is zero. This set of relationships gives us the ability to "focus" ions in a well-defined beam; the density will be constant right to the edge of the beam, and will be zero beyond that, where Poisson's equation becomes La Place's equation. If the ion source box is properly designed, the edge of the beam should coincide with the edge of the table.

In order to predict the behavior of the ions as well as the ion density and electric field strength, we must seek a solution to (11). Taking the divergence of both members of (11) we have

$$\nabla^2\Phi = M(\bar{\nabla}\rho \cdot \bar{\nabla}V + \rho\nabla^2 V) = 0 \tag{13}$$

or, using equation (3),

$$\bar{\nabla}\rho \cdot \bar{\nabla}V = \frac{4\pi}{K}\rho^2 \tag{14}$$

and substituting for V from (11)

$$\bar{\nabla}\rho \cdot \bar{\nabla}\Phi = \frac{4\pi M}{K}\rho^3 \tag{15}$$

This equation often has a closed solution if we know the distribution of Φ for the applicable boundaries (a solution to La Place's equation) and if we can choose a set of coordinates such that the two gradients lie directly along one axis so that (15) becomes an ordinary differential equation along that axis; expansion by means of harmonics and the like can sometimes then yield a formal solution for the entire region.

2. Solution for ion flow between concentric spheres

In the case of the worktable the true boundaries are much too complicated to attempt a formal solution by this means. However, since we have no need for high accuracy, we will seek some simple set of boundaries which will give us an approximate solution. One such set is to consider the table top to be a section of a sphere concentric about the needle point ion source.

In the spherical solution all gradients will lie along a radius, so (15) reduces to the ordinary differential equation

$$\frac{d\rho}{dr}\frac{d\Phi}{dr} = \frac{4\pi M}{K}\rho^3 \tag{16}$$

The density of the ion current at radius r can be written in terms of the total current for the entire sphere:

$$I = -\frac{d\phi}{dr} \quad \frac{I_T}{4\pi r^2} \tag{17}$$

where I_T is the total current. Substituting for $\frac{d\phi}{dr}$ in (16) gives

$$\frac{d\rho}{dr} = -\frac{16\pi^2 M}{I_T K} r^2 \rho^3 \tag{18}$$

which integrates to give us the expression for the ion density throughout the region:

$$\rho = \frac{1}{4\pi\sqrt{\frac{2M}{3KI_T}}\sqrt{r^3 + C}} \tag{19}$$

where C is an arbitrary constant associated with the inner boundary. If the inner boundary is a needle point, the constant disappears:

$$\rho = \frac{1}{4\pi}\sqrt{\frac{3KI_T}{2M}}\, r^{-3/2} \tag{20}$$

From (10)

$$\rho = \frac{I}{ME} \quad \frac{I_T}{4\pi MEr^2} \tag{21}$$

Eliminating ρ between (20) and (21) gives us the expression for the strength of the electric field throughout the region:

$$E = \sqrt{\frac{2I_T}{3KMr}} \tag{22}$$

It is significant to note at this point that the presence of the ion beam leads to a more uniform electric field; without the ions, the electric field in a spherical system would fall off inversely as the square of the distance from the needle point, whereas in the ion beam it falls off only with the square root of the radius. (22) can be integrated to yield the expression for the electric potential throughout the region:

$$V = -\int E dr = V_p - 2\sqrt{\frac{2I_T}{3KM}}\sqrt{r} \tag{23}$$

where V_p is the potential applied to the needle point. Here the total current I_T is for an entire sphere concentric with the point source; a constant must be entered to allow for the fact that the table top approximates only a segment of such a sphere.

3. Solution for ion flow between infinite parallel planes

The spherical solution derived in the previous section will quite accurately describe the upper part of our region, closest to the needle point, since the exact shape of the table top will have little effect on the ion distribution in this region. If we wish to examine the region close to the table top, however, it will be more accurate to use a solution for ion flow between parallel planes.

Our basic differential equation now becomes, from (15)

$$\frac{d\rho}{dx} \frac{d\phi}{cs} = \frac{4\pi M}{K} \rho^3 \tag{24}$$

where x is considered the distance measured down from an upper plane boundary. The current density (I) will now be a constant, reducing (24) to

$$\frac{d\rho}{dx} = - \frac{4\pi M}{KI} \rho^3 \tag{25}$$

which may be integrated to give us an expression for the ion density near the table top:

$$\rho = \sqrt{\frac{KI}{8\pi M}} \frac{1}{\sqrt{x + c}} \tag{26}$$

Comparing this with (19) shows that the ion density is more nearly constant as we approach the table. The current (I) must be adjusted, of course, to fit this solution together with the spherical solution at some point above the table. Eliminating ρ by means of (10), we have the expression for the strength of the electric field near the table

$$E = \sqrt{\frac{8\pi I}{KM}} \sqrt{x + c} \tag{27}$$

where the arbitrary constant c will be later adjusted to fit the two solutions together. It is interesting to note that the strength of the electric field is now increasing as we approach the table (x is measured downward to be consistent with r of the spherical solution). This is due to electric flux arising from ions in transit. We may now integrate (27) to give us the expression for the potential near the table:

$$V = V_a - \frac{2}{3} \sqrt{\frac{8\pi I}{KM}} (x + c)^{3/2} \tag{28}$$

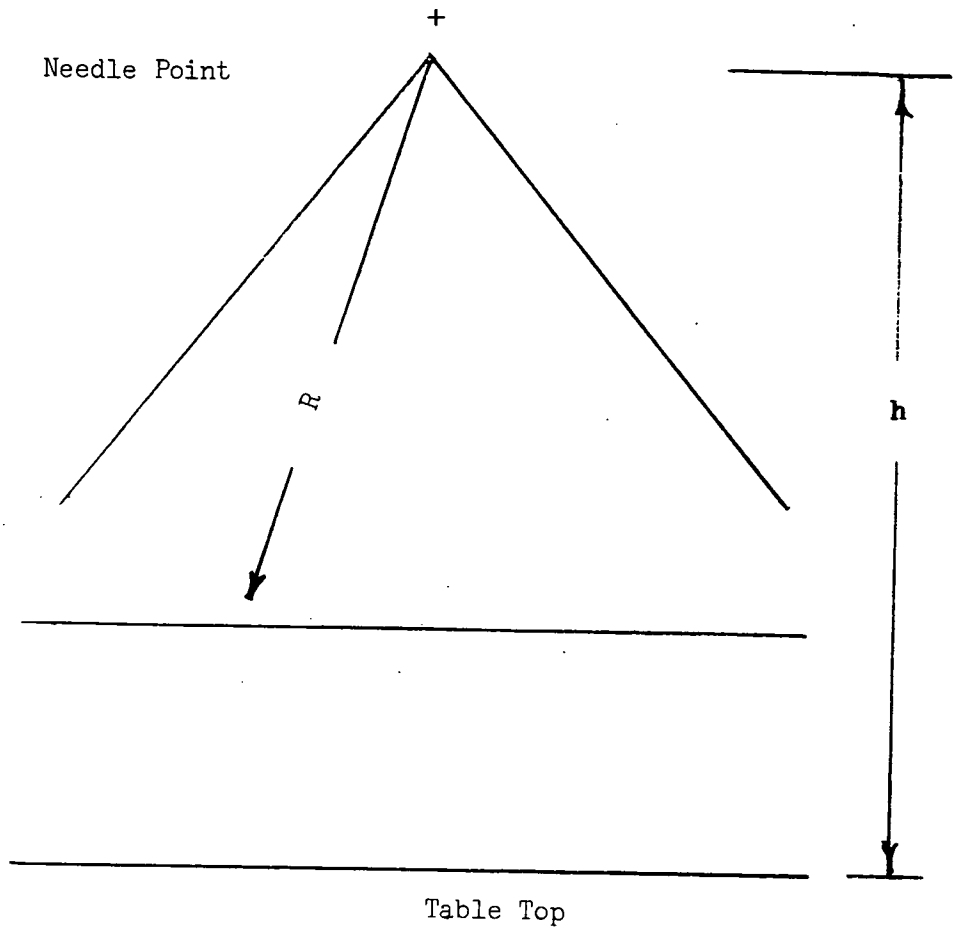

Figure 14. An approximate mathematical model of the table is formed by piecing together spherical and plane solutions to Poisson's equation.

where V_a is the potential at the upper plane.

4. Approximate solution for the table

If the table top has an area A, we may express both I and I_T in terms of the total measured current I_m

$$I = \frac{I_m}{A} \qquad I_T = 4\pi R^2 I = \frac{4\pi R^2}{A} I_m \tag{29}$$

where R is the maximum radius of the spherical solution. (See figure 1.) If we now let r be the distance from the needle point in both solutions, x + c becomes r. The potential at the upper boundary of the lower solution V_a must be equal to the potential at radius R in the upper solution. Making these substitutions gives us our two expressions for electric potential

$$\text{Upper region:} \quad V = V_P - 4\sqrt{\frac{2\pi R^2 I_m}{3KMA}}\ \sqrt{r} \tag{30}$$

$$\text{Lower region:} \quad V = V_P - \frac{4}{3}\sqrt{\frac{2\pi I_m}{KMA}}\ (\sqrt{3}\, R^{3/2} + r^{3/2}) \tag{31}$$

in terms of applied voltage V_p and measured current I_m. Similarly, our electric field strength is given by

$$\text{Upper region:} \quad E = 2\sqrt{\frac{2\pi R^2 I_m}{3KMA}}\ \frac{1}{\sqrt{r}} \tag{32}$$

$$\text{Lower region:} \quad E = 2\sqrt{\frac{2\pi I_m}{KMA}}\ \sqrt{r} \tag{33}$$

It is these last two expressions that determine the force with which an object of a given charge will be attracted to the table. Two things may be noted: the force will be proportional to the square root of the current I_m and thus a reduction in current does not proportionally reduce the force, and in both regions the force varies inversely with the square root of the mobility M. This tells us that the less the mobility, the greater the force, hence the decision to use positive ions rather than negative, since positive ions have only about half the mobility of negative ions.

The attractive force we might expect will be

$$f = EVC \tag{34}$$

where C is the capacitance of the object. This assumes that the object has had time to charge up to whatever potential V exists at that point.

APPENDIX II

NO. 340-20 DIETZGEN GRAPH PAPER
20 X 20 PER INCH

EUGENE DIETZGEN CO.
MADE IN U. S. A.

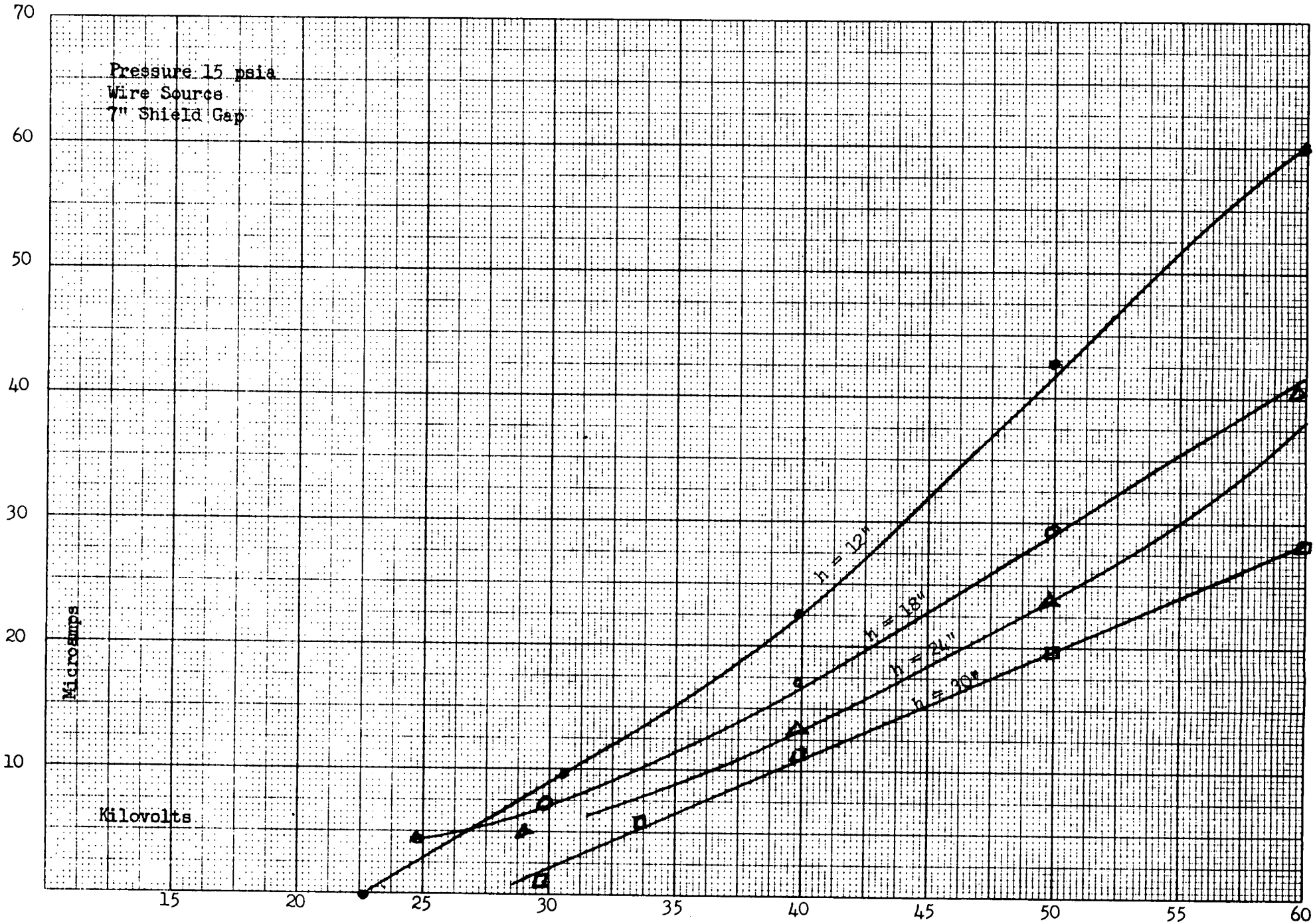

Figure 15

NO. 340-20 DIETZGEN GRAPH PAPER
20 X 20 PER INCH

EUGENE DIETZGEN CO.
MADE IN U. S. A.

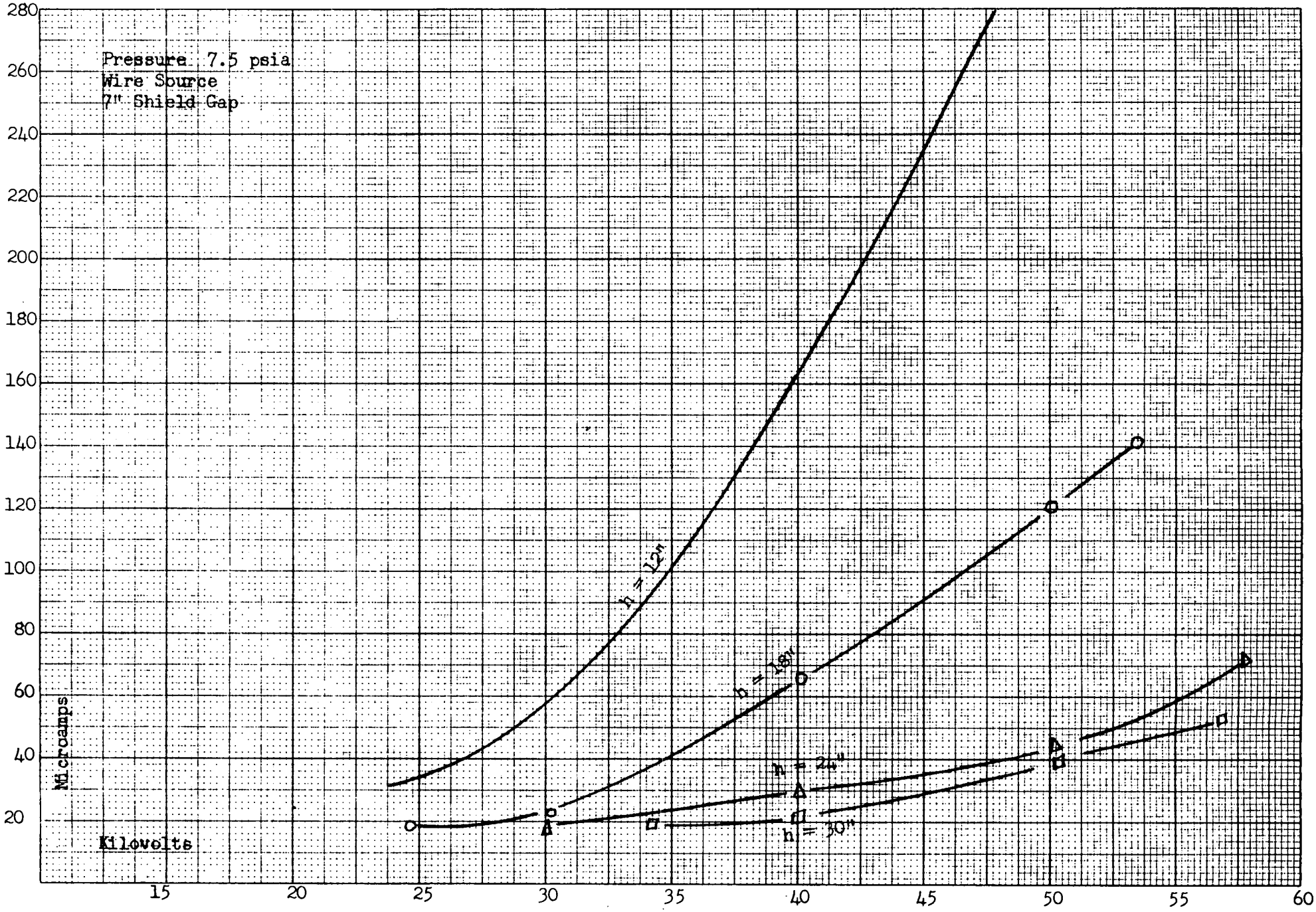

Figure 16

NO. 340-20 DIETZGEN GRAPH PAPER
20 X 20 PER INCH

EUGENE DIETZGEN CO.
MADE IN U. S. A.

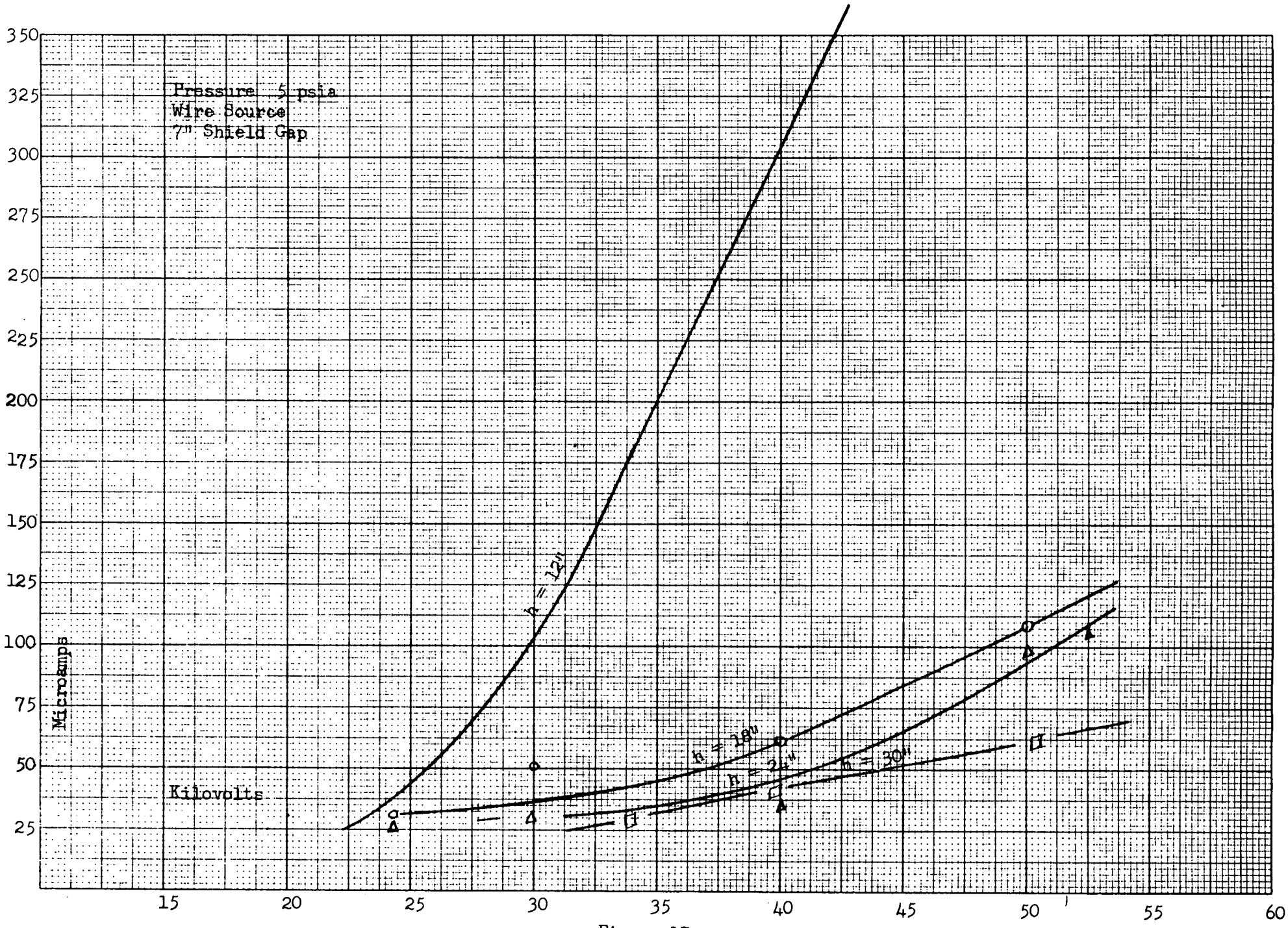

Figure 17

NO. 340-20 DIETZGEN GRAPH PAPER
20 X 20 PER INCH
EUGENE DIETZGEN CO.
MADE IN U. S. A.

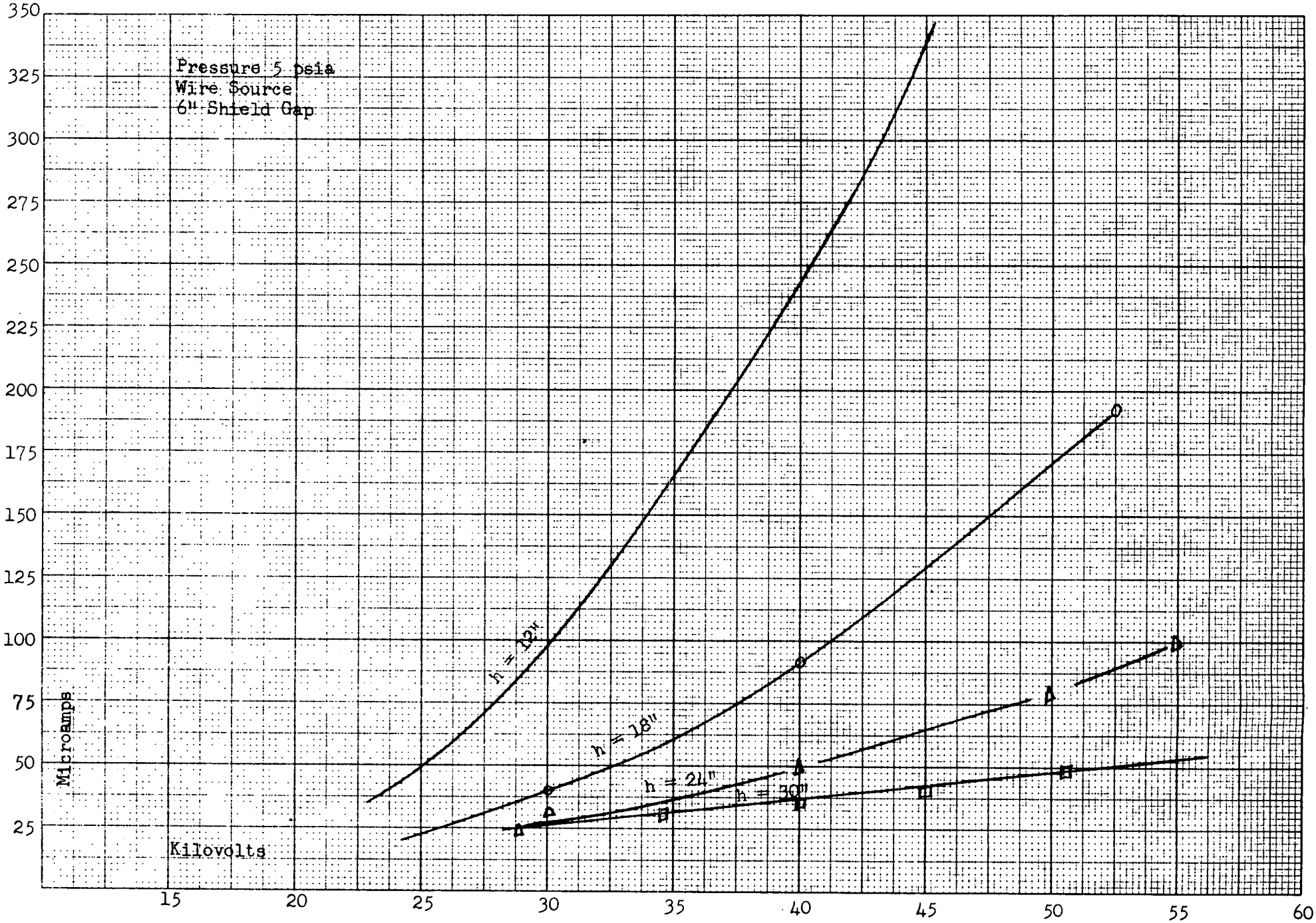

Figure 18

NO. 340-20 DIETZGEN GRAPH PAPER
20 X 20 PER INCH

EUGENE DIETZGEN CO.
MADE IN U. S. A.

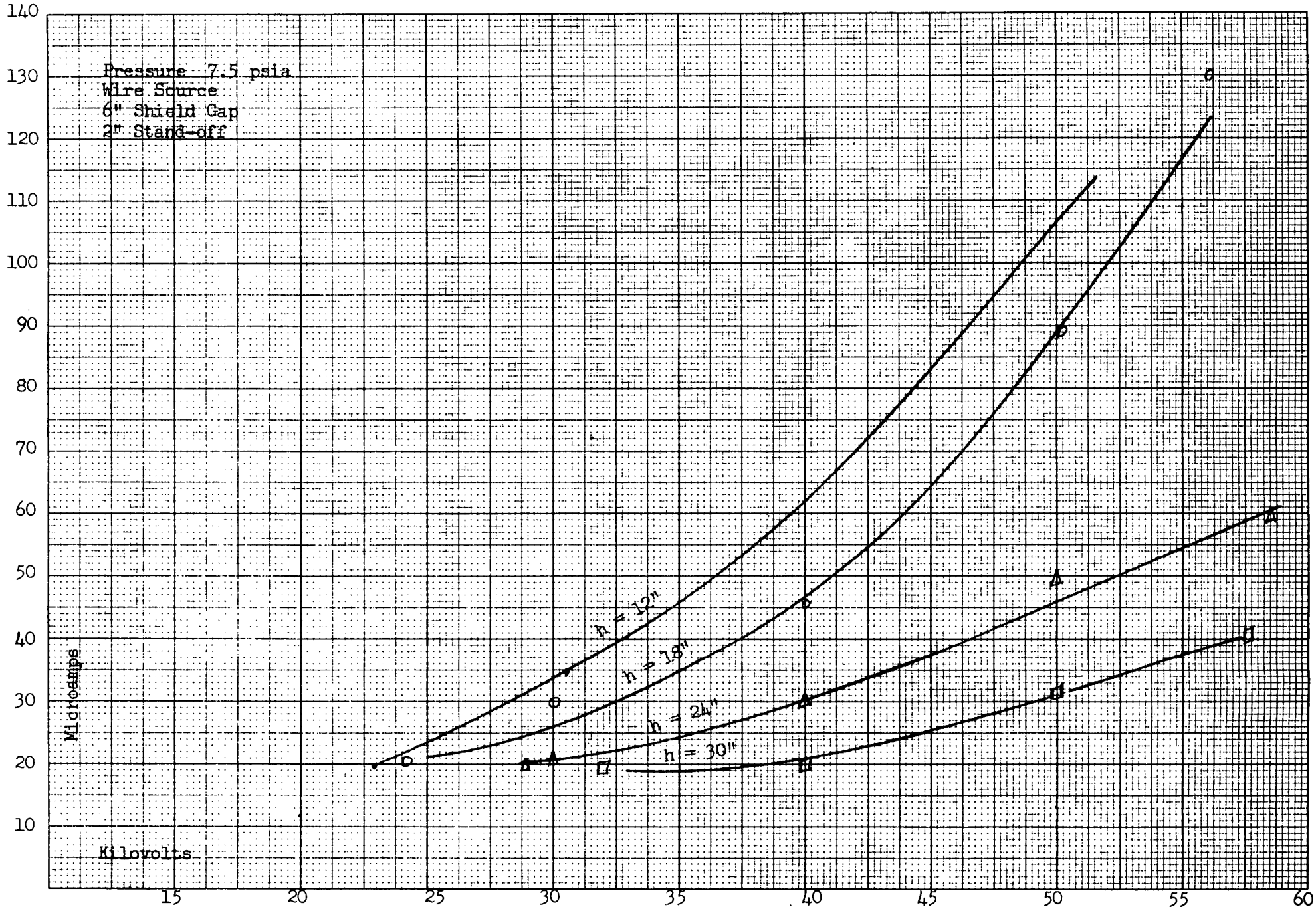

Figure 19

NO. 340-20 DIETZGEN GRAPH PAPER
20 X 20 PER INCH
EUGENE DIETZGEN CO.
MADE IN U. S. A.

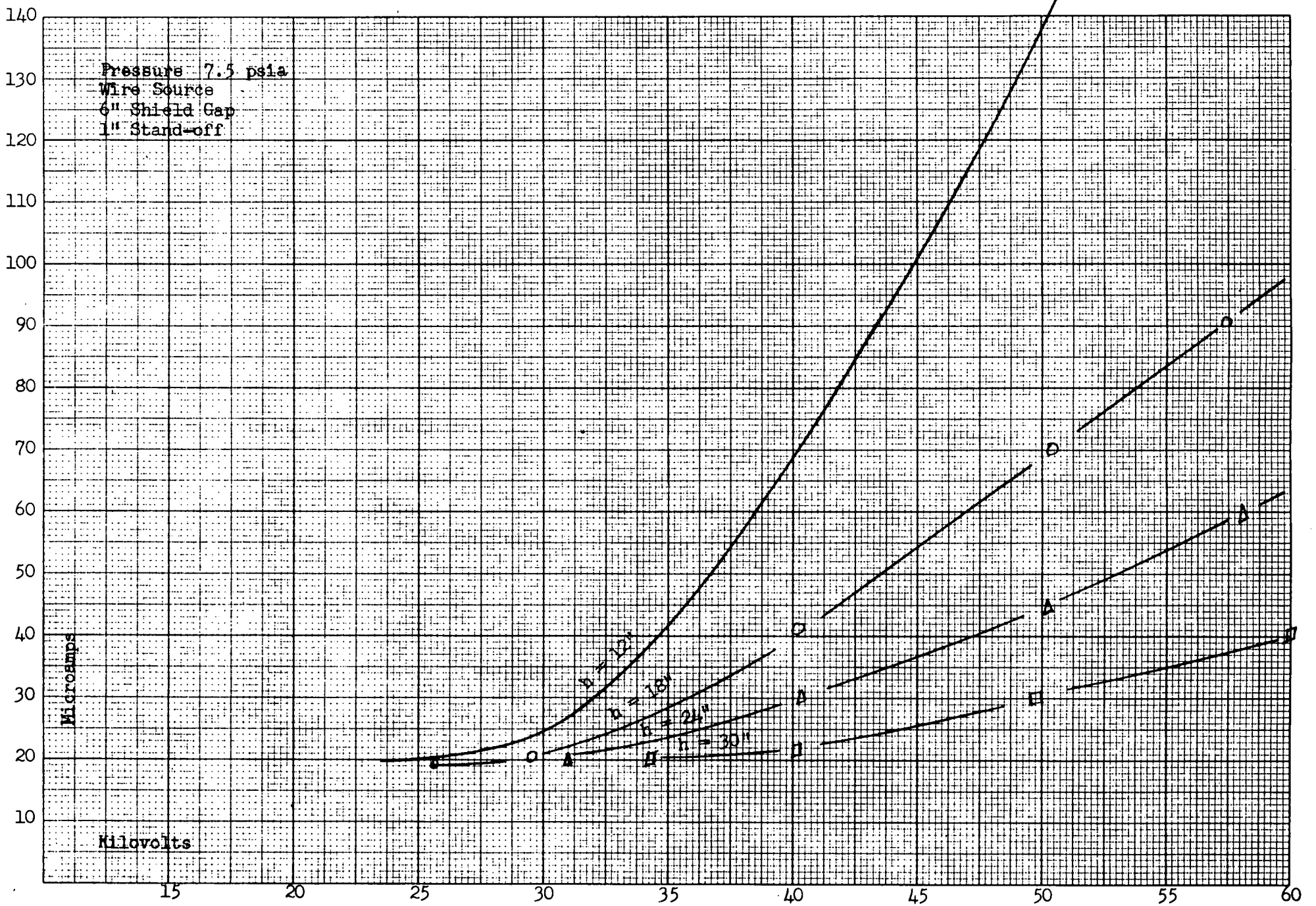

Figure 20

NO. 340-20 DIETZGEN GRAPH PAPER
20 X 20 PER INCH
EUGENE DIETZGEN CO.
MADE IN U. S. A.

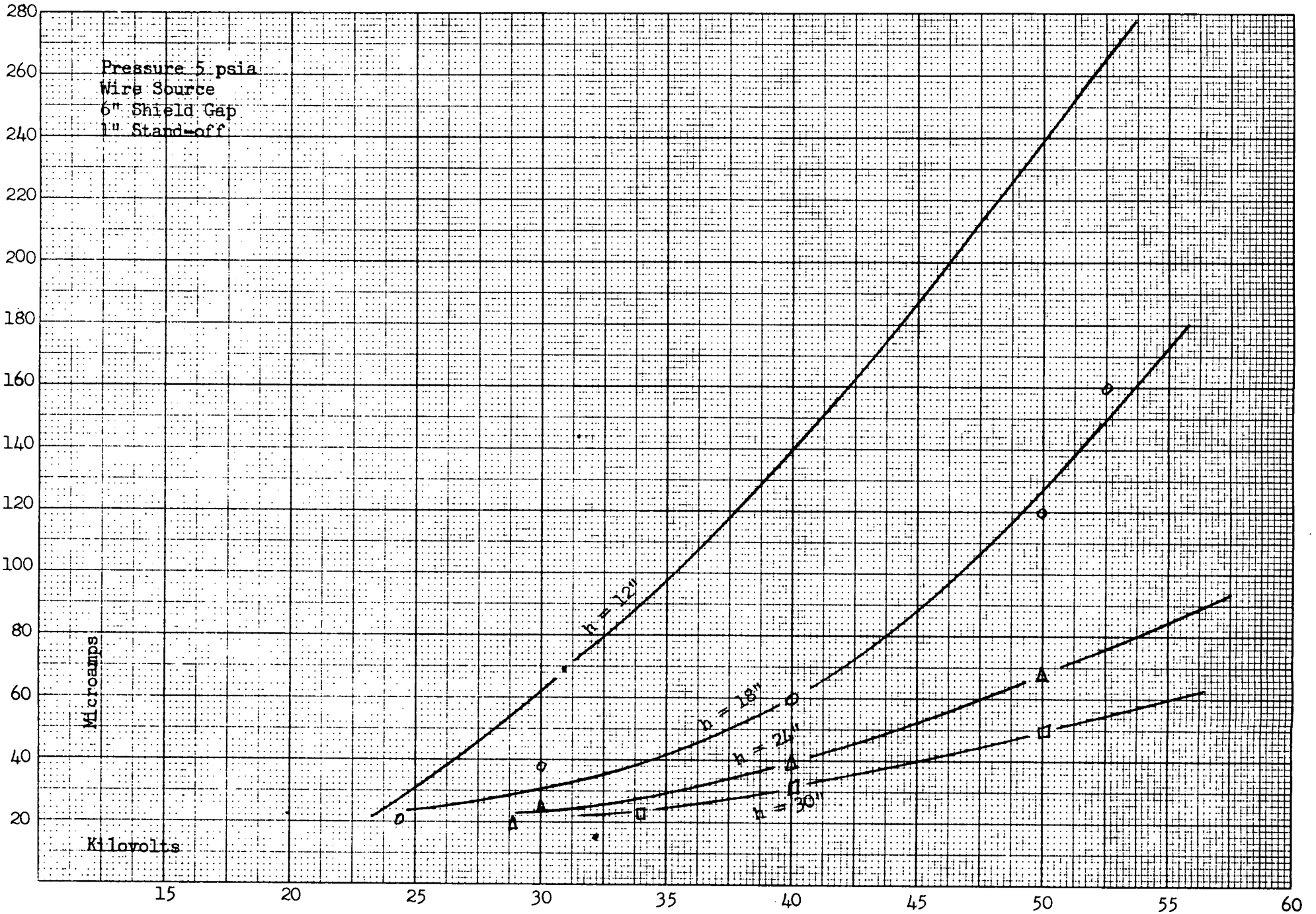

Figure 21

NO. 340-20 DIETZGEN GRAPH PAPER
20 X 20 PER INCH
EUGENE DIETZGEN CO.
MADE IN U. S. A.

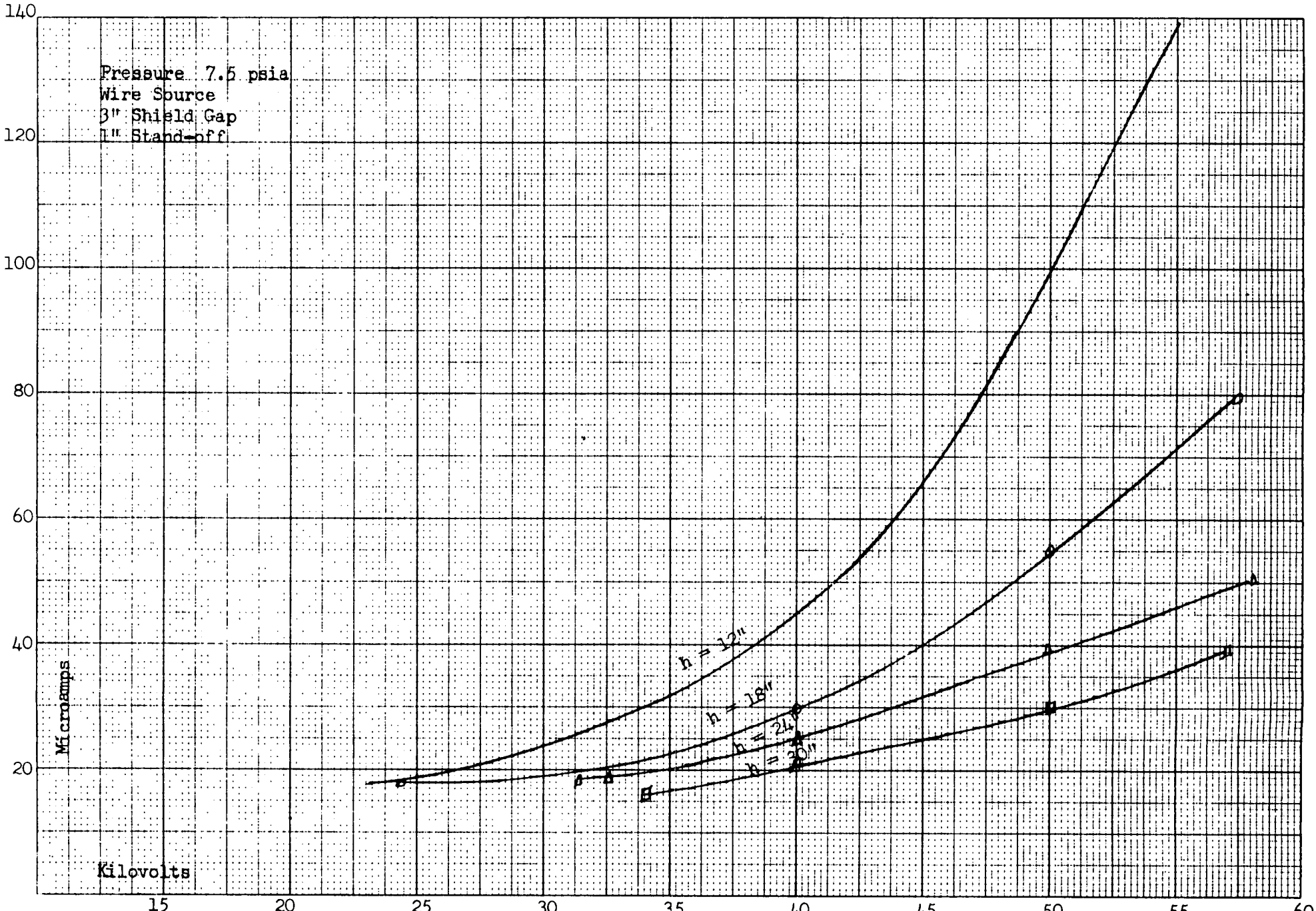

Figure 22

NO. 340-20 DIETZGEN GRAPH PAPER
20 X 20 PER INCH
EUGENE DIETZGEN CO.
MADE IN U. S. A.

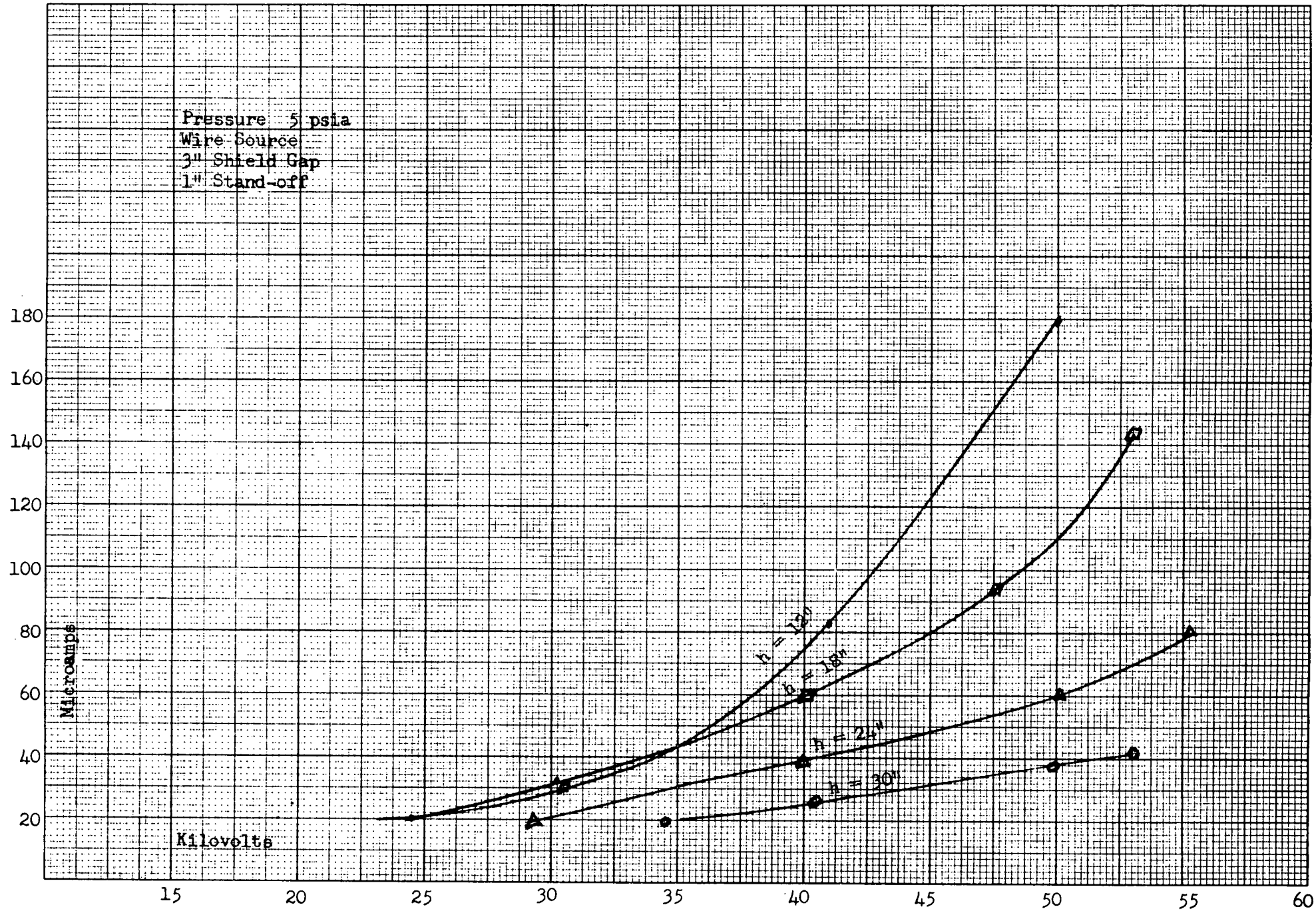

Figure 23

NO. 340-20 DIETZGEN GRAPH PAPER
20 X 20 PER INCH

EUGENE DIETZGEN CO.
MADE IN U. S. A.

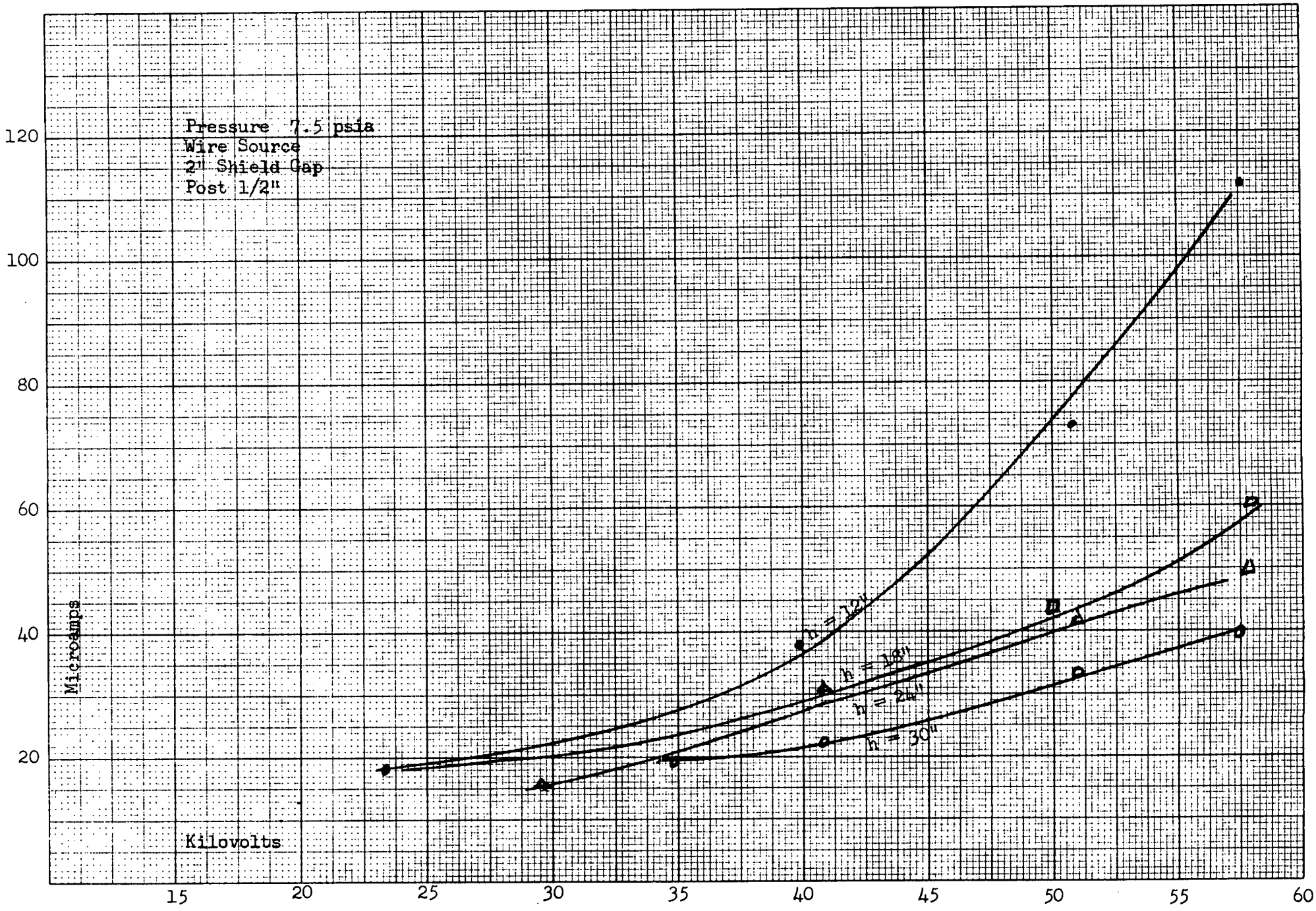

Figure 24

NO. 340-20 DIETZGEN GRAPH PAPER
20 X 20 PER INCH

EUGENE DIETZGEN CO.
MADE IN U. S. A.

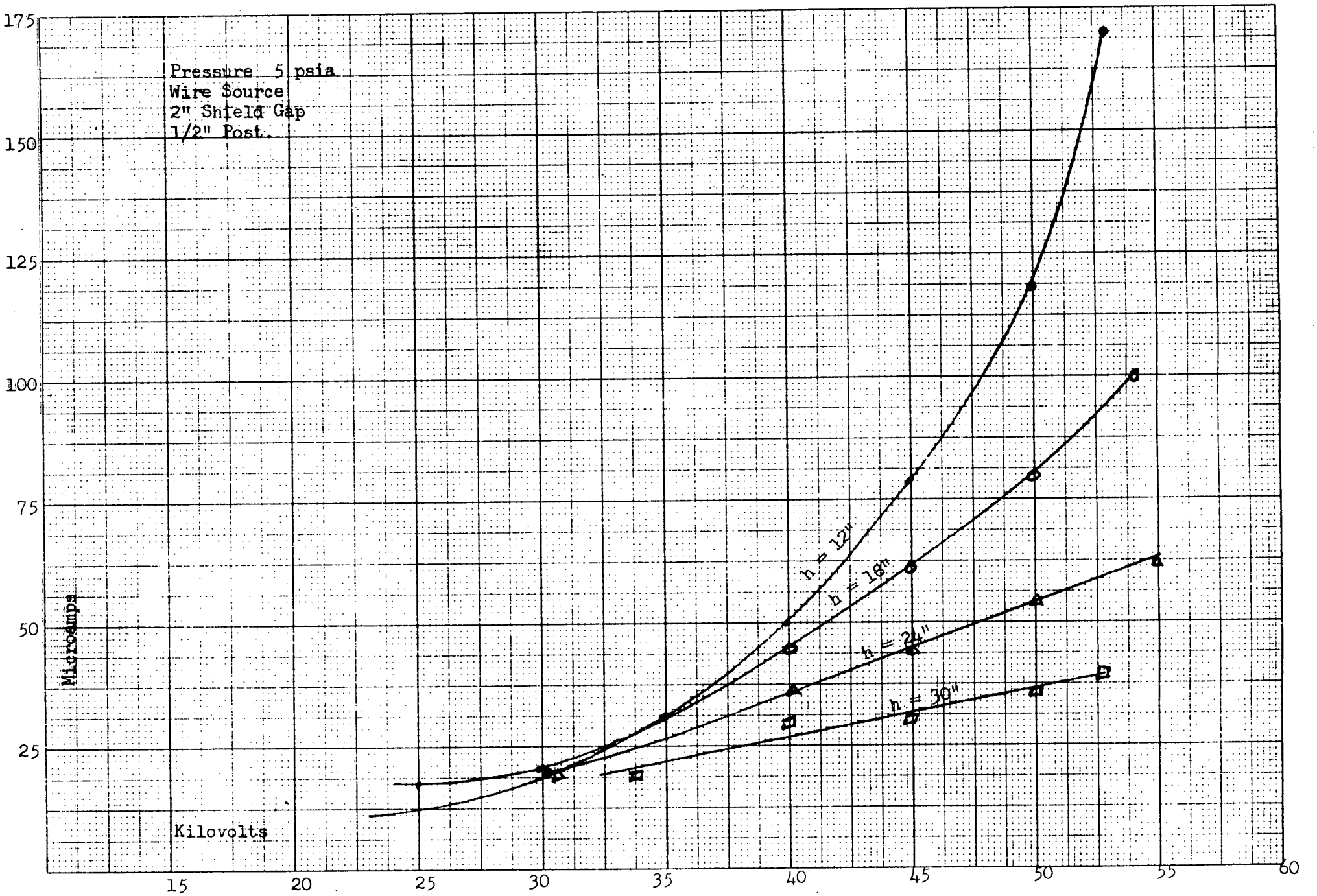

Figure 25

NO. 340-20 DIETZGEN GRAPH PAPER
20 X 20 PER INCH

EUGENE DIETZGEN CO.
MADE IN U. S. A.

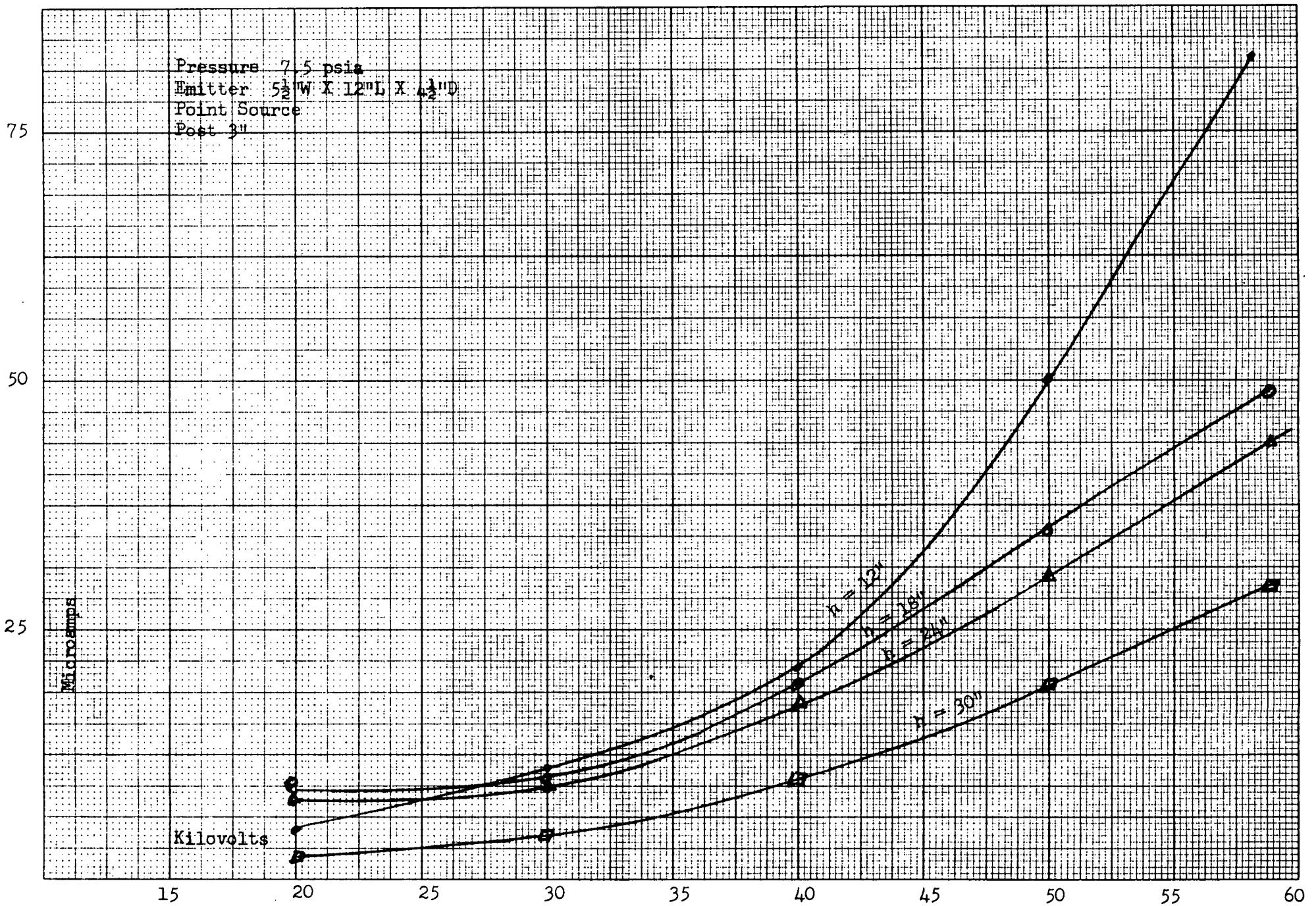

Figure 26

NO. 340-20 DIETZGEN GRAPH PAPER
20 X 20 PER INCH

EUGENE DIETZGEN CO.
MADE IN U. S. A.

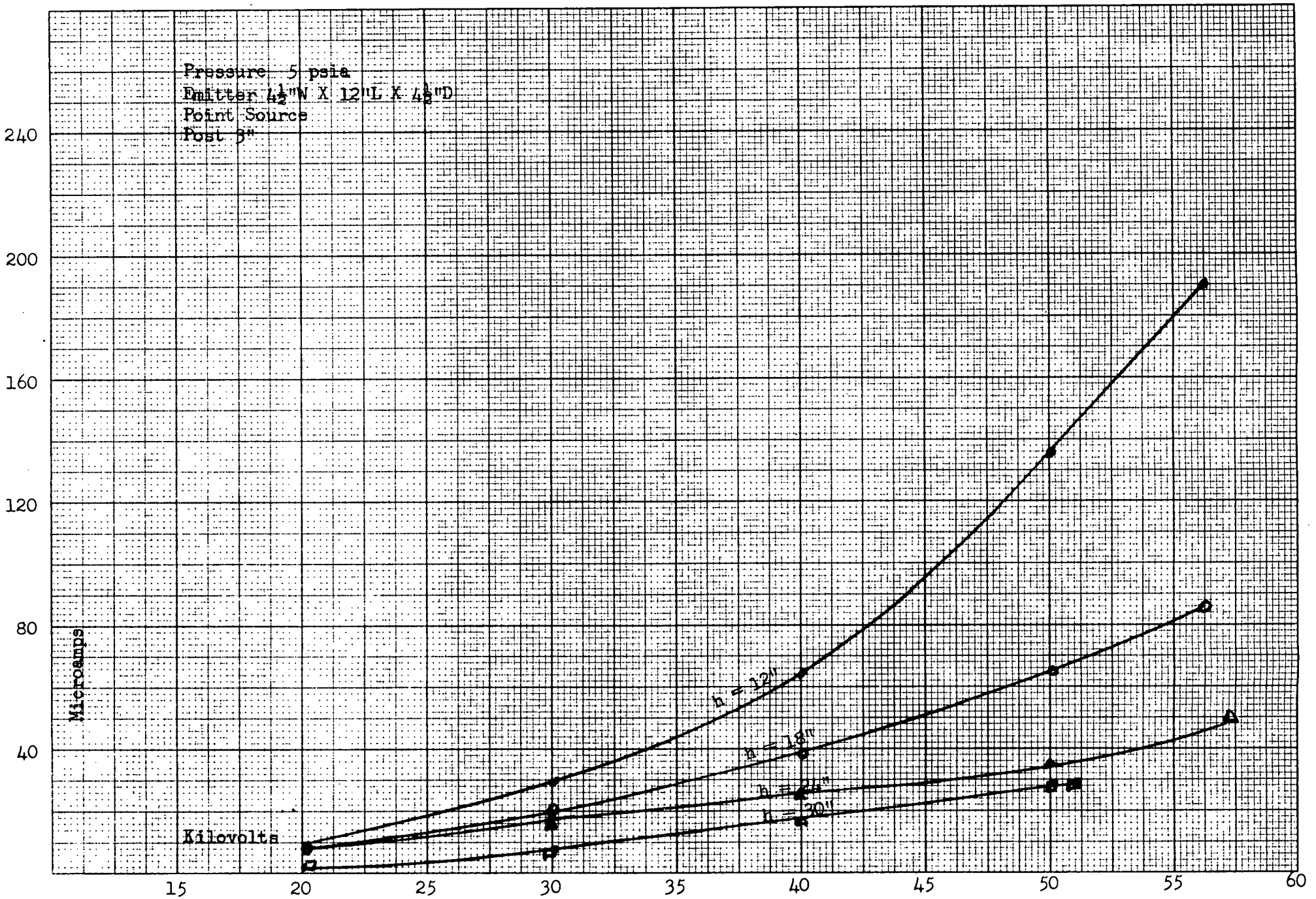

Figure 27

NO. 340-20 DIETZGEN GRAPH PAPER
20 X 20 PER INCH

EUGENE DIETZGEN CO.
MADE IN U. S. A.

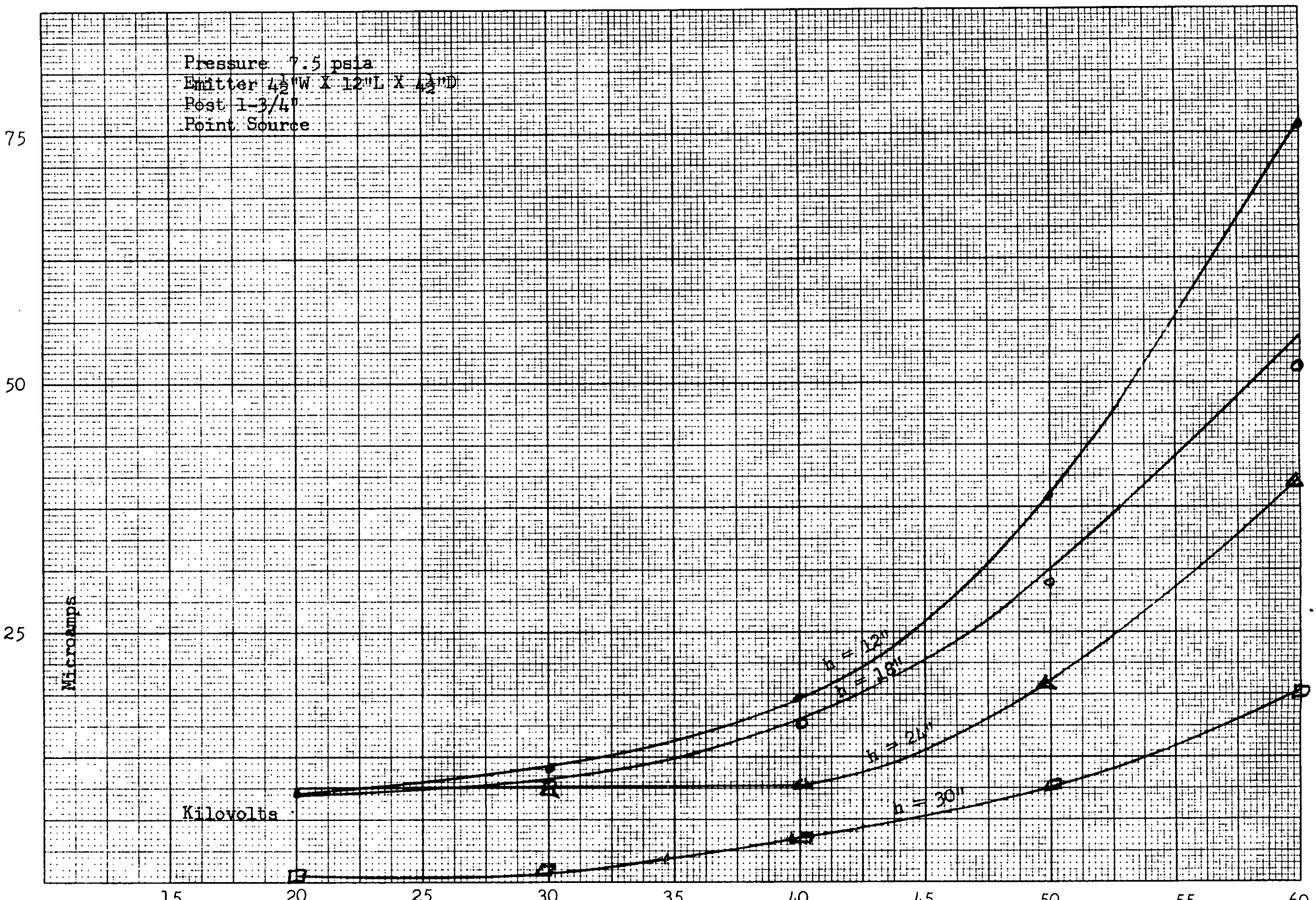

Figure 28

NO. 340-20 DIETZGEN GRAPH PAPER
20 X 20 PER INCH
EUGENE DIETZGEN CO.
MADE IN U. S. A.

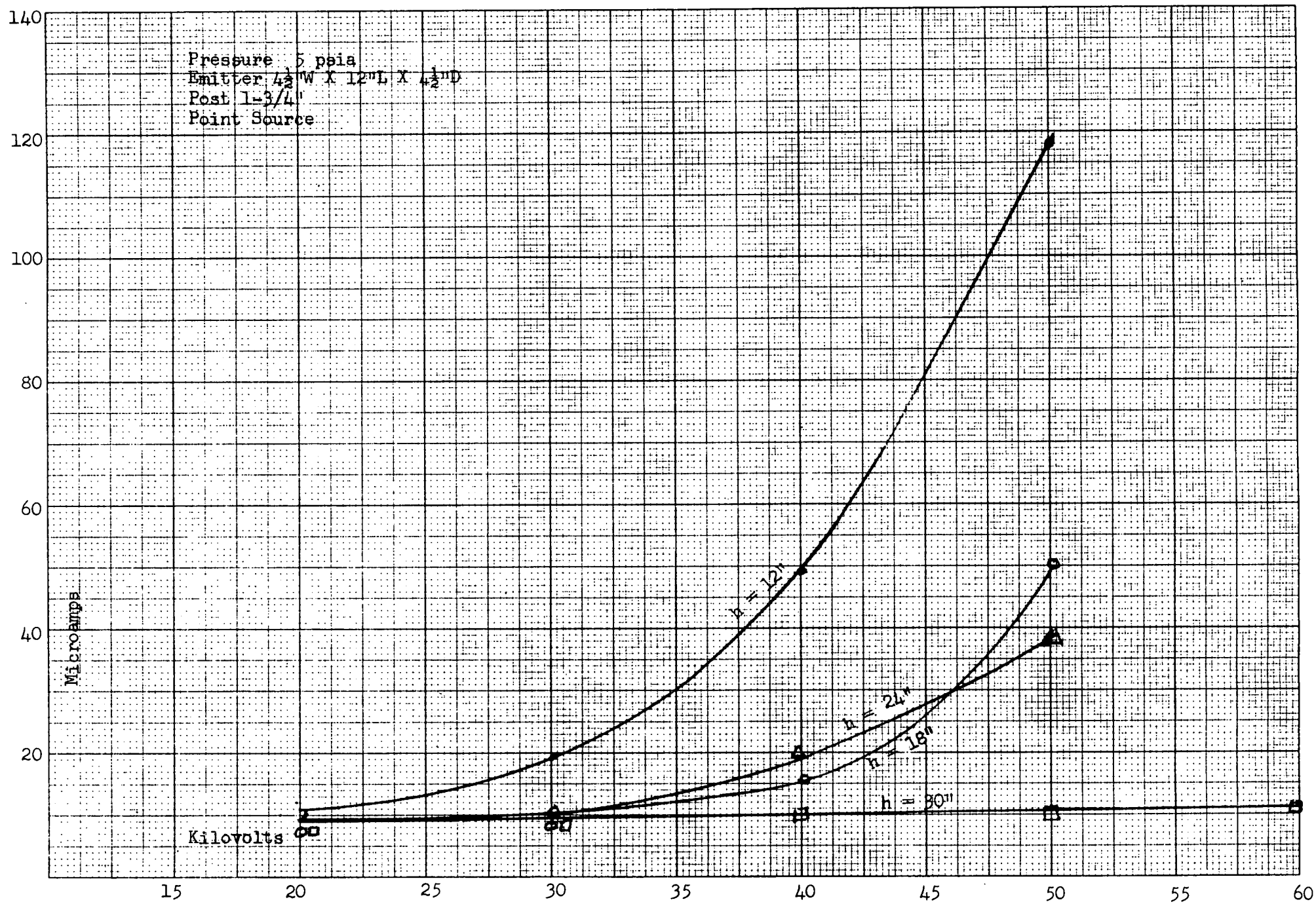

Figure 29

NO. 340-20 DIETZGEN GRAPH PAPER
20 X 20 PER INCH
EUGENE DIETZGEN CO.
MADE IN U. S. A.

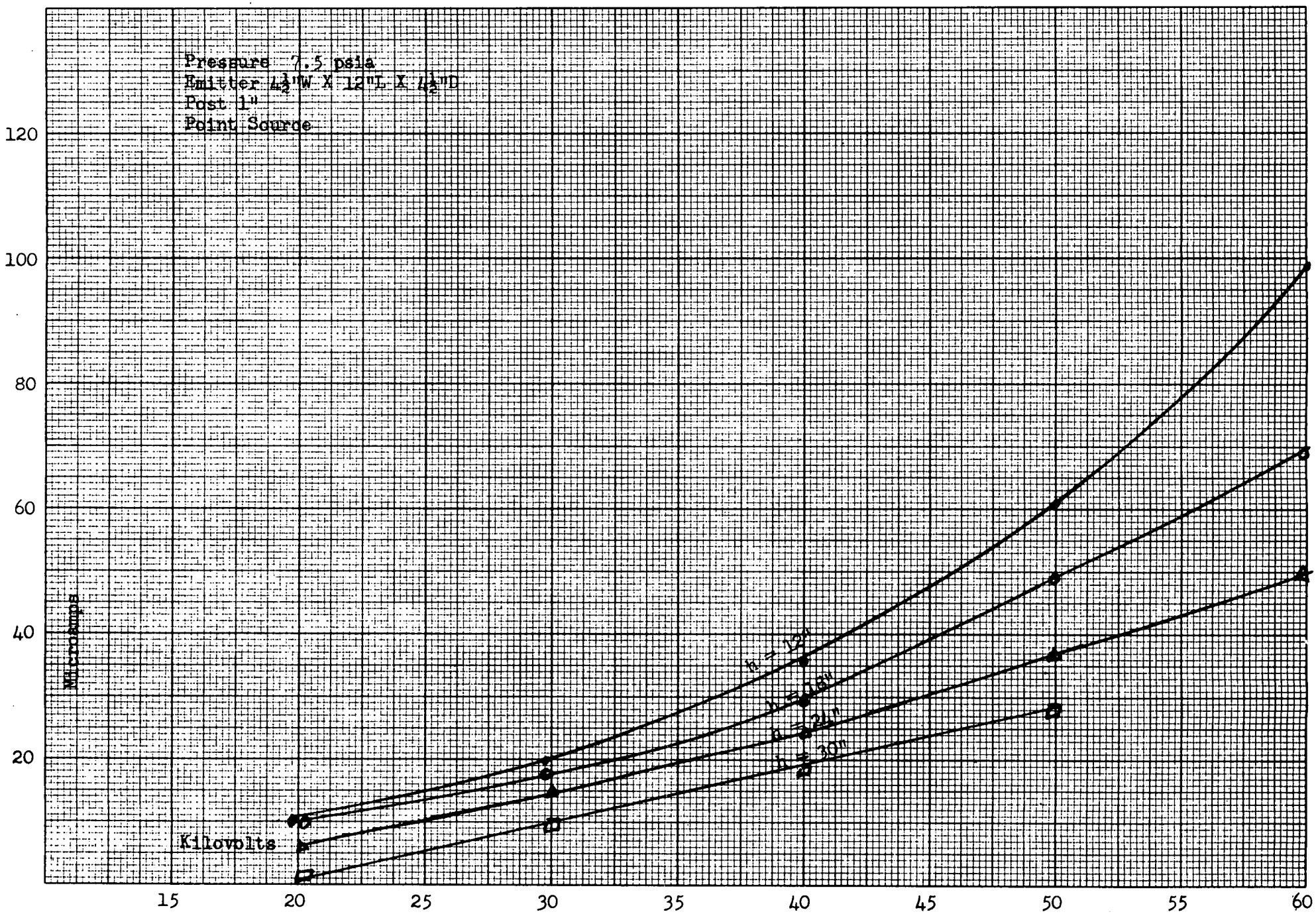

Figure 30

NO. 340-20 DIETZGEN GRAPH PAPER
20 X 20 PER INCH
EUGENE DIETZGEN CO.
MADE IN U. S. A.

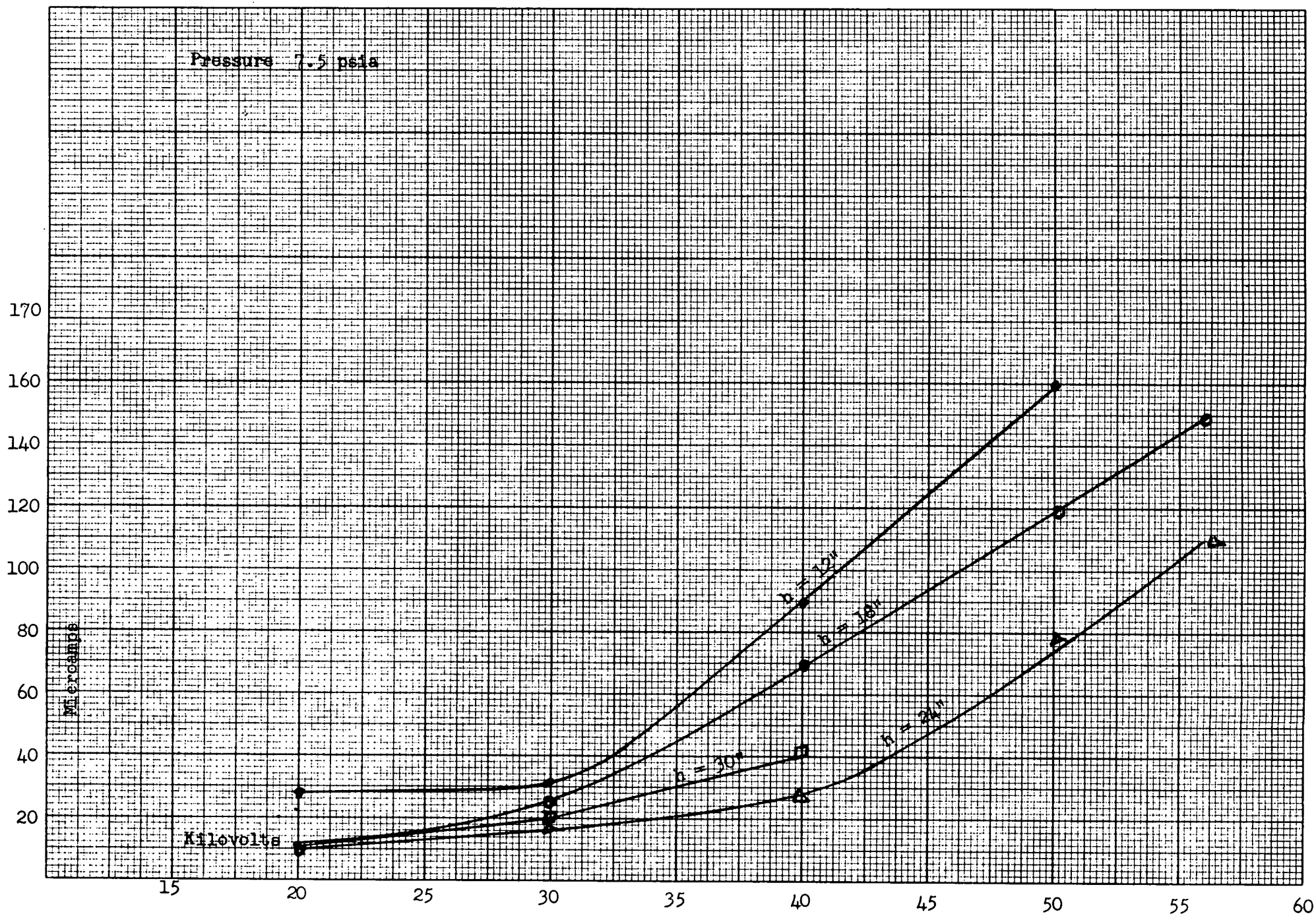

Figure 31

NO. 340-20 DIETZGEN GRAPH PAPER
20 X 20 PER INCH
EUGENE DIETZGEN CO.
MADE IN U. S. A.

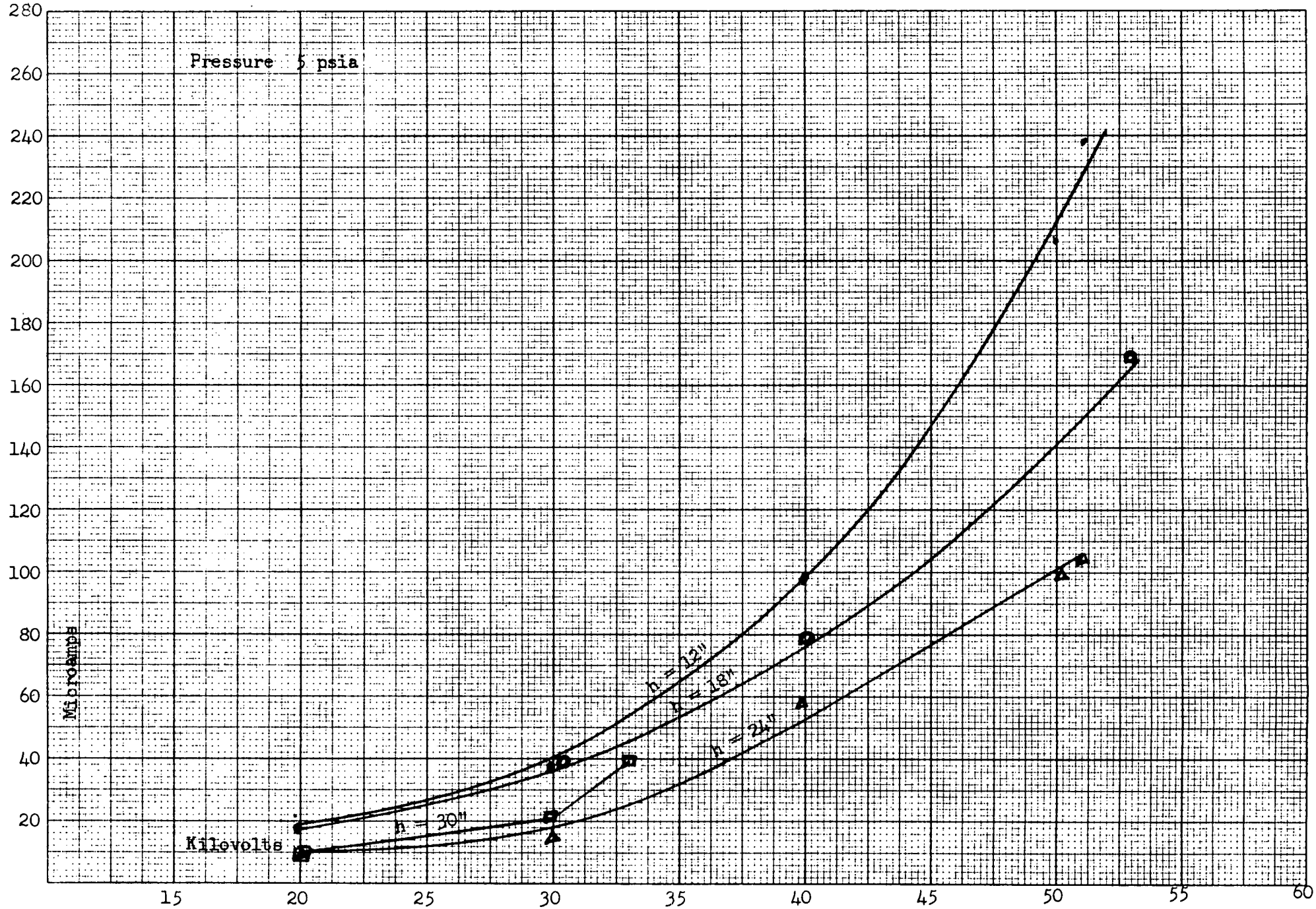

Figure 32

NO. 340-20 DIETZGEN GRAPH PAPER
20 X 20 PER INCH

EUGENE DIETZGEN CO.
MADE IN U. S. A.

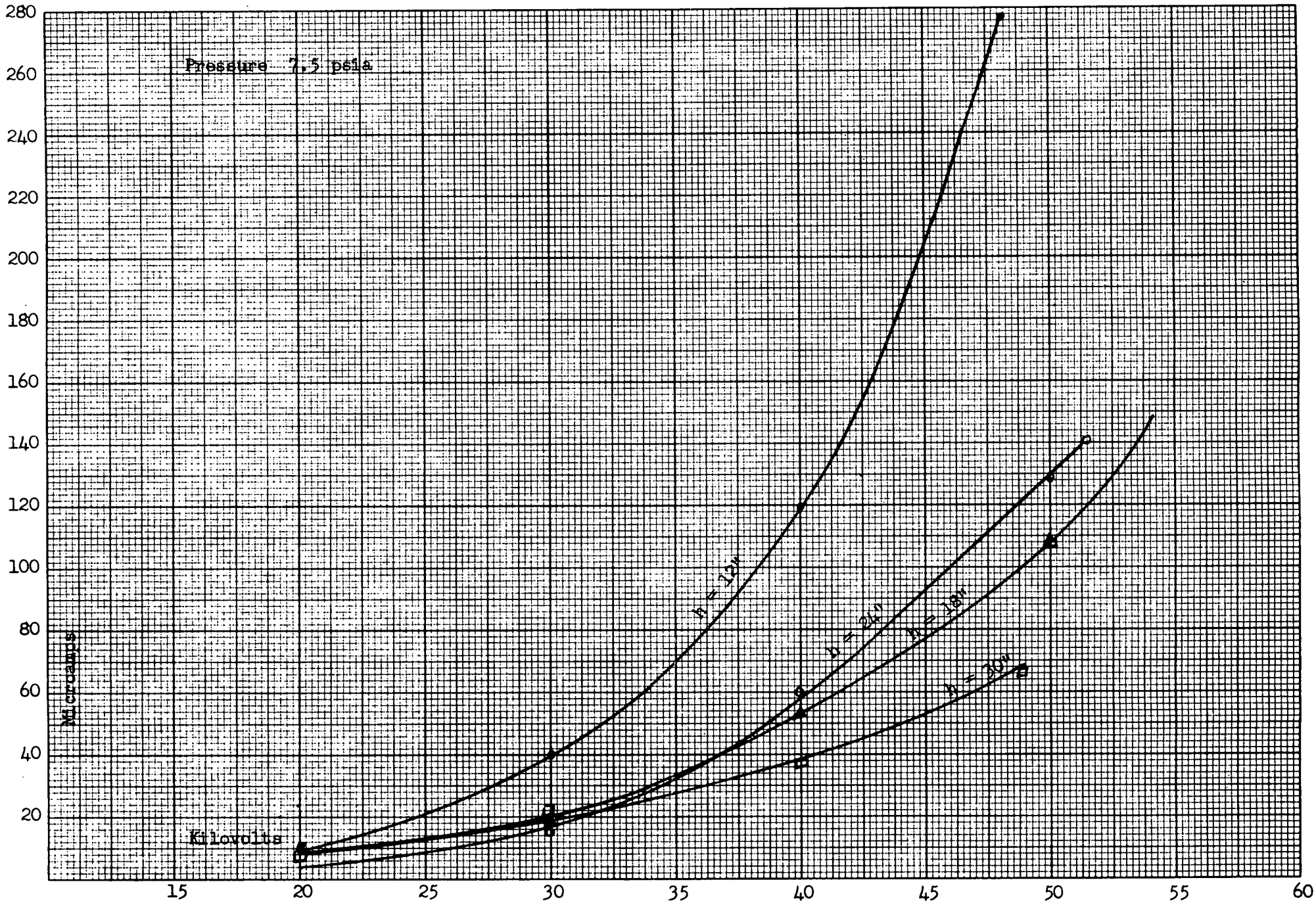

Figure 33

K+E 10 X 10 TO THE CENTIMETER 46 1510
18 X 25 CM. MADE IN U.S.A.
KEUFFEL & ESSER CO.

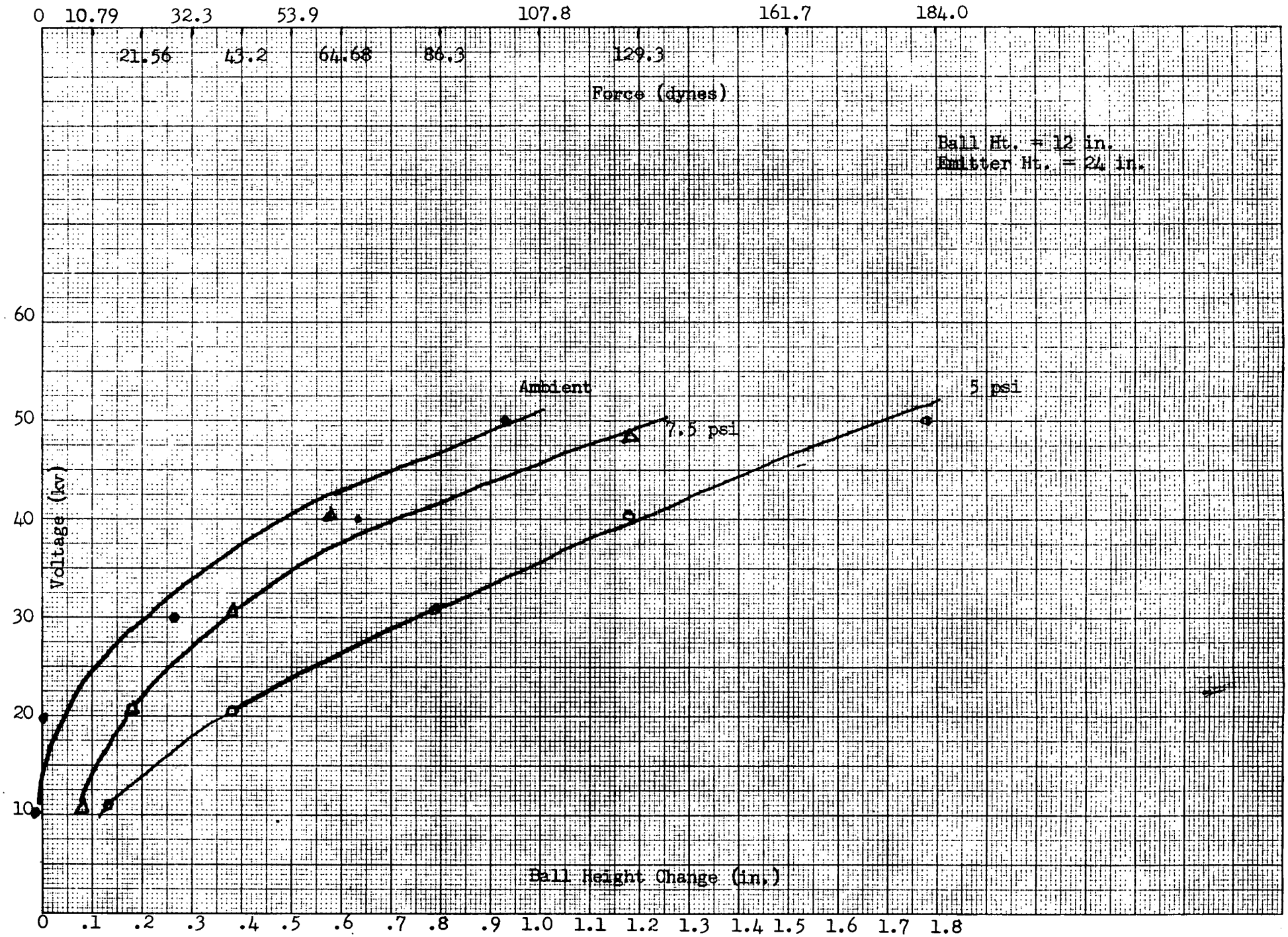

Figure 34

K+E 10 X 10 TO THE CENTIMETER 46 1510
18 X 25 CM. MADE IN U.S.A.
KEUFFEL & ESSER CO.

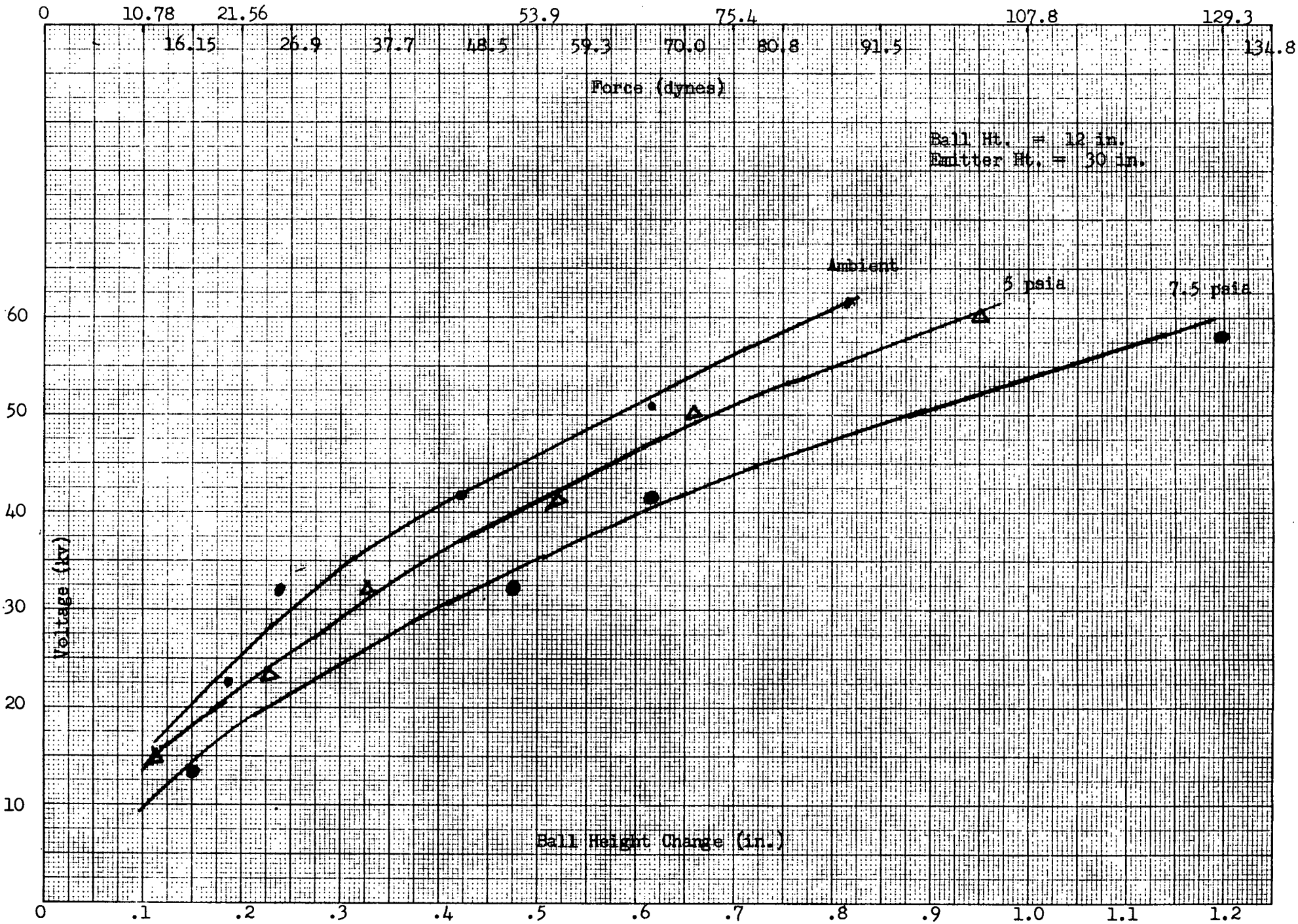

Figure 35

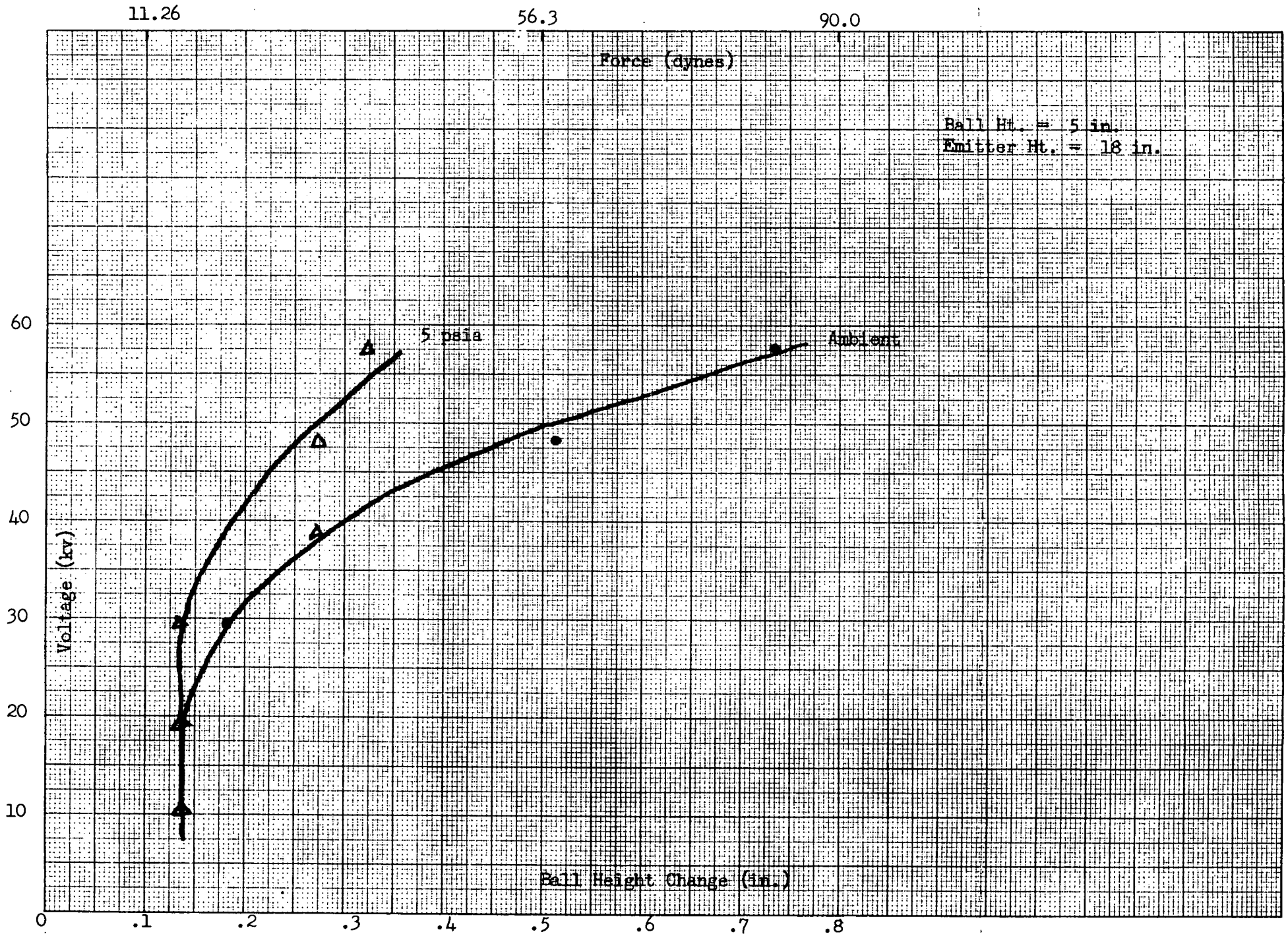
11.26
56.3
90.0
Force (dynes)
Ball Ht. = 5 in.
Emitter Ht. = 18 in.
5 psia
Ambient
Voltage (kv)
60
50
40
30
20
10
0
.1
.2
.3
.4
.5
.6
.7
.8
Ball Height Change (in.)

Figure 36

K+E 10 X 10 TO THE CENTIMETER 46 1510
18 X 25 CM. MADE IN U.S.A.
KEUFFEL & ESSER CO.

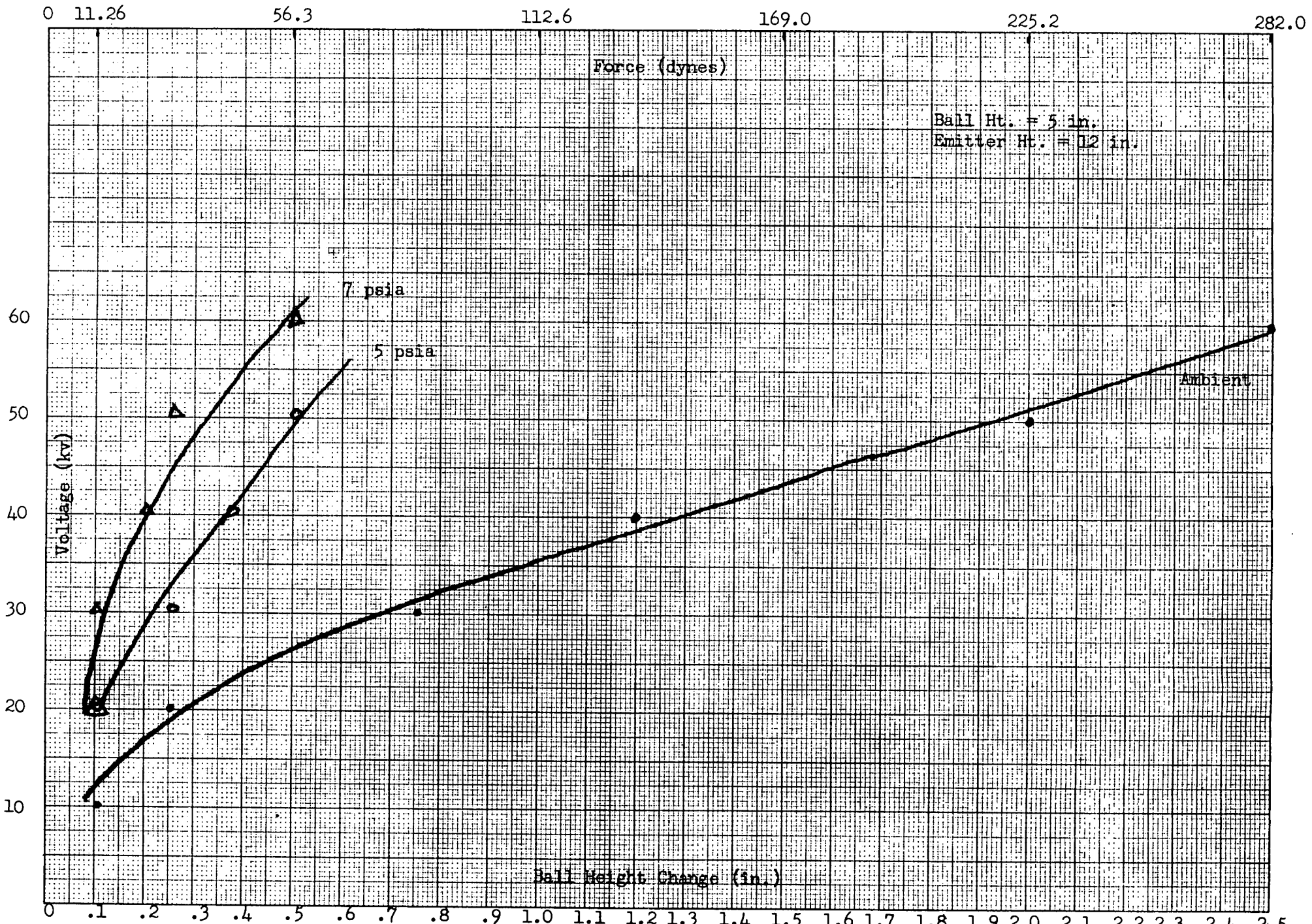

Figure 37

K+E 10 X 10 TO THE CENTIMETER 46 1510
18 X 25 CM. MADE IN U.S.A.
KEUFFEL & ESSER CO.

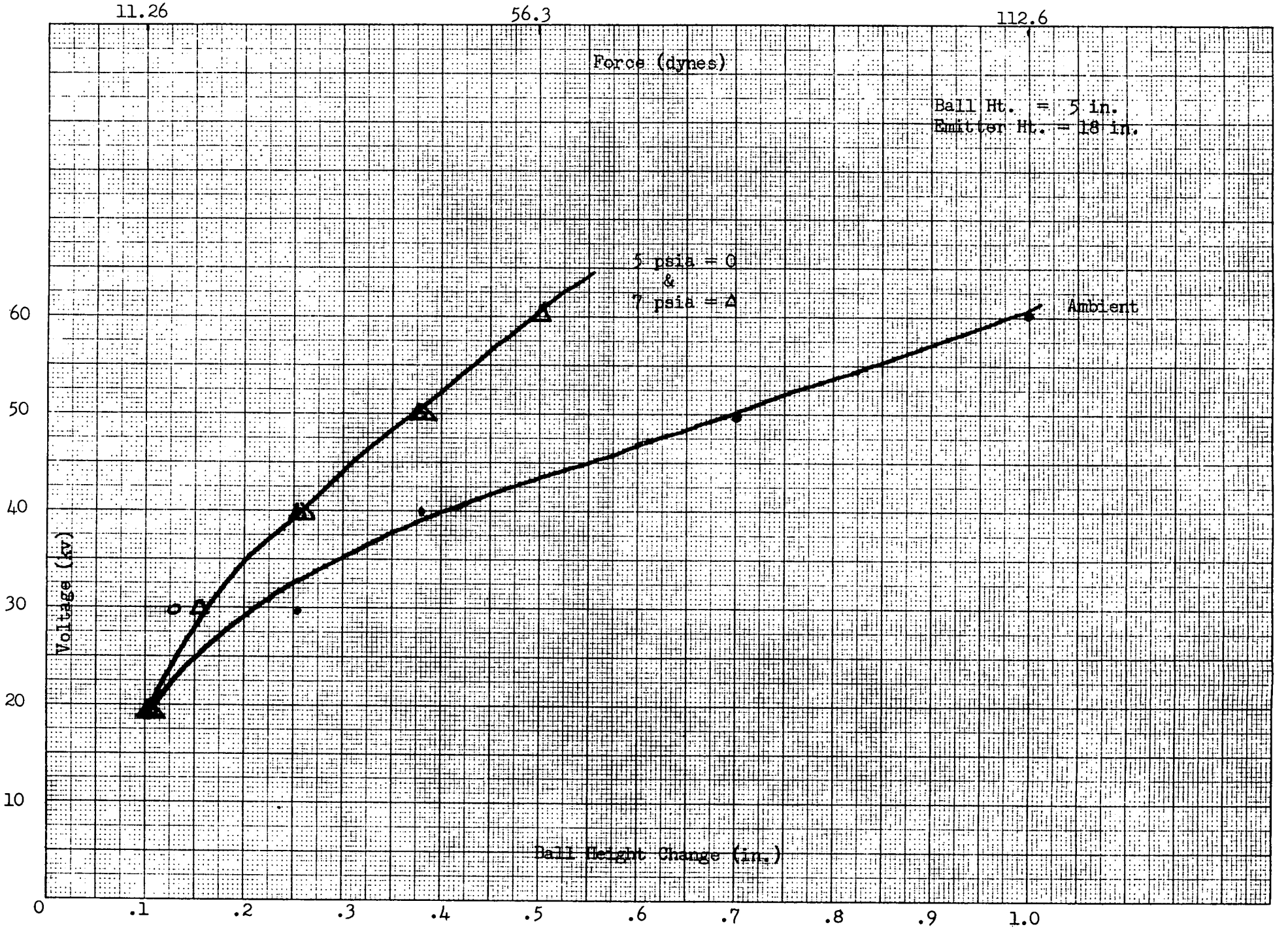

Figure 38

K+E 10 X 10 TO THE CENTIMETER 46 1510
18 X 25 CM. MADE IN U.S.A.
KEUFFEL & ESSER CO.

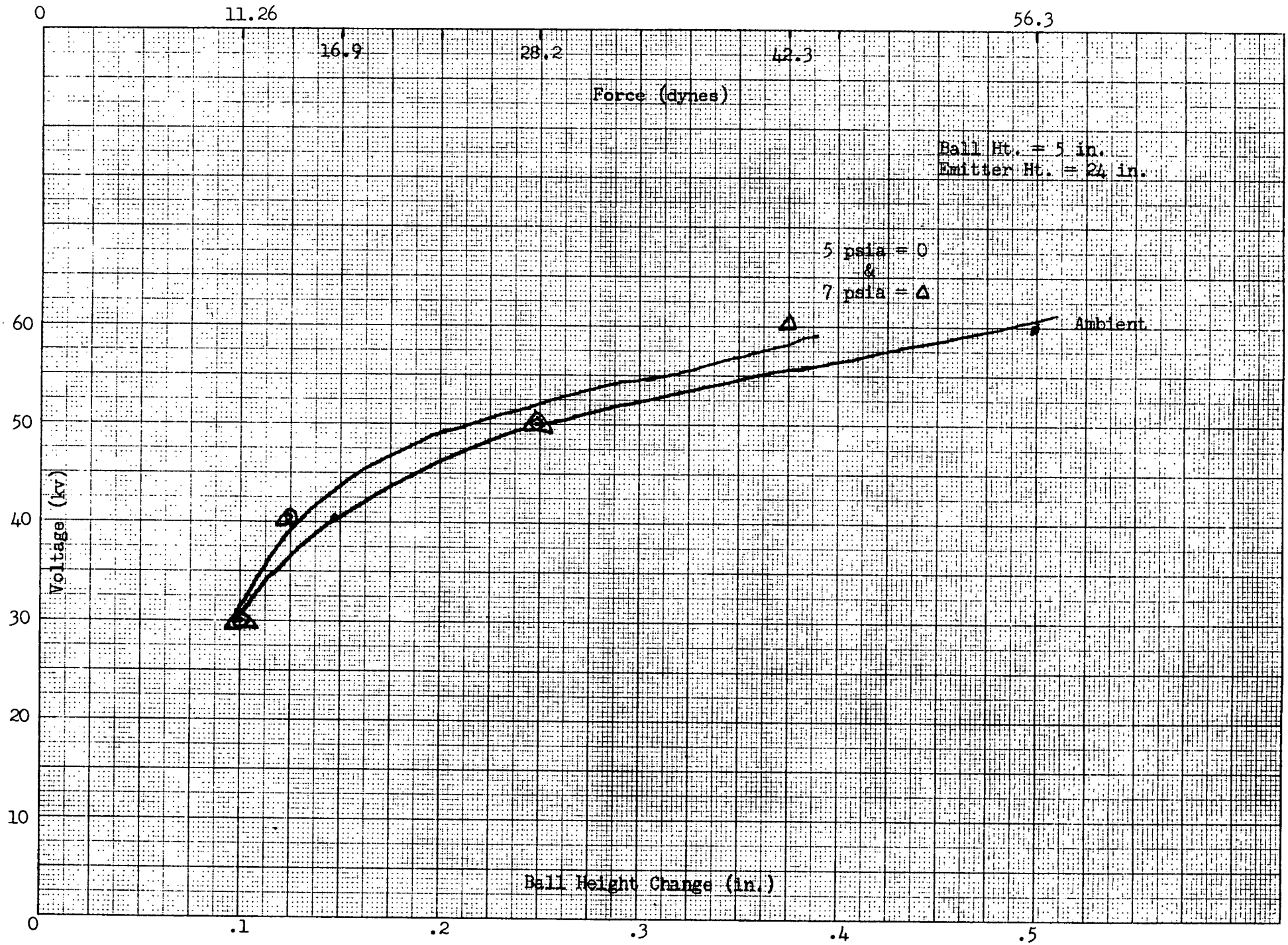

Figure 39

K+E 10 X 10 TO THE CENTIMETER 46 1540
18 X 25 CM. MADE IN U.S.A.
KEUFFEL & ESSER CO.

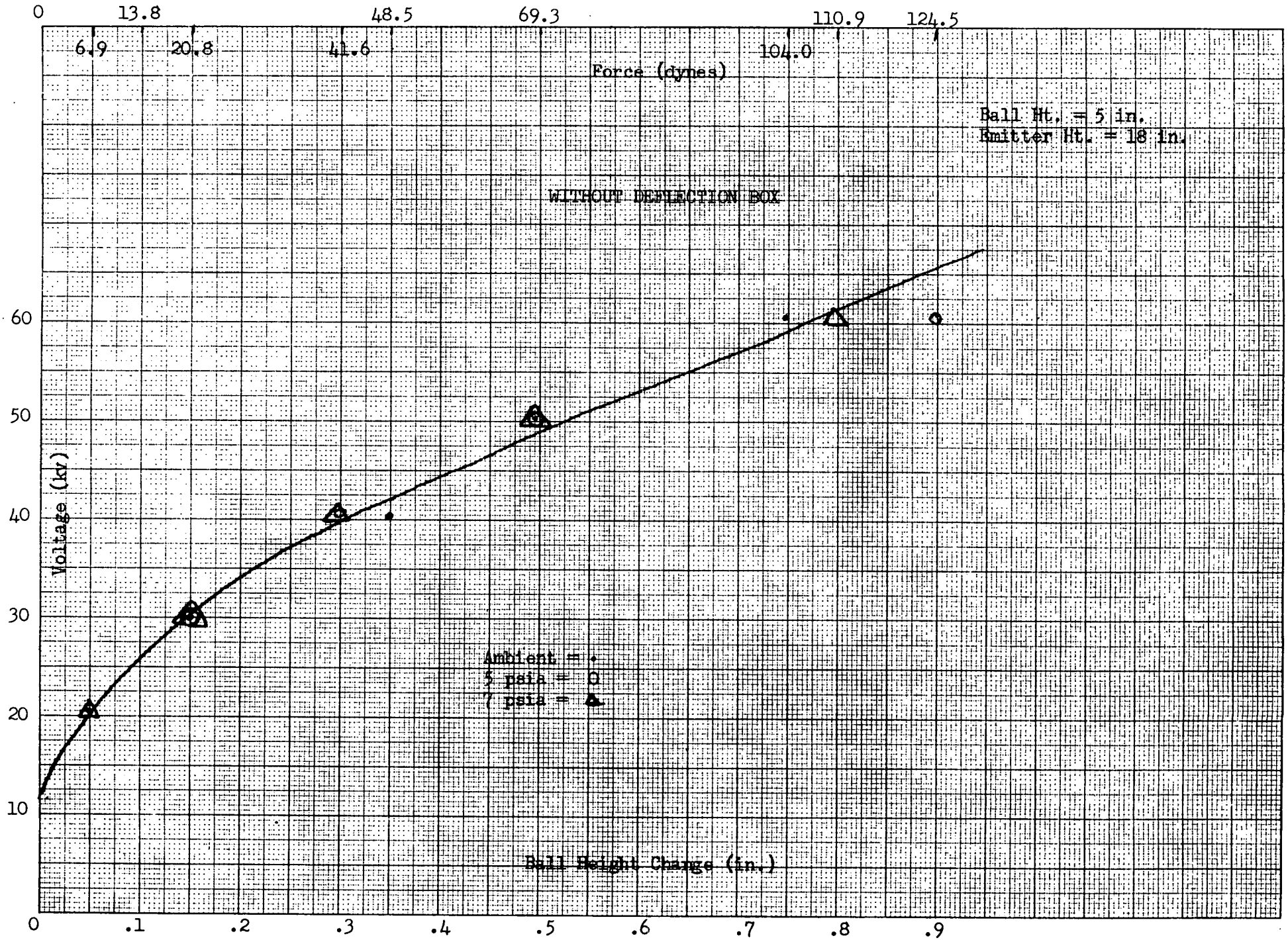

Figure 40

K+E 10 X 10 TO THE CENTIMETER 46 1510
18 X 25 CM. MADE IN U.S.A.
KEUFFEL & ESSER CO.

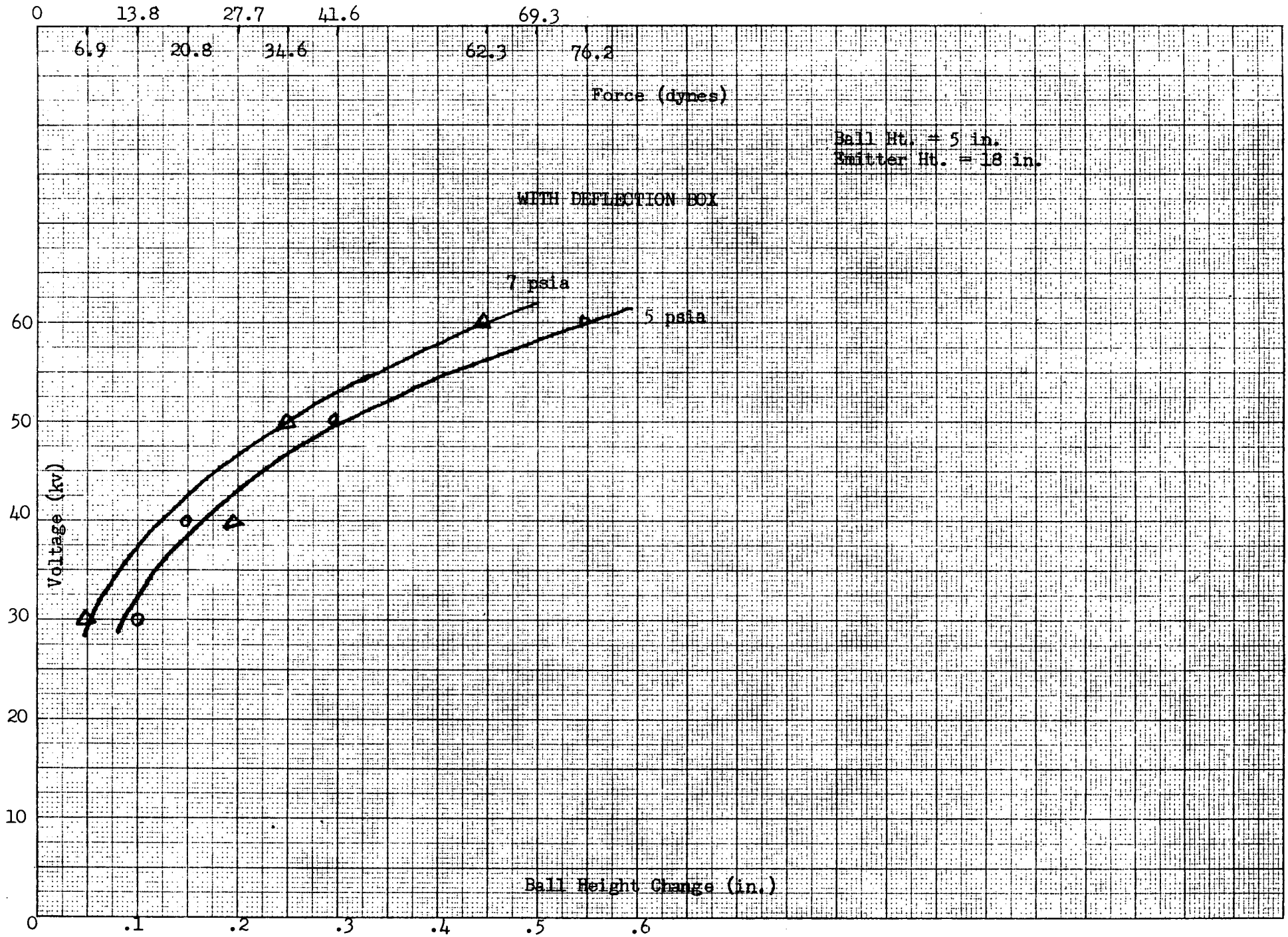

Figure 41

K+E 10 X 10 TO THE CENTIMETER 46 1510
18 X 25 CM. MADE IN U.S.A.
KEUFFEL & ESSER CO.

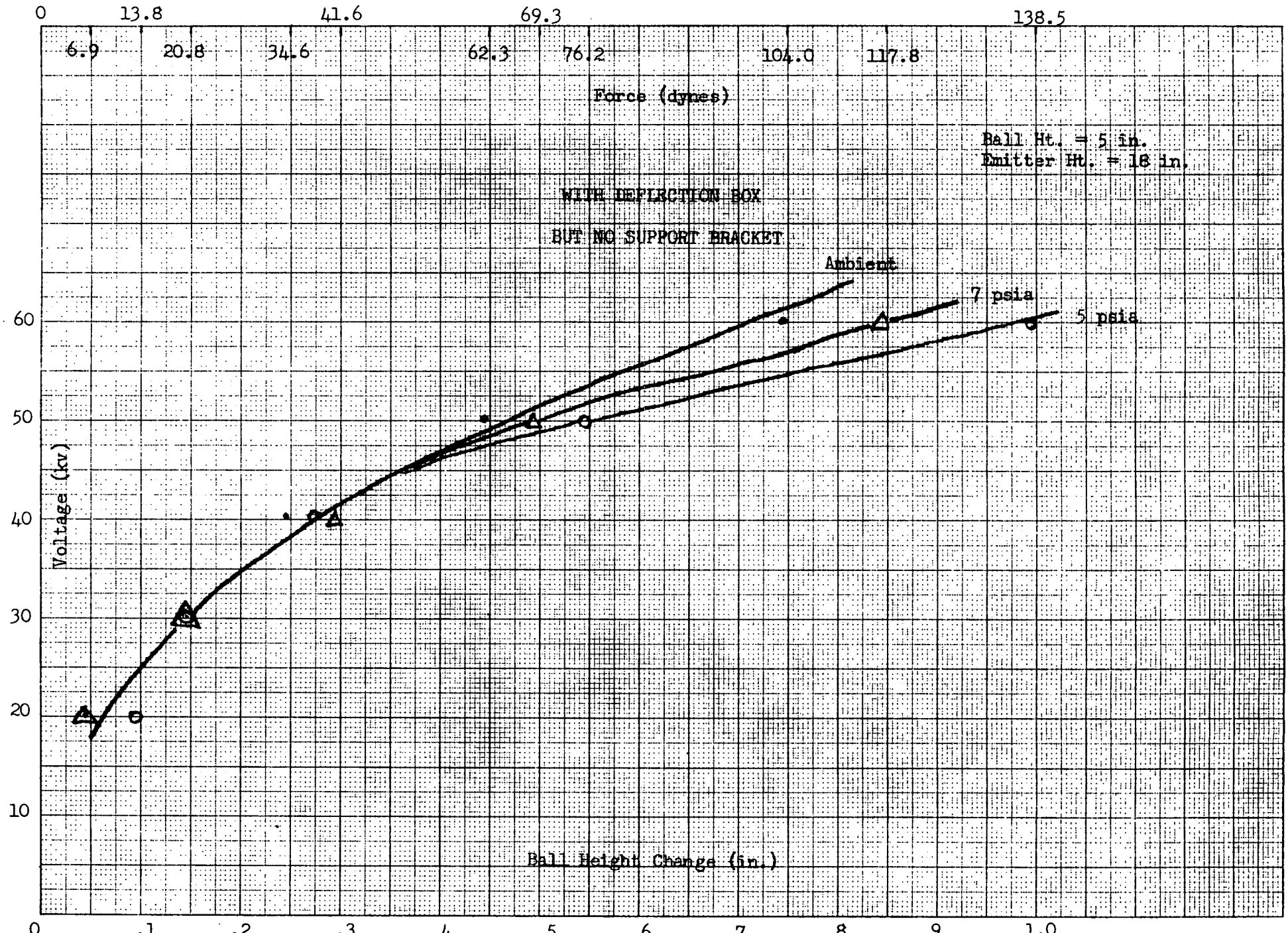

Figure 42

K+E 10 X 10 TO THE CENTIMETER 46 1510
18 X 25 CM MADE IN U.S.A.
KEUFFEL & ESSER CO.

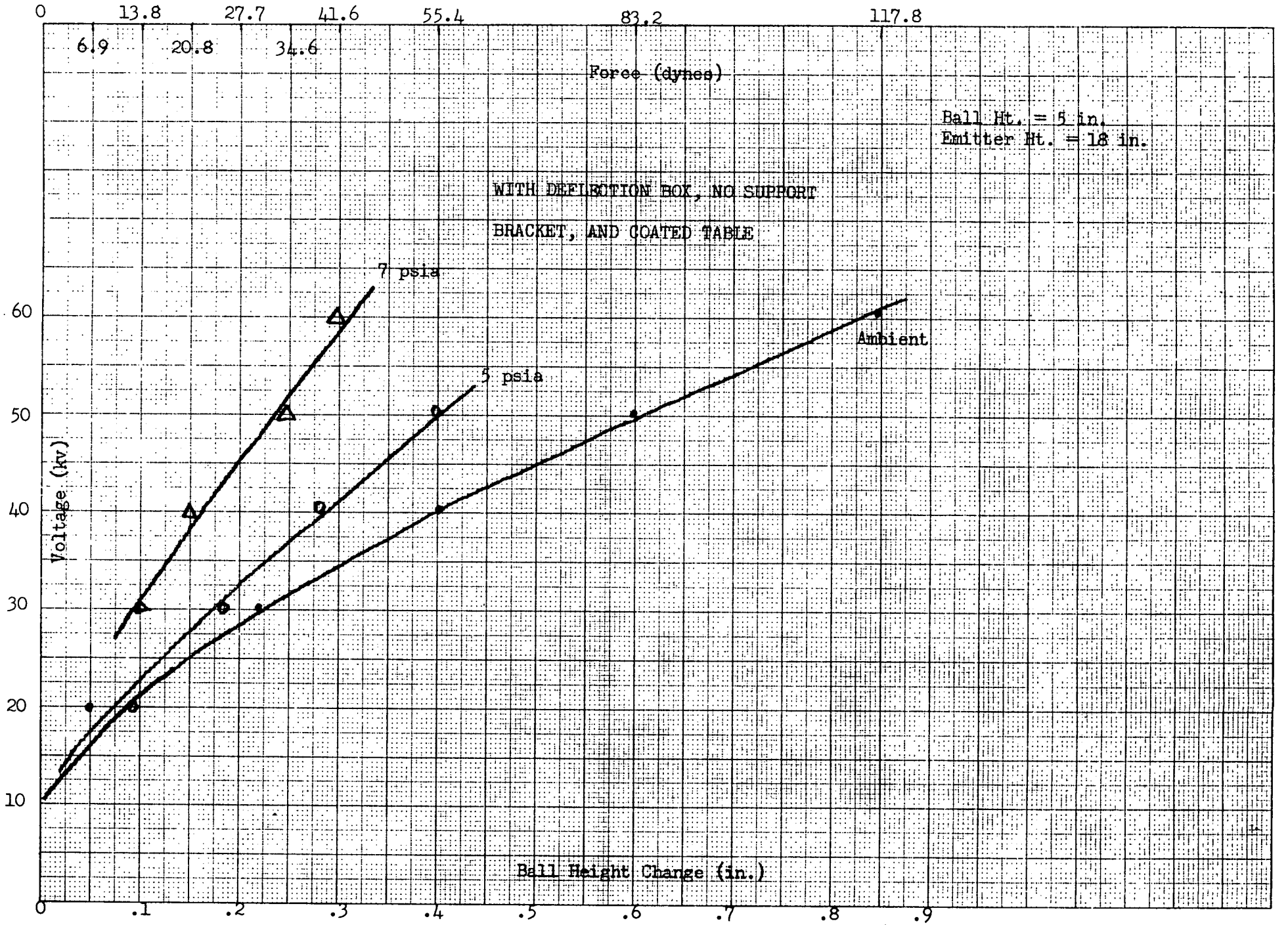

Figure 43

K+E 10 X 10 TO THE CENTIMETER 46 1510
18 X 25 CM. MADE IN U.S.A.
KEUFFEL & ESSER CO.

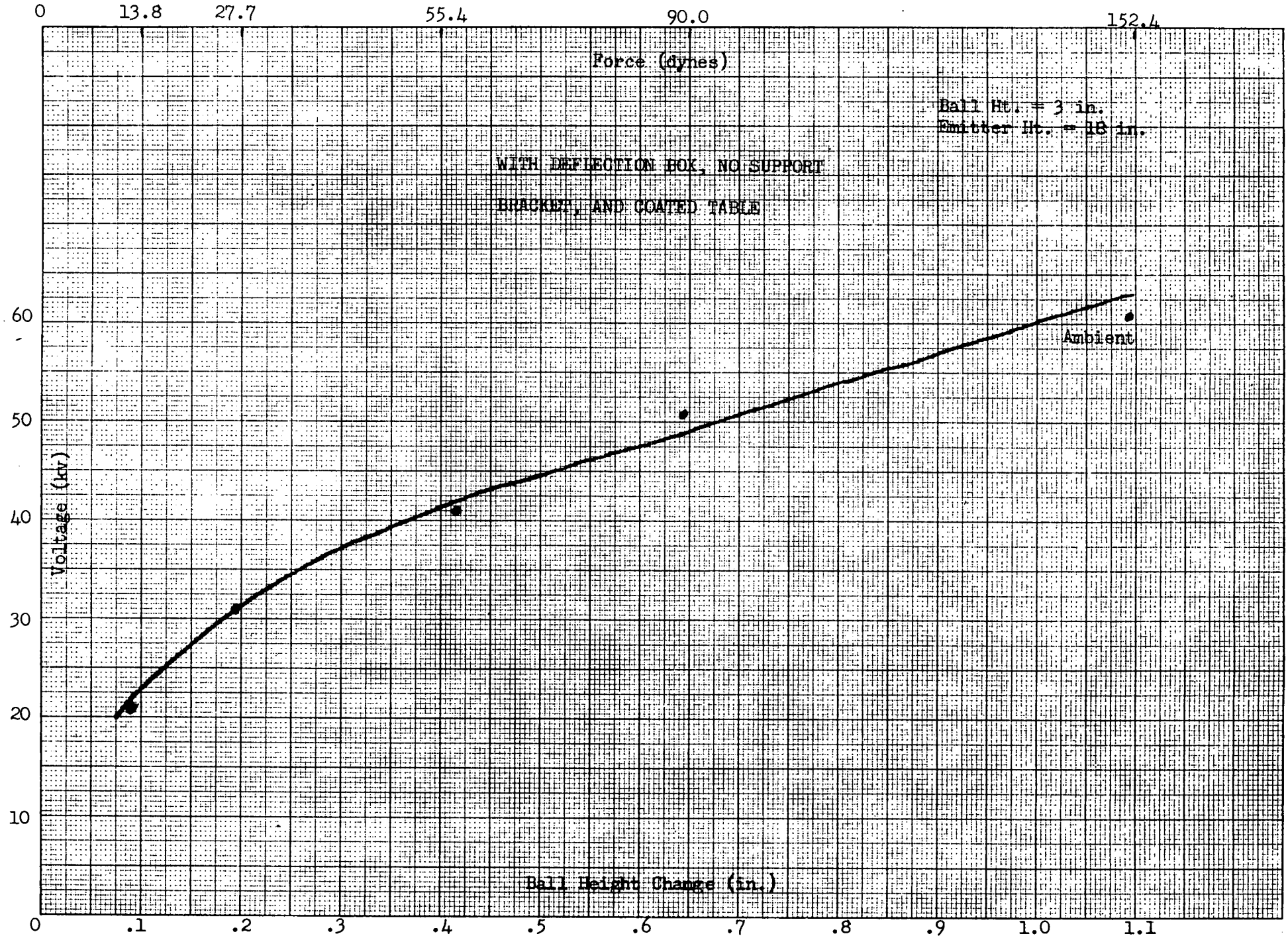

Figure 44

K+E 10 X 10 TO THE CENTIMETER 46 15.10
18 X 25 CM MADE IN U.S.A.
KEUFFEL & ESSER CO.

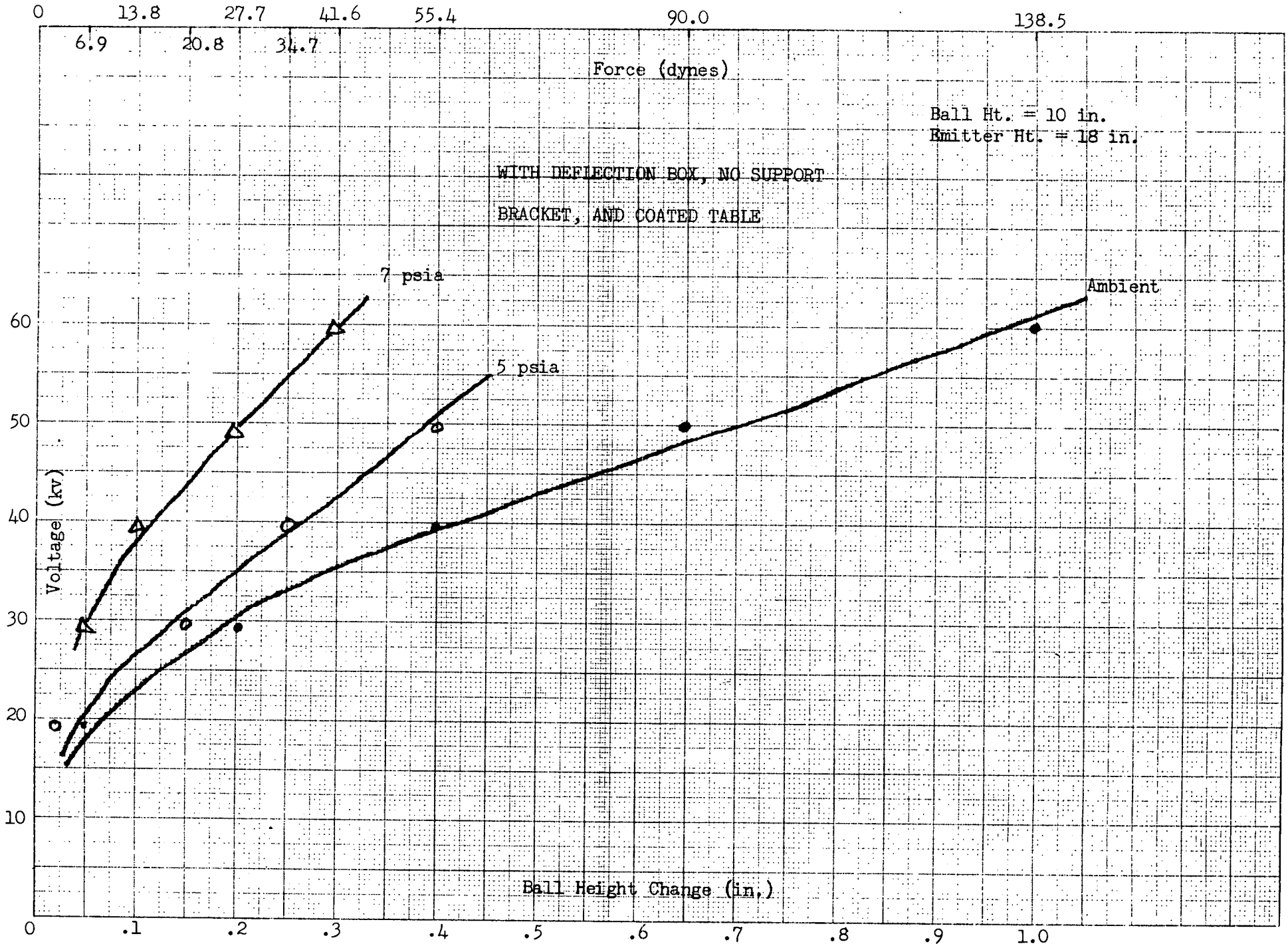

Figure 45

K+E 10 X 10 TO THE CENTIMETER 46 1540
18 X 25 CM MADE IN U.S.A.
KEUFFEL & ESSER CO.

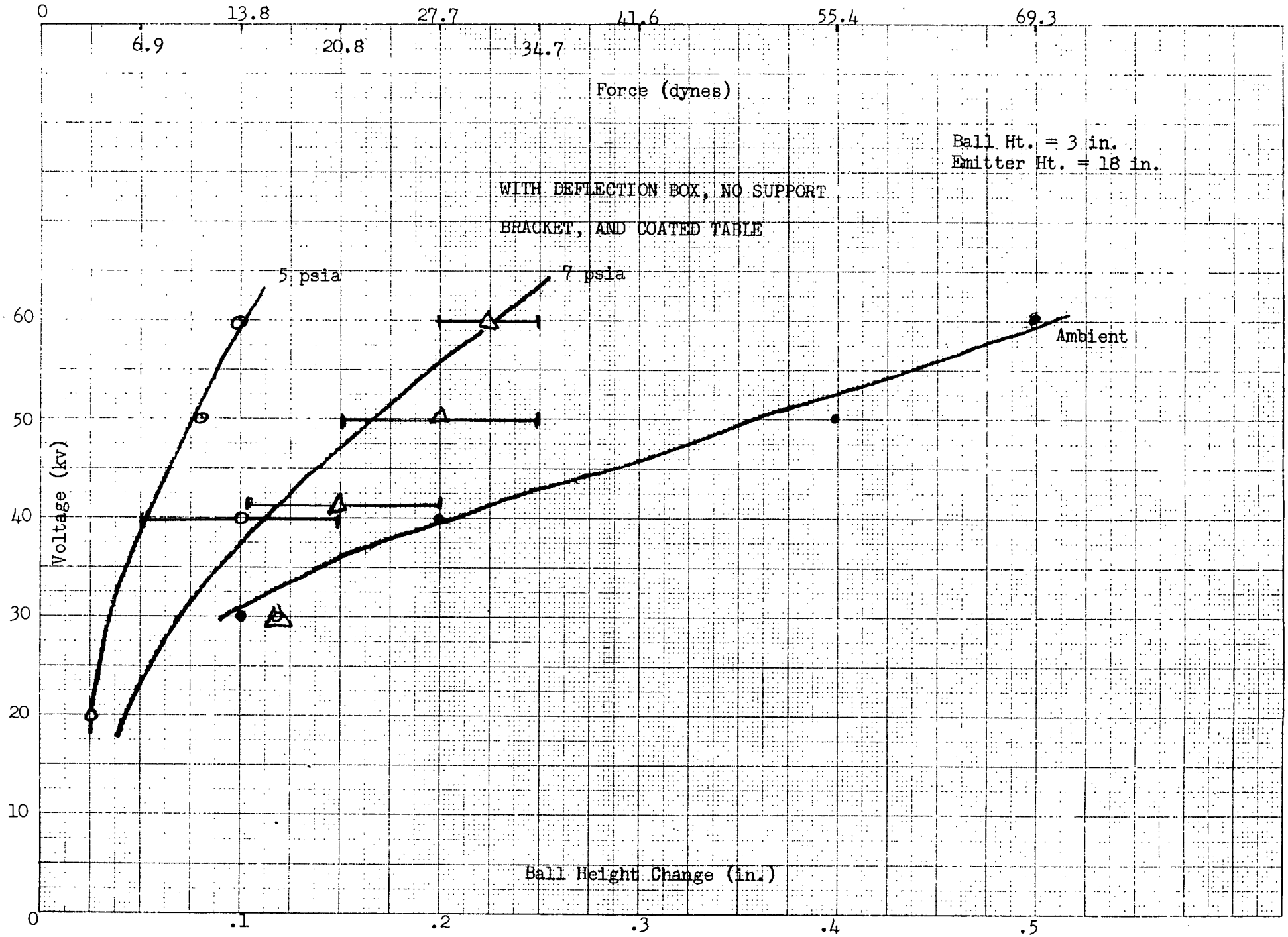

Figure 46

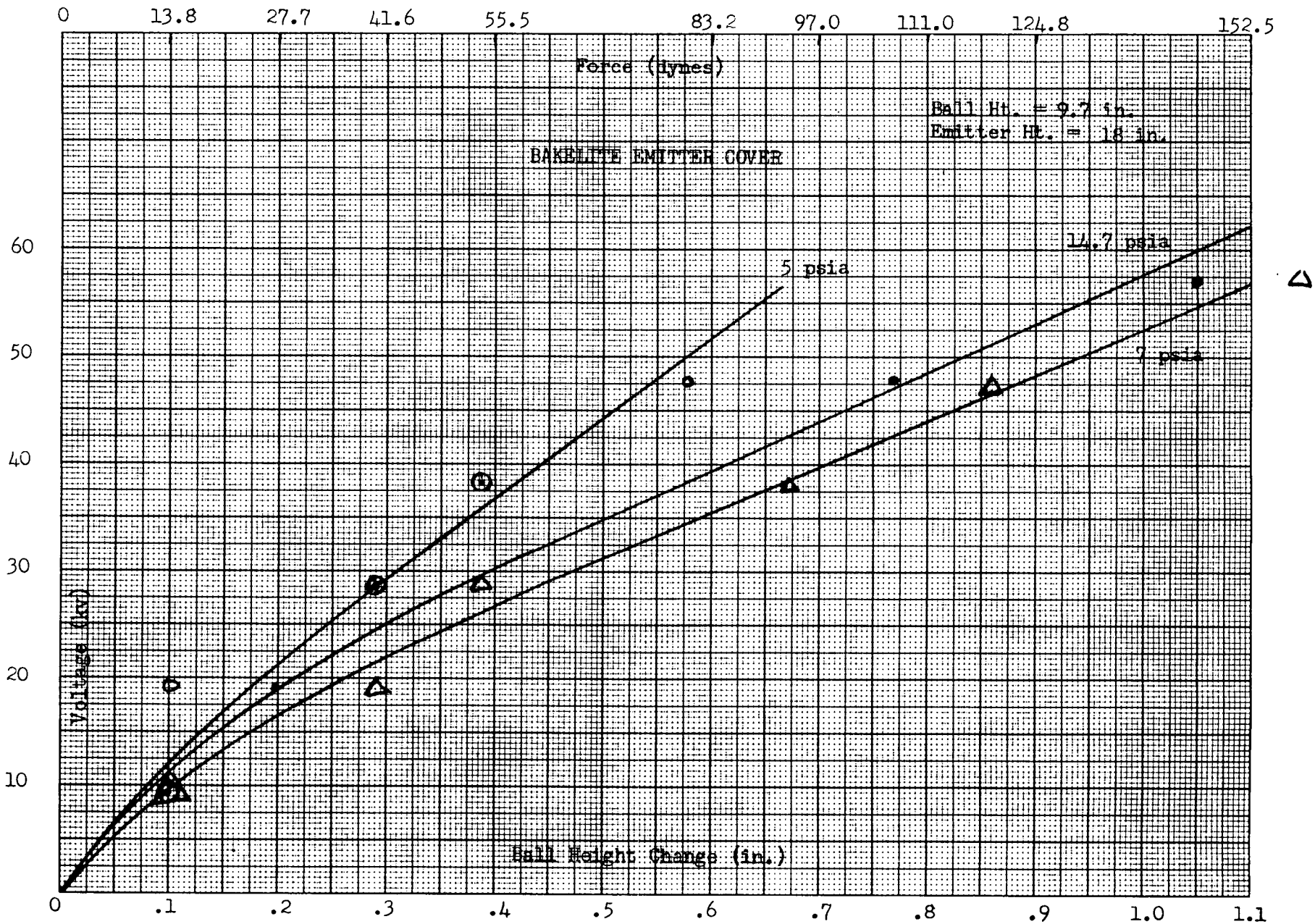
0
13.8
27.7
41.6
55.5
83.2
97.0
111.0
124.8
152.5
Force (dynes)
Ball Ht. = 9.7 in.
Emitter Ht. = 18 in.
BAKELITE EMITTER COVER
14.7 psia
5 psia
7 psia
60
50
40
30
20
10
Voltage (kv)
Ball Height Change (in.)
0
.1
.2
.3
.4
.5
.6
.7
.8
.9
1.0
1.1

Figure 47

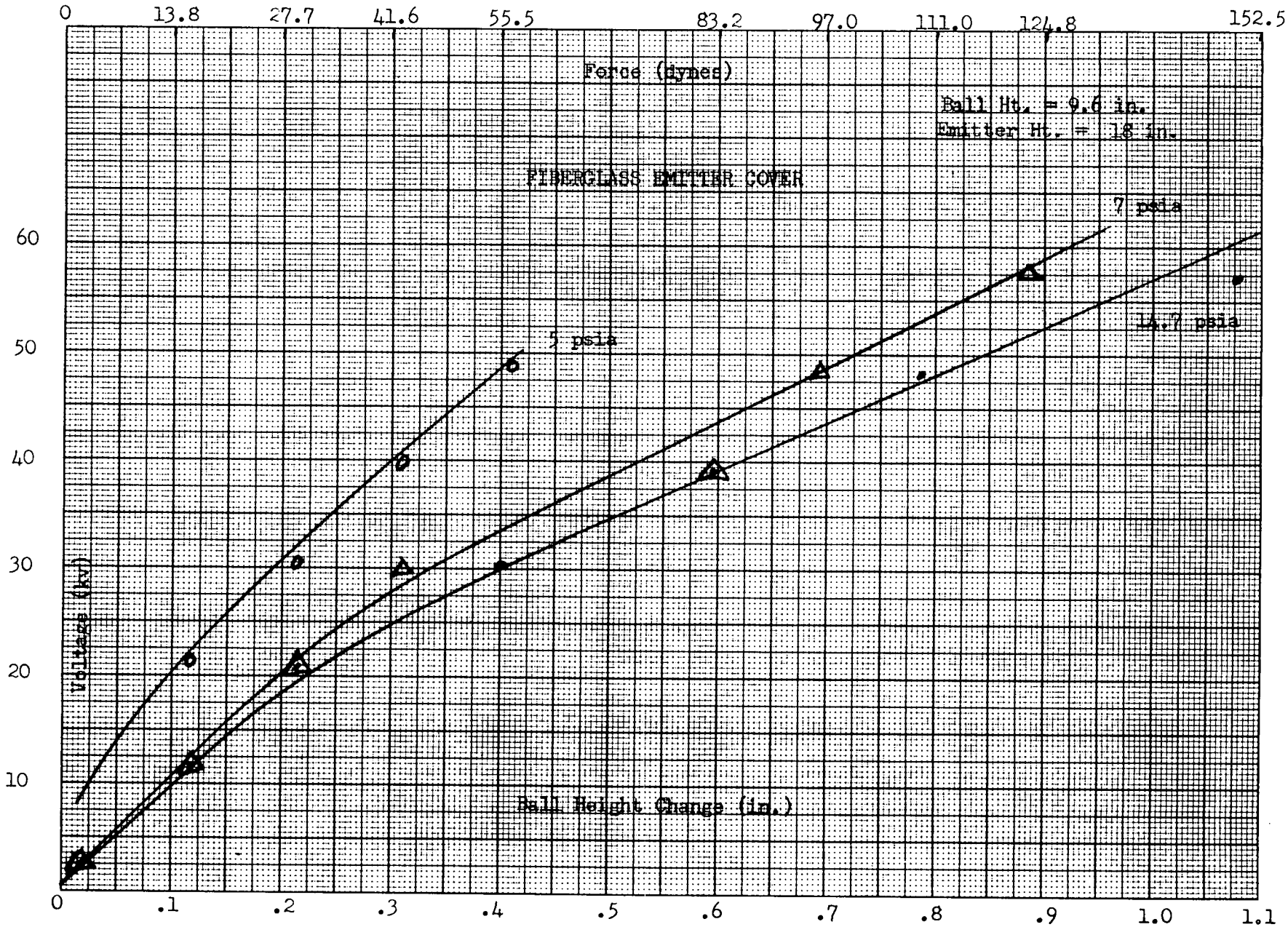
0
13.8
27.7
41.6
55.5
83.2
97.0
111.0
124.8
152.5
Force (dynes)
Ball Ht. = 9.6 in.
Emitter Ht. = 18 in.
FIBERGLASS EMITTER COVER
7 psia
5 psia
14.7 psia
60
50
40
30
20
10
Voltage (kv)
Ball Height Change (in.)
0
.1
.2
.3
.4
.5
.6
.7
.8
.9
1.0
1.1

Figure 48

K+E 10 X 10 TO THE CENTIMETER 46 1510
18 X 25 CM. MADE IN U.S.A.
KEUFFEL & ESSER CO.

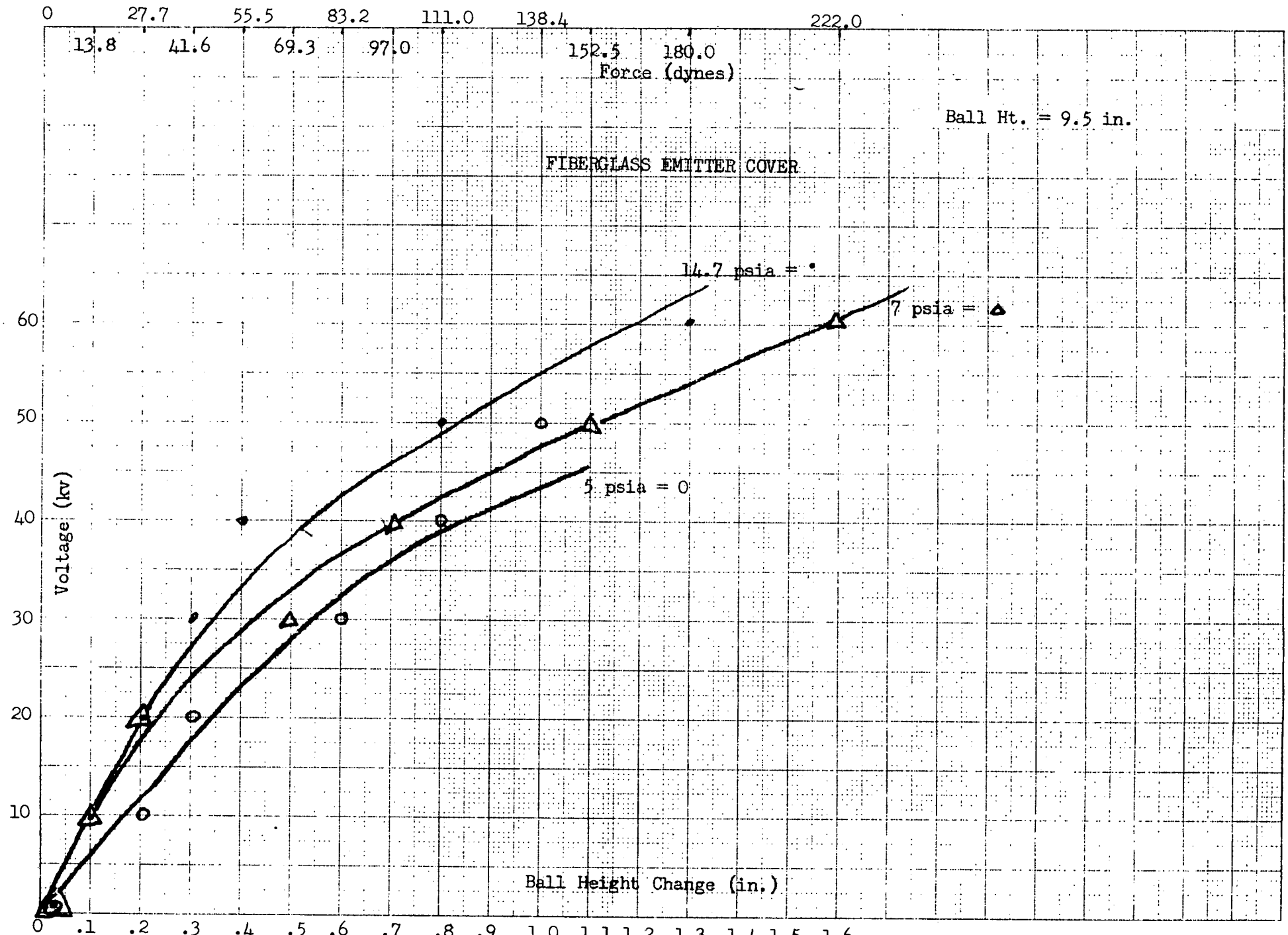

Figure 49

K+E 10 X 10 TO THE CENTIMETER 46 1510
13 X 25 CM MADE IN U.S.A.
KEUFFEL & ESSER CO.

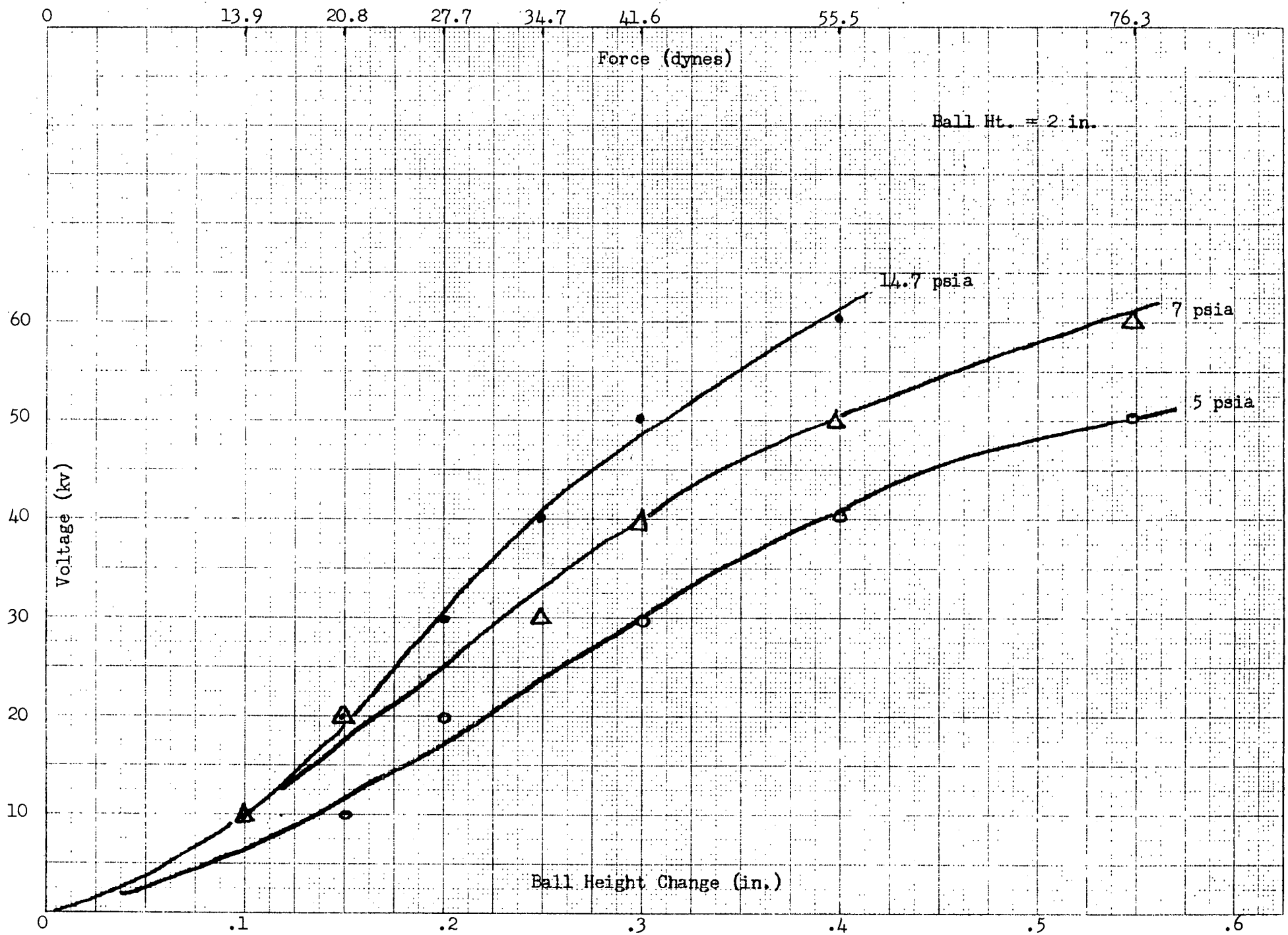

Figure 50

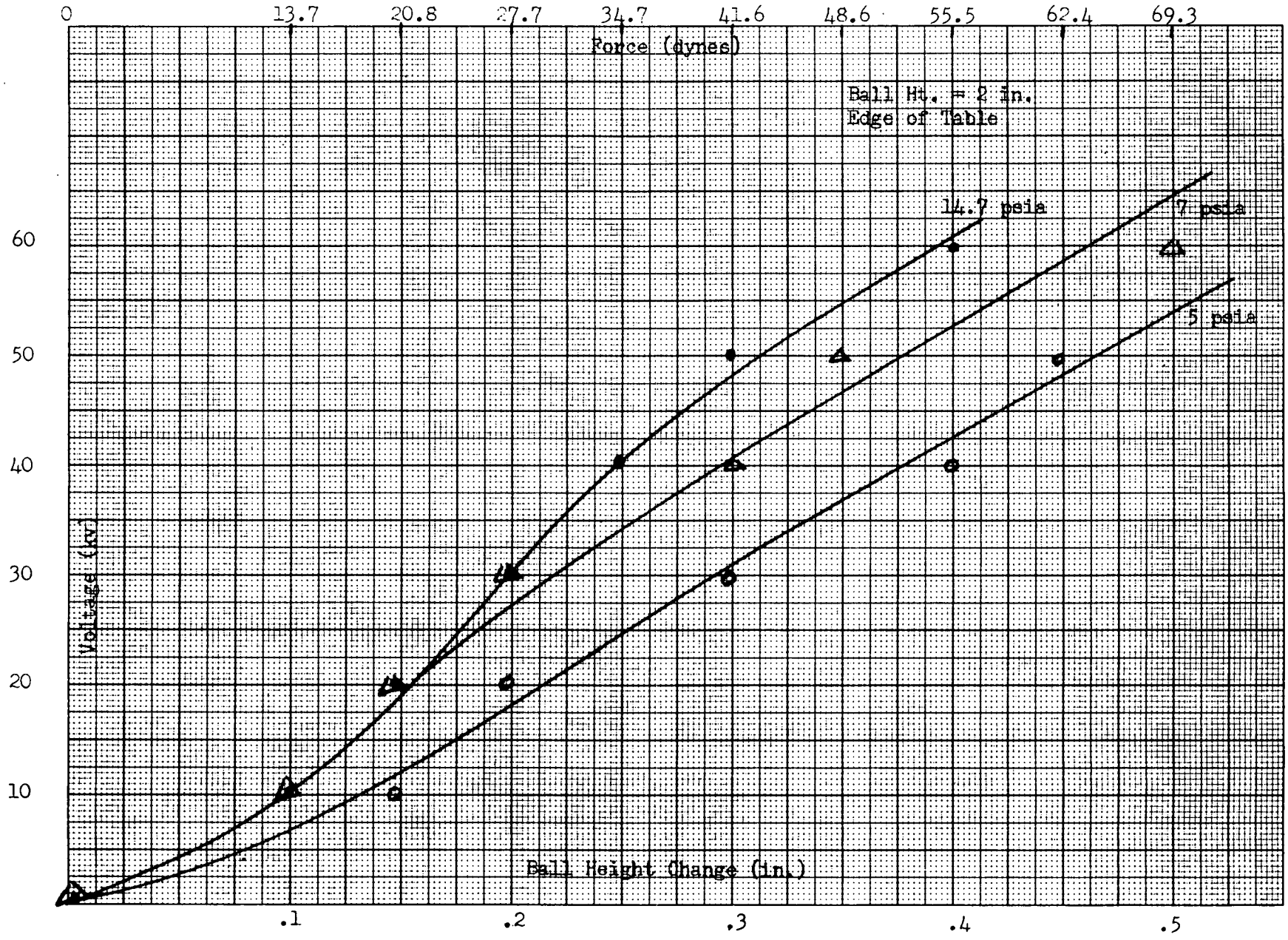
0
13.7
20.8
27.7
34.7
41.6
48.6
55.5
62.4
69.3
Force (dynes)
Ball Ht. = 2 in.
Edge of Table
14.7 psia
7 psia
5 psia
60
50
40
30
20
10
Voltage (kv)
Ball Height Change (in.)
.1
.2
.3
.4
.5

Figure 51

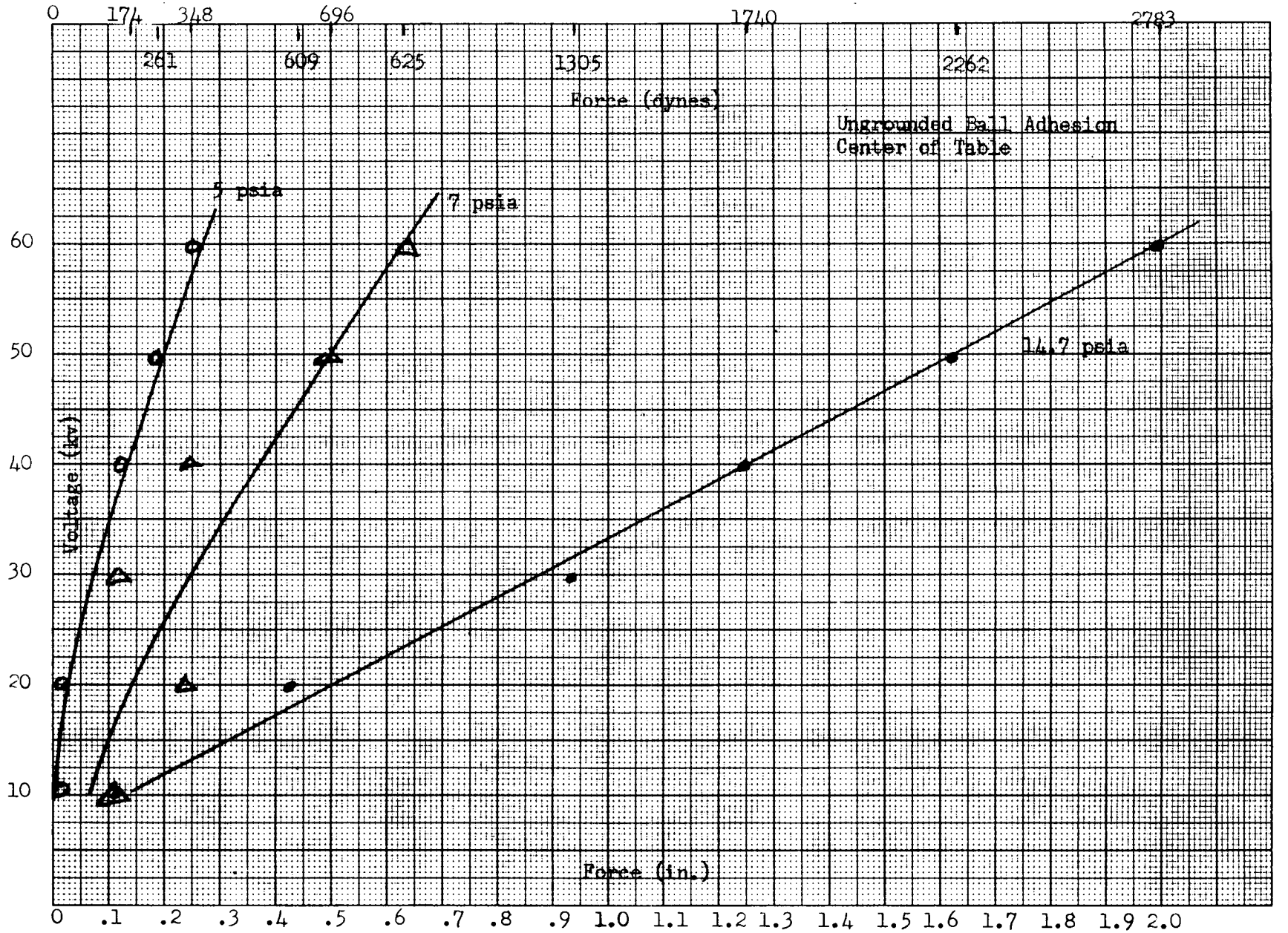
0
174
348
696
1740
2783
261
609
625
1305
2262
Force (dynes)
Ungrounded Ball Adhesion
Center of Table
5 psia
7 psia
14.7 psia
60
50
40
30
20
10
Voltage (kv)
Force (in.)
0
.1
.2
.3
.4
.5
.6
.7
.8
.9
1.0
1.1
1.2
1.3
1.4
1.5
1.6
1.7
1.8
1.9
2.0

Figure 52

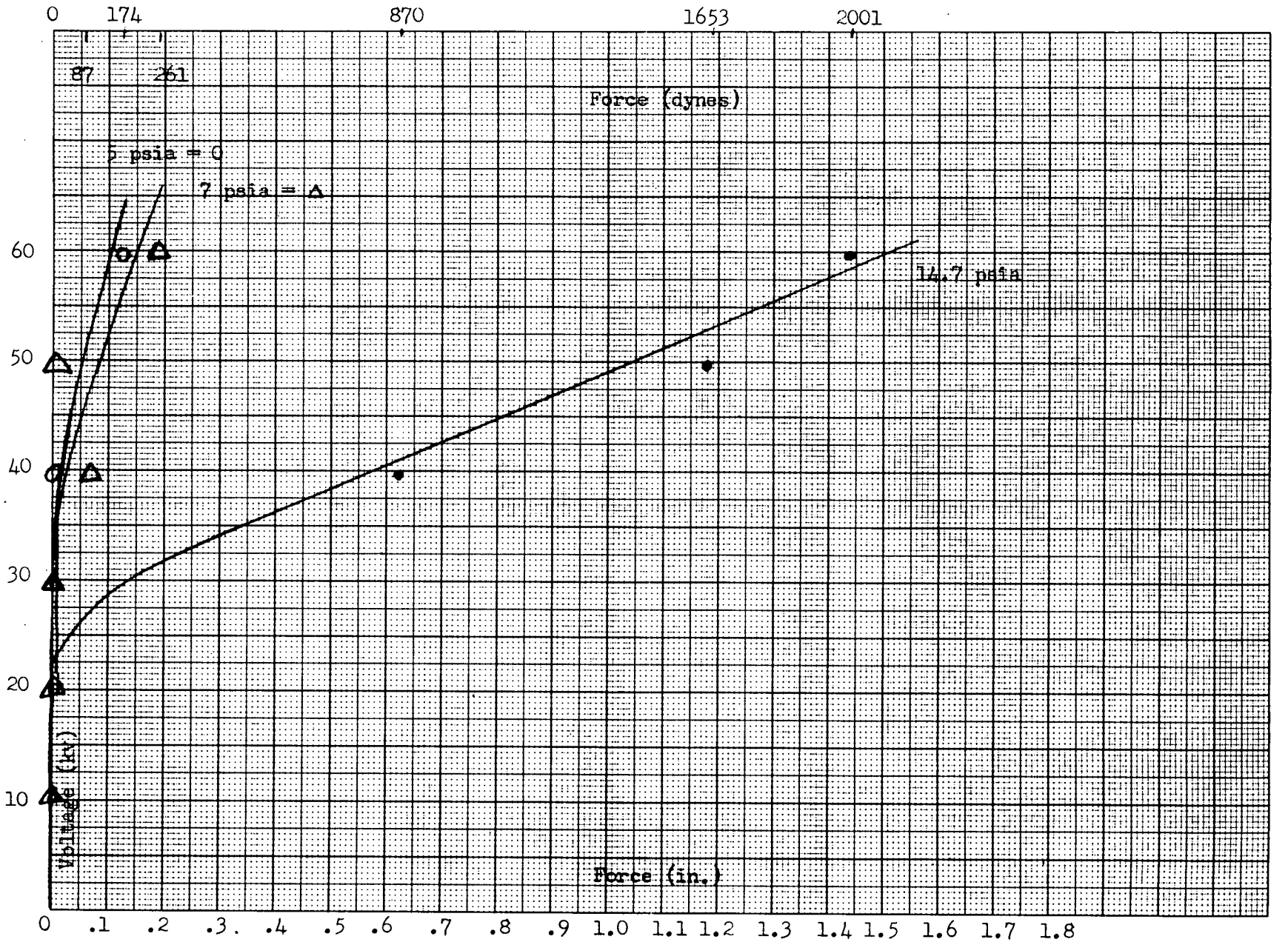

Figure 53

CLEARPRINT PAPER CO. NO. C38 MILLIMETERS BOTH WAYS 100 X 250 DIVISIONS:
PRINTED IN U.S.A. ON CLEARPRINT TECHNICAL PAPER NO. 1012

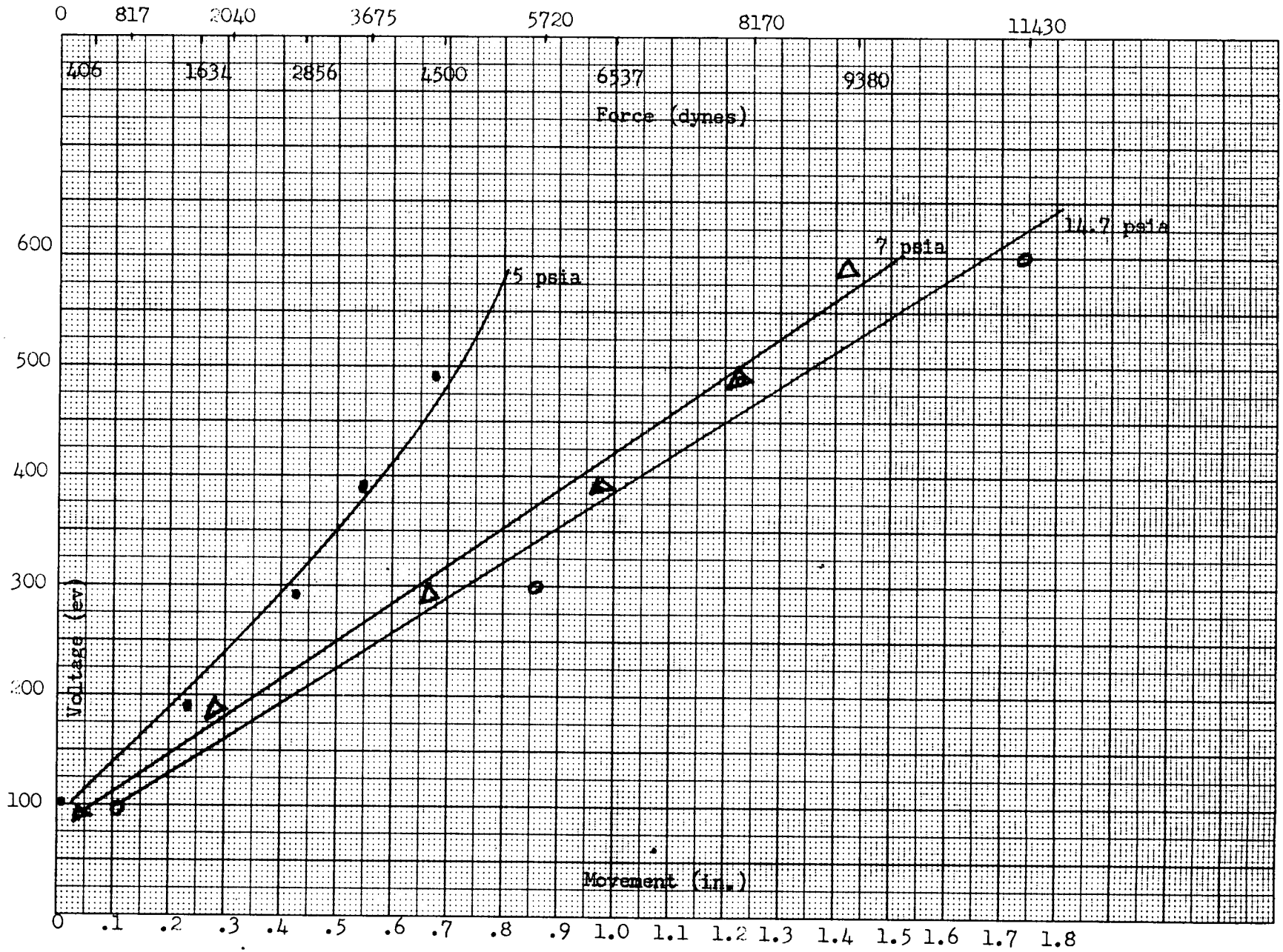
0
817
2040
3675
5720
8170
11430
406
1634
2856
4500
6537
9380
Force (dynes)
600
500
400
300
200
100
Voltage (ev)
5 psia
7 psia
14.7 psia
Movement (in.)
0
.1
.2
.3
.4
.5
.6
.7
.8
.9
1.0
1.1
1.2
1.3
1.4
1.5
1.6
1.7
1.8

Figure 54

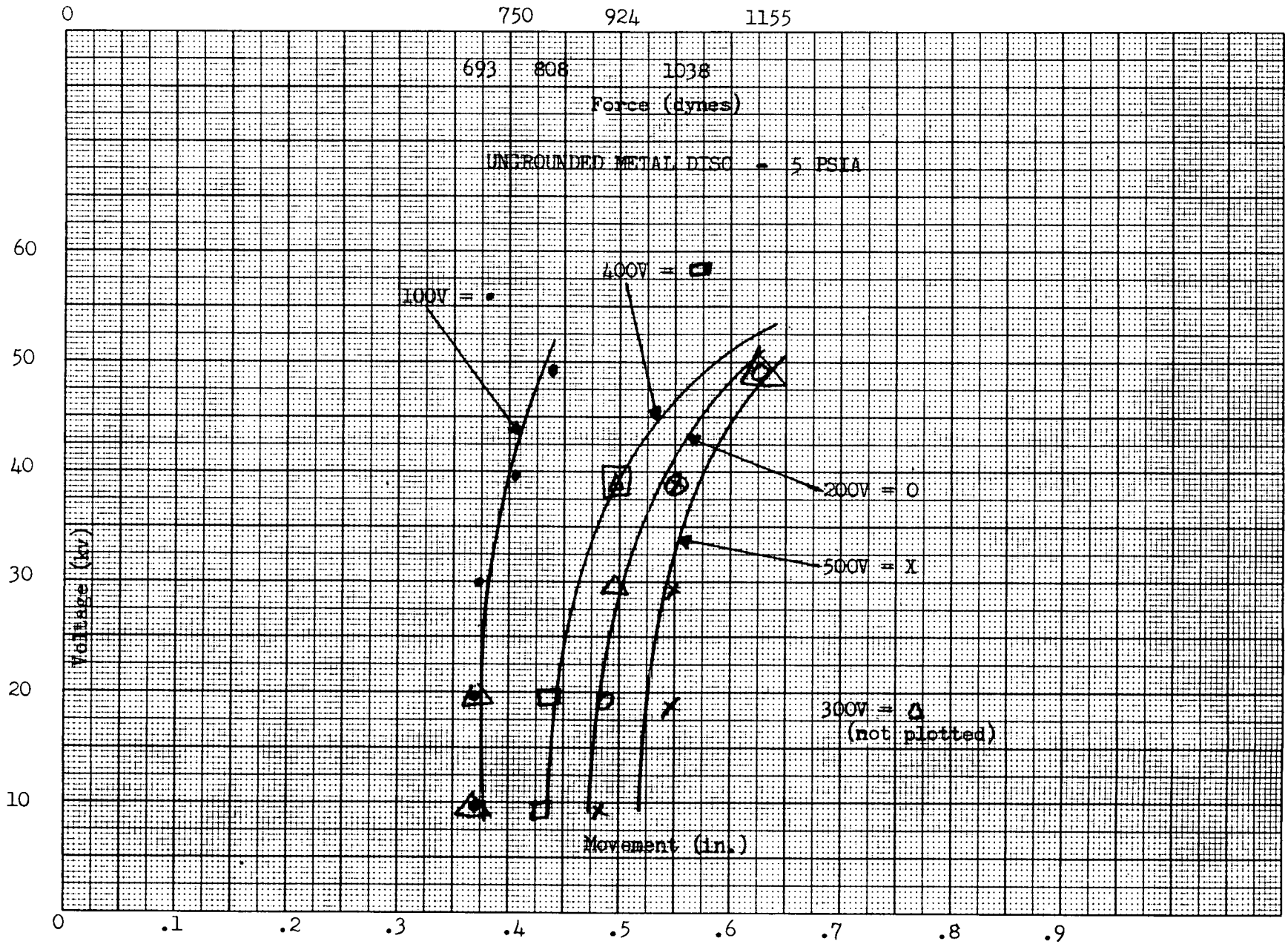
0
750
924
1155
693
808
1038
Force (dynes)
UNGROUNDED METAL DISC - 5 PSIA
60
50
40
30
20
10
100V = •
400V = □
200V = O
500V = X
300V = △
(not plotted)
Voltage (kV)
Movement (in.)
0
.1
.2
.3
.4
.5
.6
.7
.8
.9

Figure 55

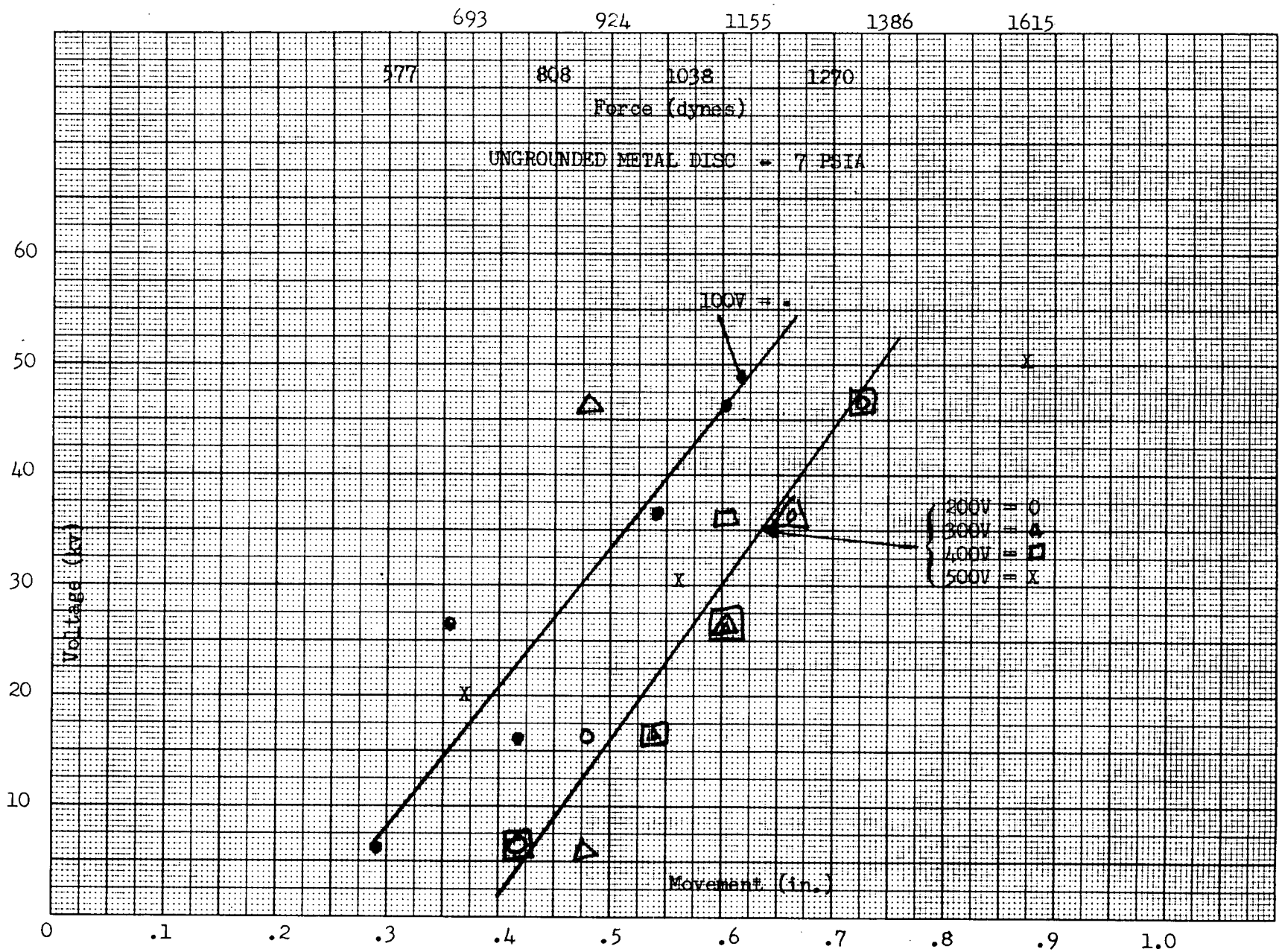

Figure 56

CLEARPRINT PAPER CO. NO. C98 MILLIMETERS BOTH WAYS 180 X 250 DIVISIONS
PRINTED IN U.S.A. ON CLEARPRINT TECHNICAL PAPER NO. 1015

K+E 10 X 10 TO THE CENTIMETER 46 1510
10 X 25 CM. MADE IN U.S.A.
KEUFFEL & ESSER CO.

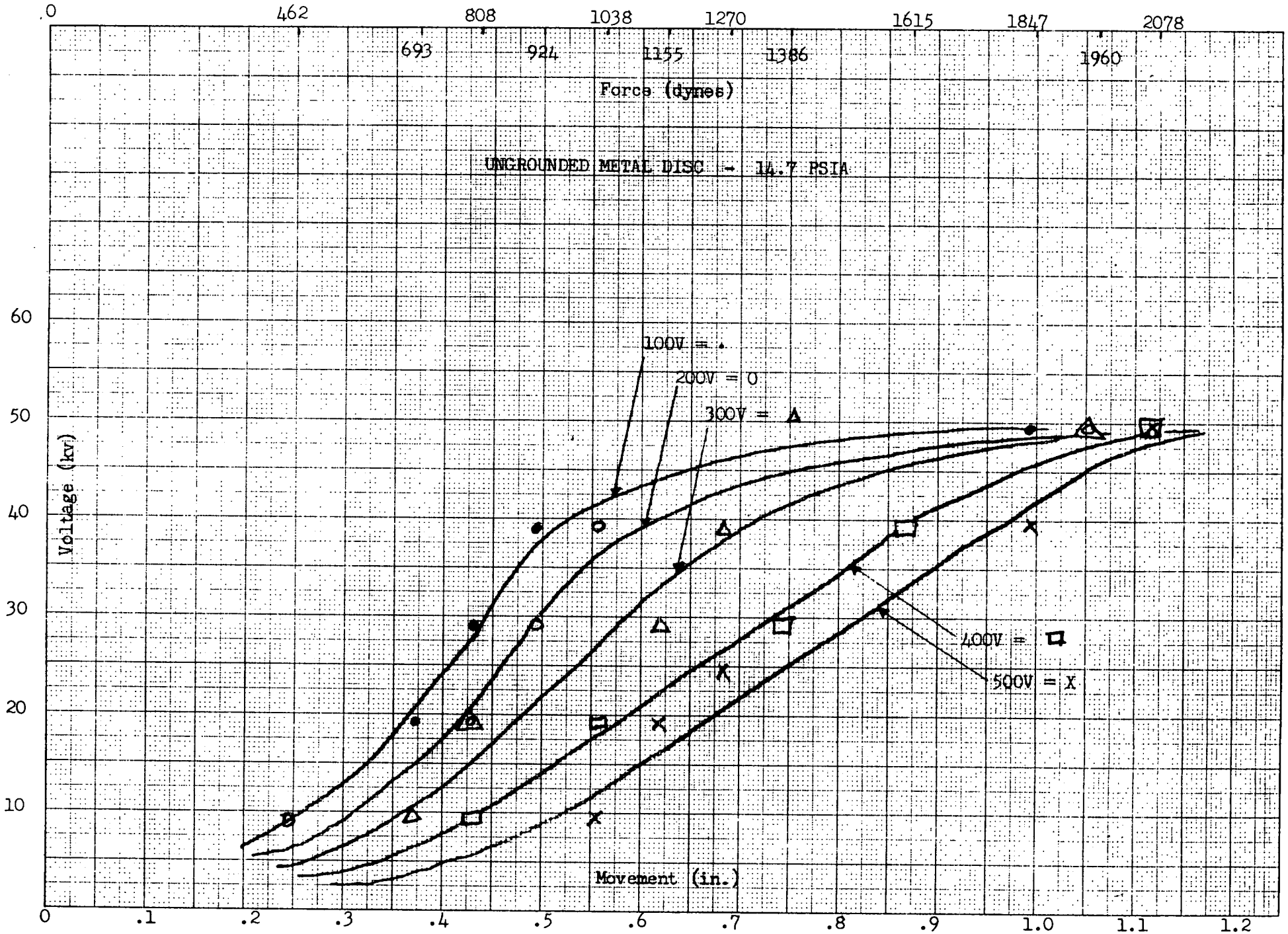

Figure 57

K+E 10 X 10 TO THE CENTIMETER 46 1510
18 X 25 CM. MADE IN U.S.A.
KEUFFEL & ESSER CO.

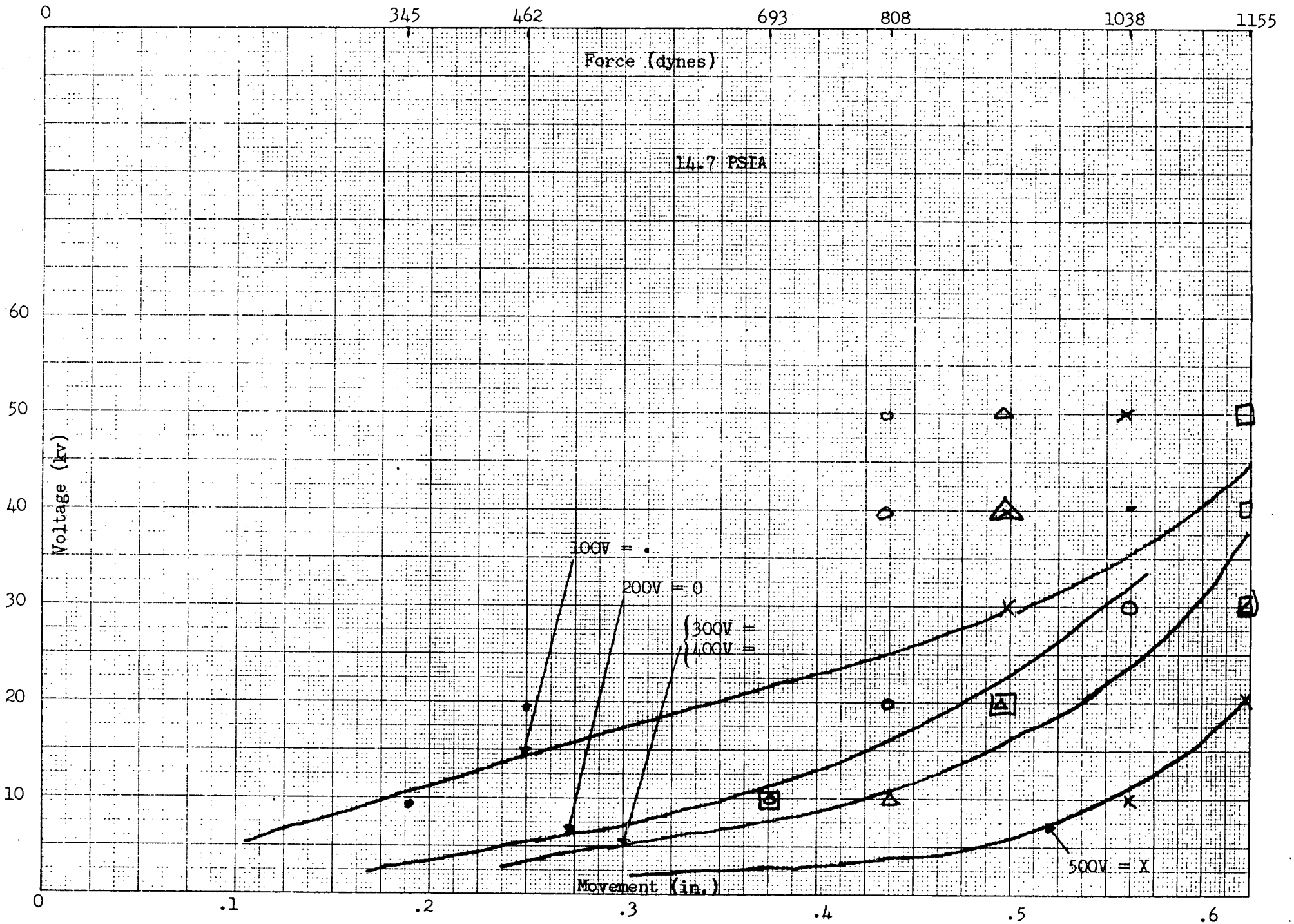

Figure 58

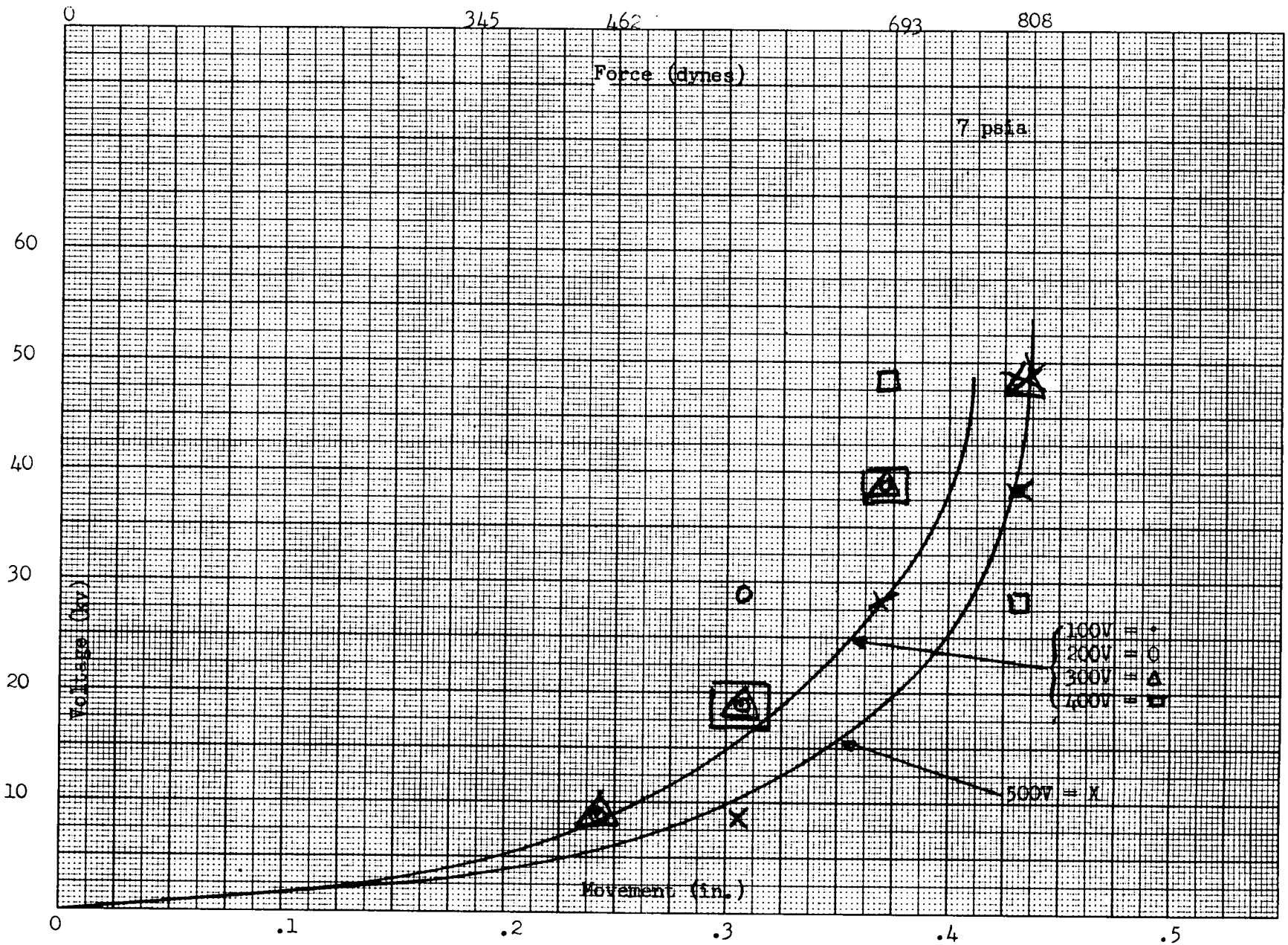
0
345
462
693
808
Force (dynes)
7 psia
60
50
40
30
20
10
Voltage (kv)
100V = •
200V = O
300V = Δ
400V = □
500V = X
Movement (in.)
0
.1
.2
.3
.4
.5

Figure 59

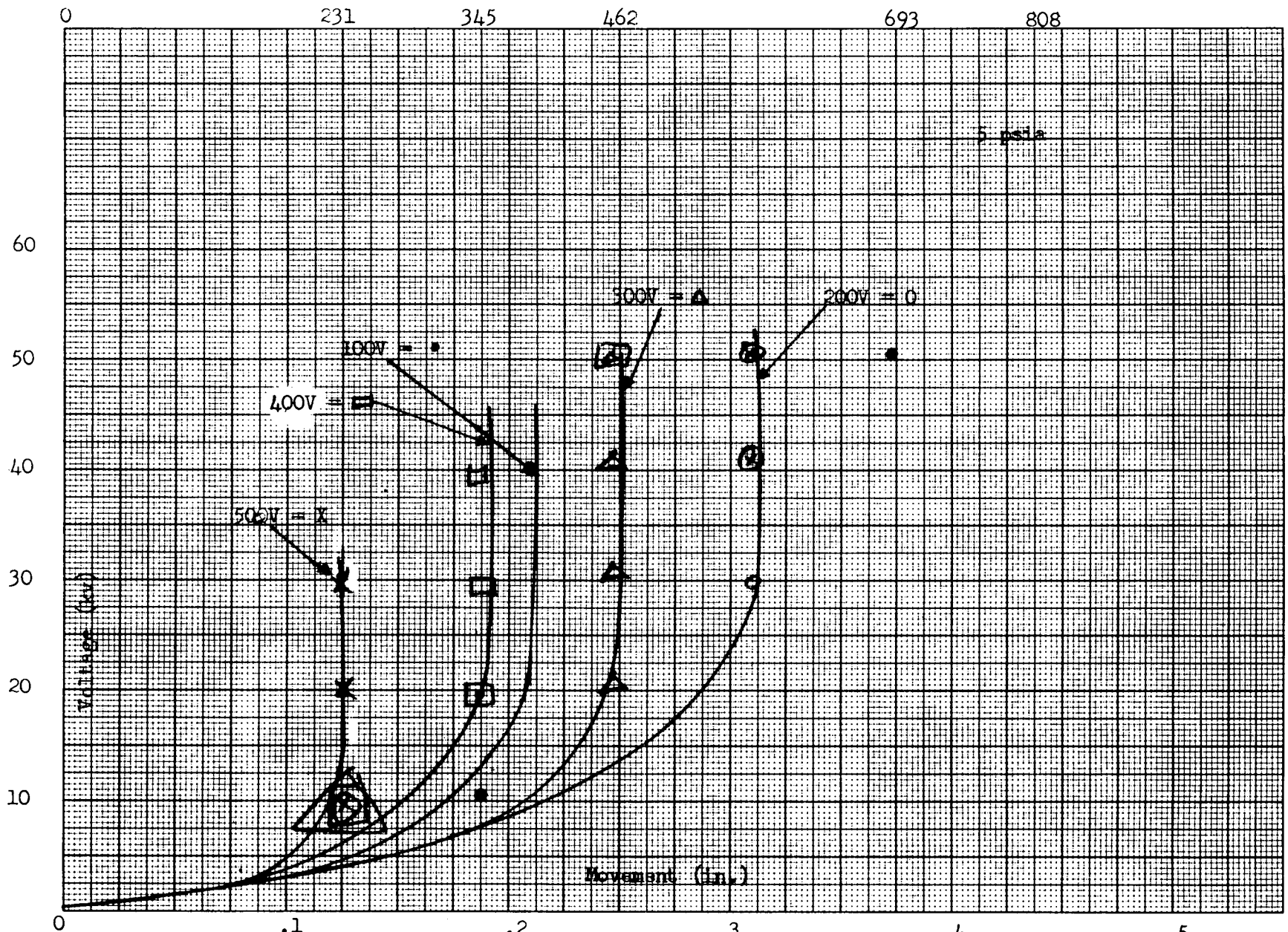
0
231
345
462
693
808
5 psia
60
50
40
30
20
10
300V = Δ
200V = O
100V = •
400V = □
500V = X
Voltage (kv)
Movement (in.)
0
.1
.2
.3
.4
.5

Figure 60

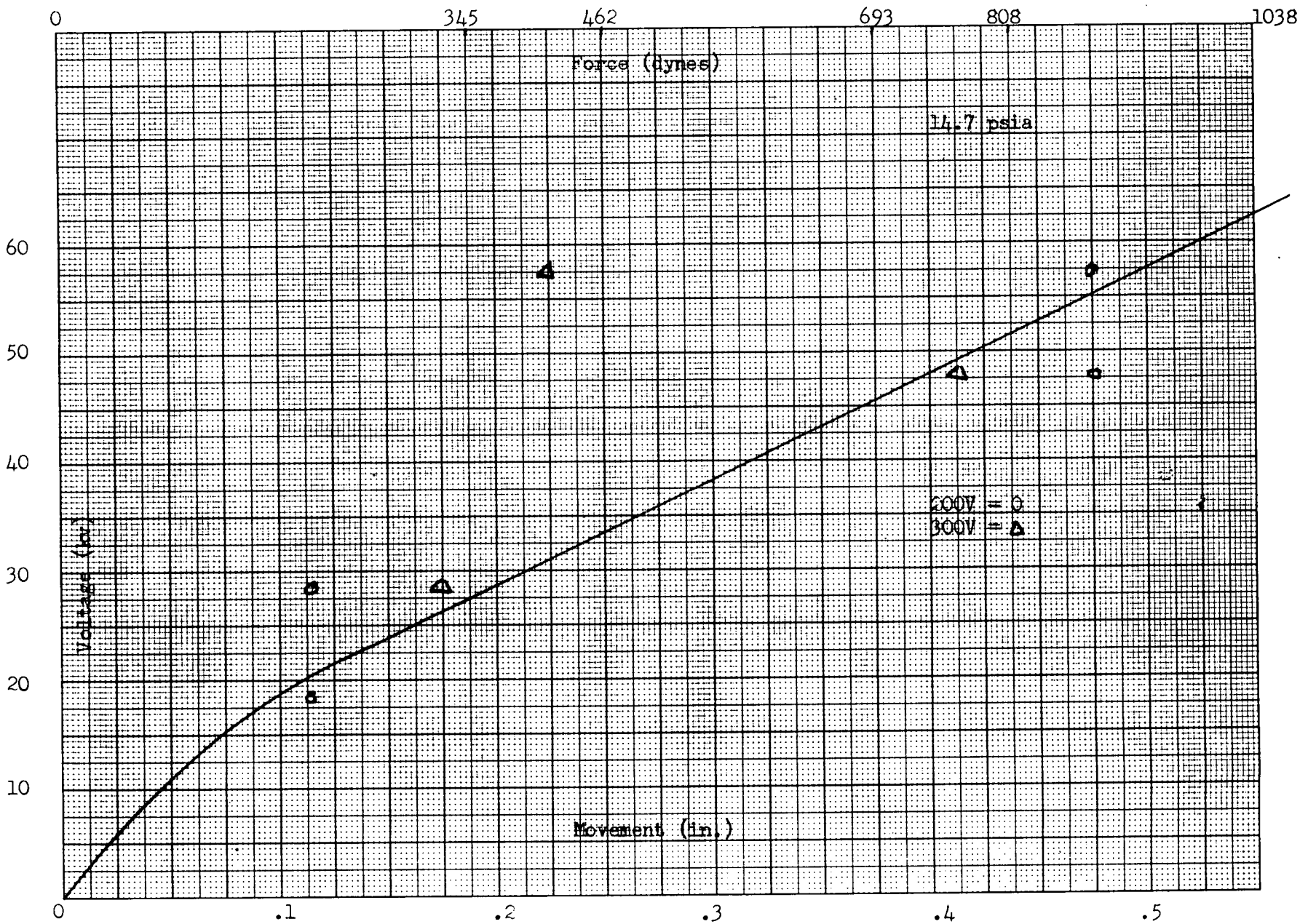
0
345
462
693
808
1038
Force (dynes)
14.7 psia
60
50
40
30
20
10
Voltage (kv)
200V = O
300V = Δ
Movement (in.)
0
.1
.2
.3
.4
.5

Figure 61

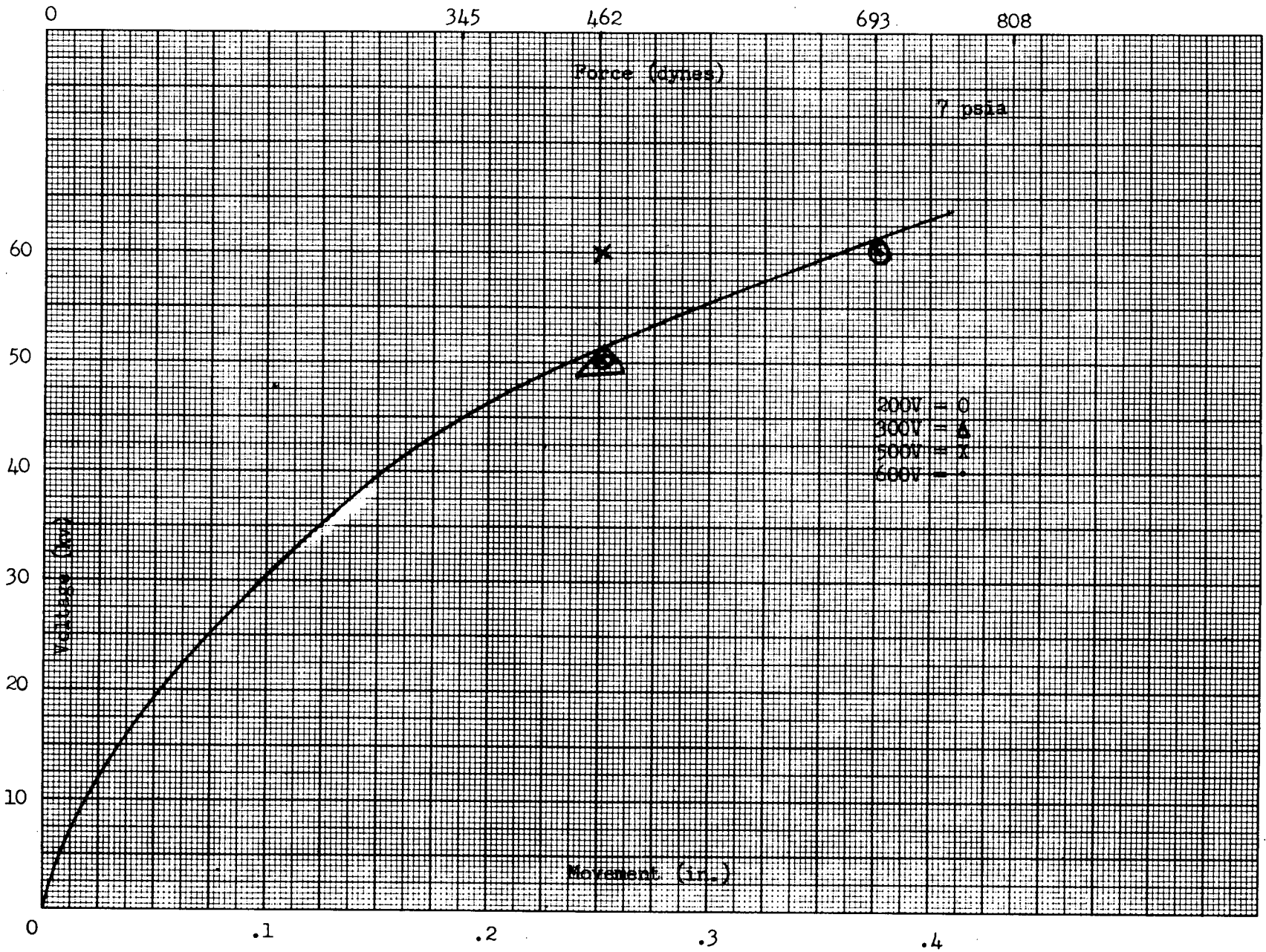
0
345
462
693
808
Force (dynes)
7 psia
60
50
40
30
20
10
Voltage (mv)
200V = O
300V = Δ
500V = X
600V = •
0
.1
.2
.3
.4
Movement (in.)

Figure 62

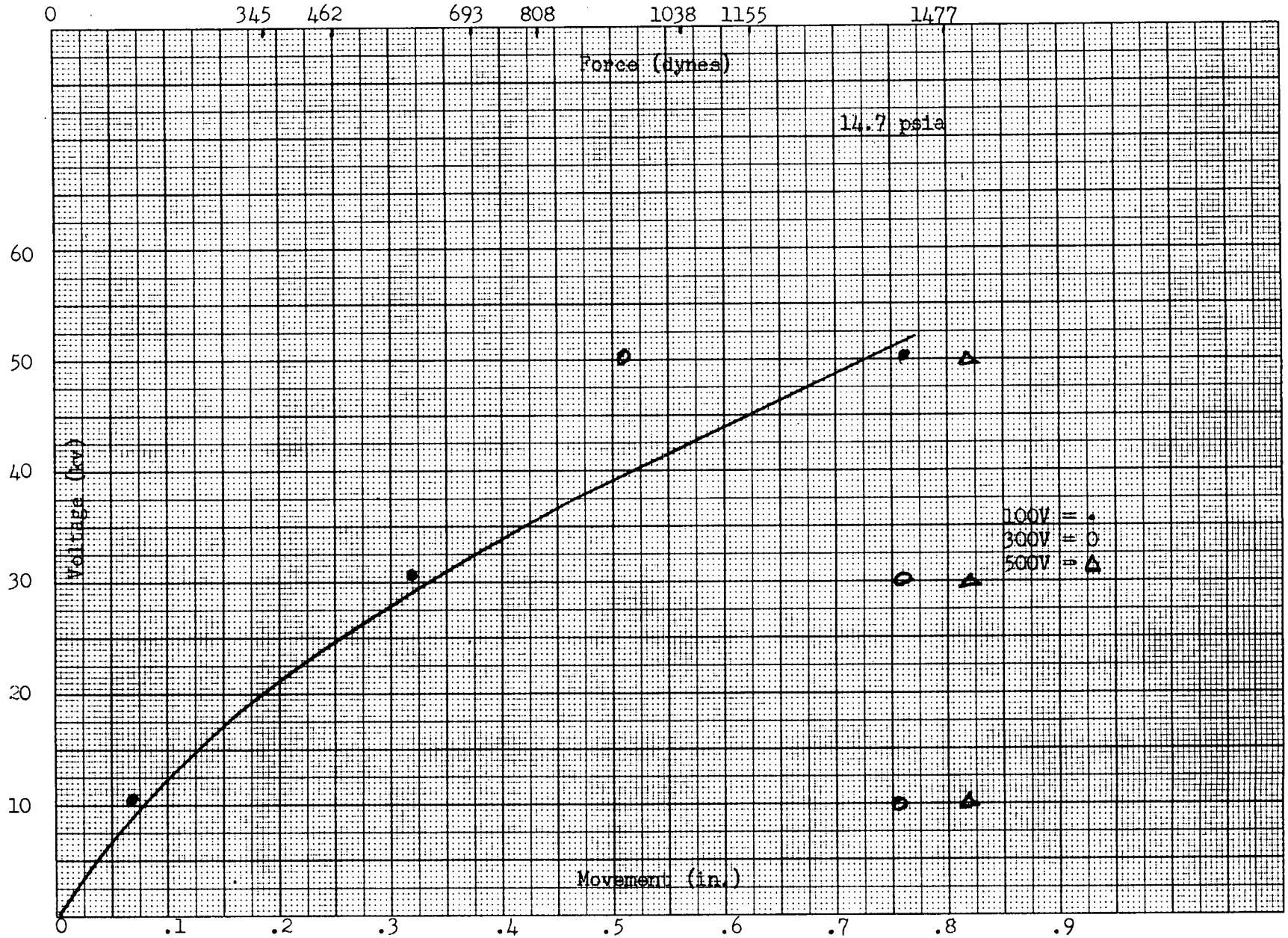
0
345
462
693
808
1038
1155
1477
Force (dynes)
14.7 psia
60
50
40
30
20
10
Voltage (kv)
100V = •
300V = O
500V = Δ
Movement (in.)
0
.1
.2
.3
.4
.5
.6
.7
.8
.9

Figure 63

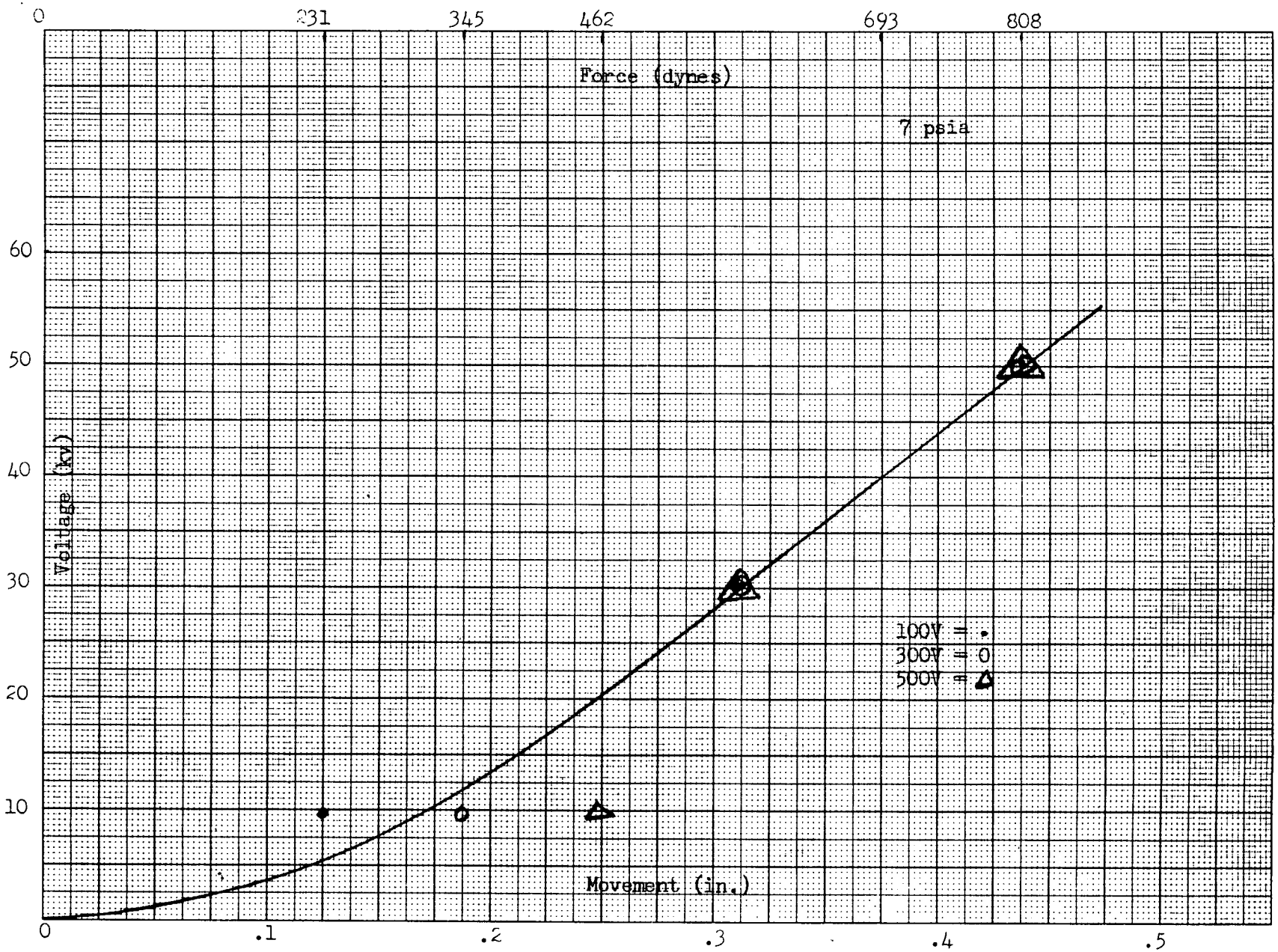
0
231
345
462
693
808
Force (dynes)
7 psia
60
50
40
30
20
10
Voltage (kv)
100V = •
300V = o
500V = △
Movement (in.)
0
.1
.2
.3
.4
.5

Figure 64

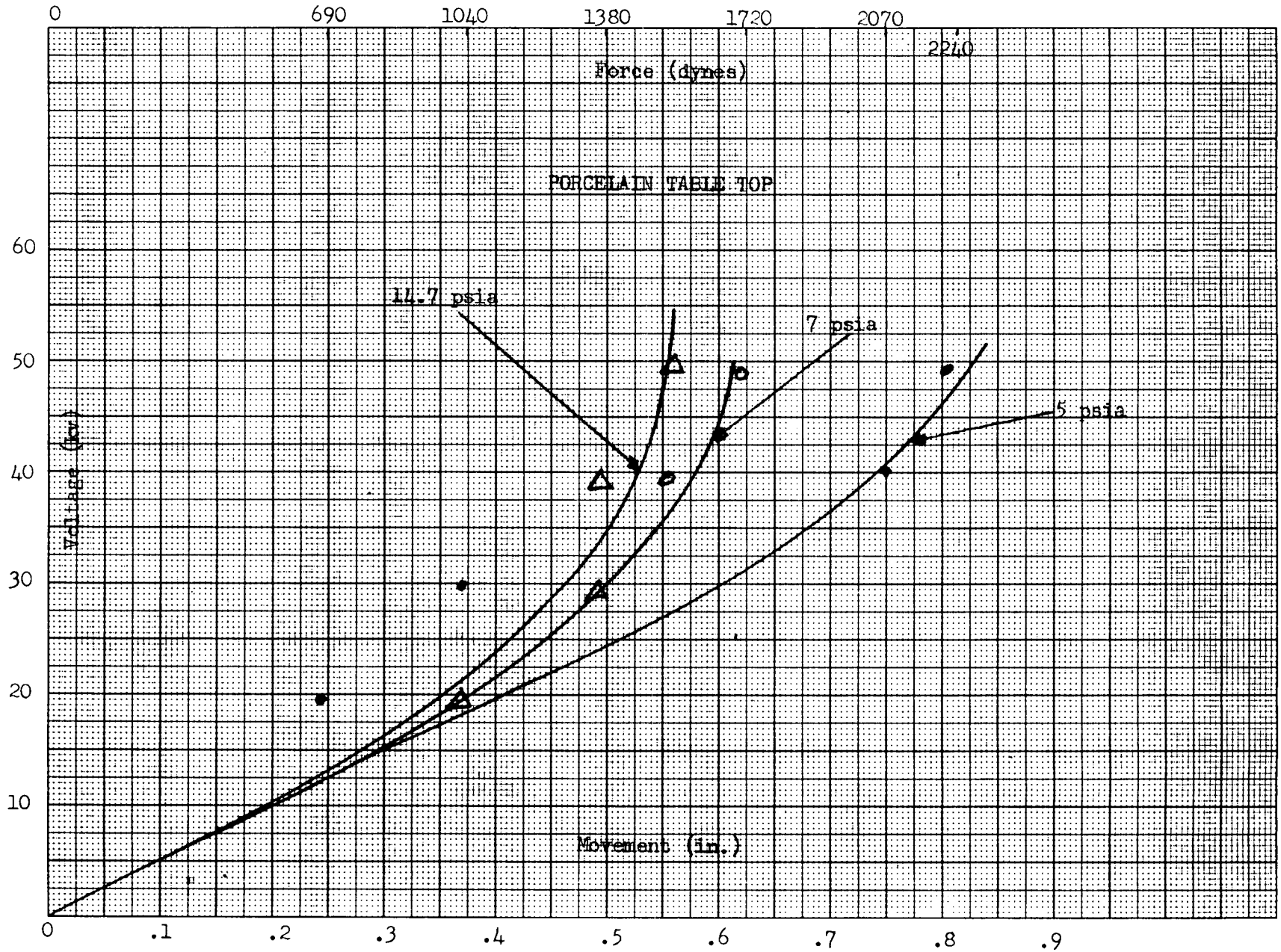
0
690
1040
1380
1720
2070
2240
Force (dynes)
PORCELAIN TABLE TOP
60
50
40
30
20
10
Voltage (kv)
14.7 psia
7 psia
5 psia
Movement (in.)
0
.1
.2
.3
.4
.5
.6
.7
.8
.9

Figure 65

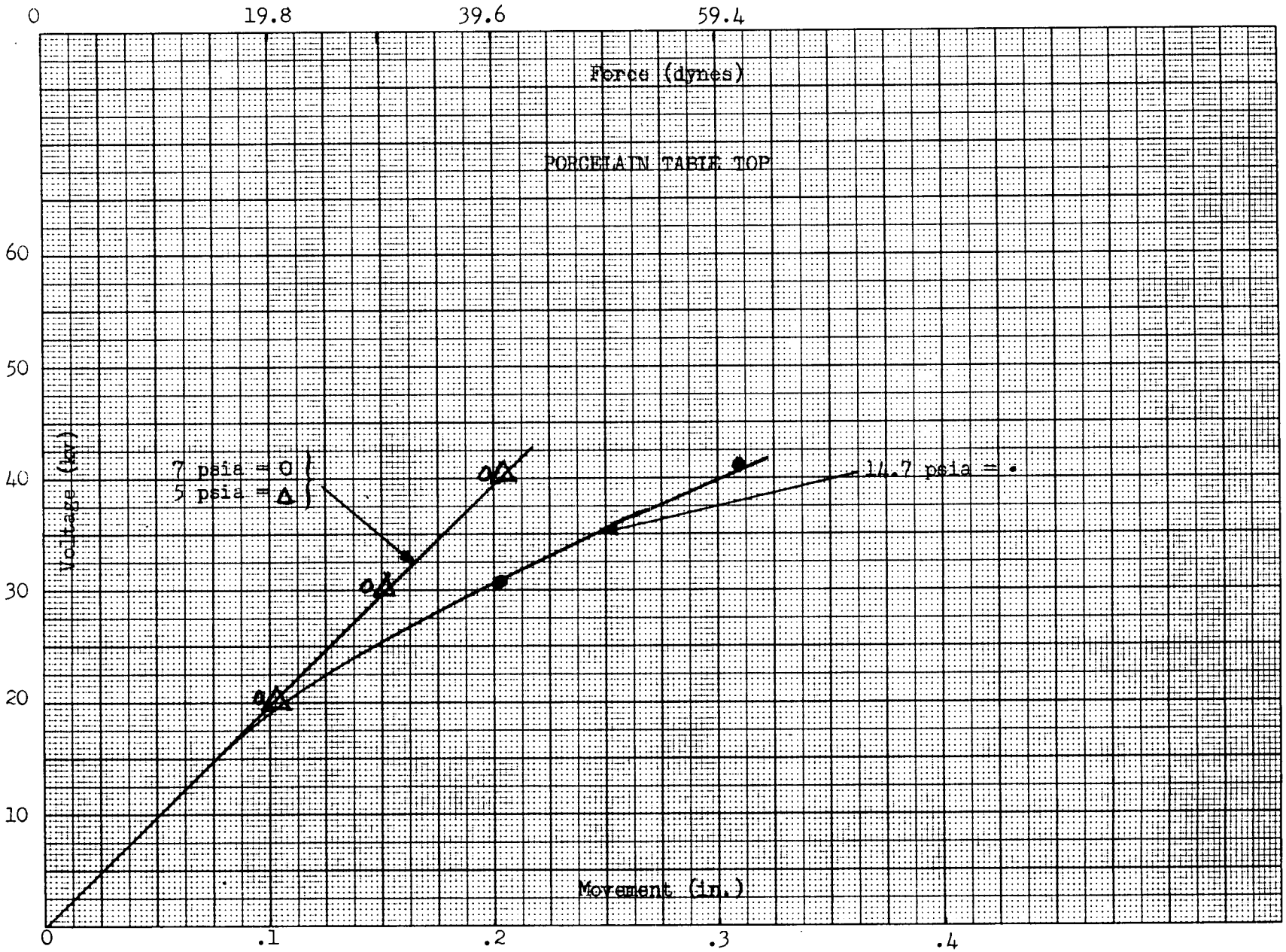
0
19.8
39.6
59.4
Force (dynes)
PORCELAIN TABLE TOP
60
50
40
30
20
10
Voltage (mv)
7 psia = O
5 psia = Δ
14.7 psia = •
0
.1
.2
.3
.4
Movement (in.)

Figure 66

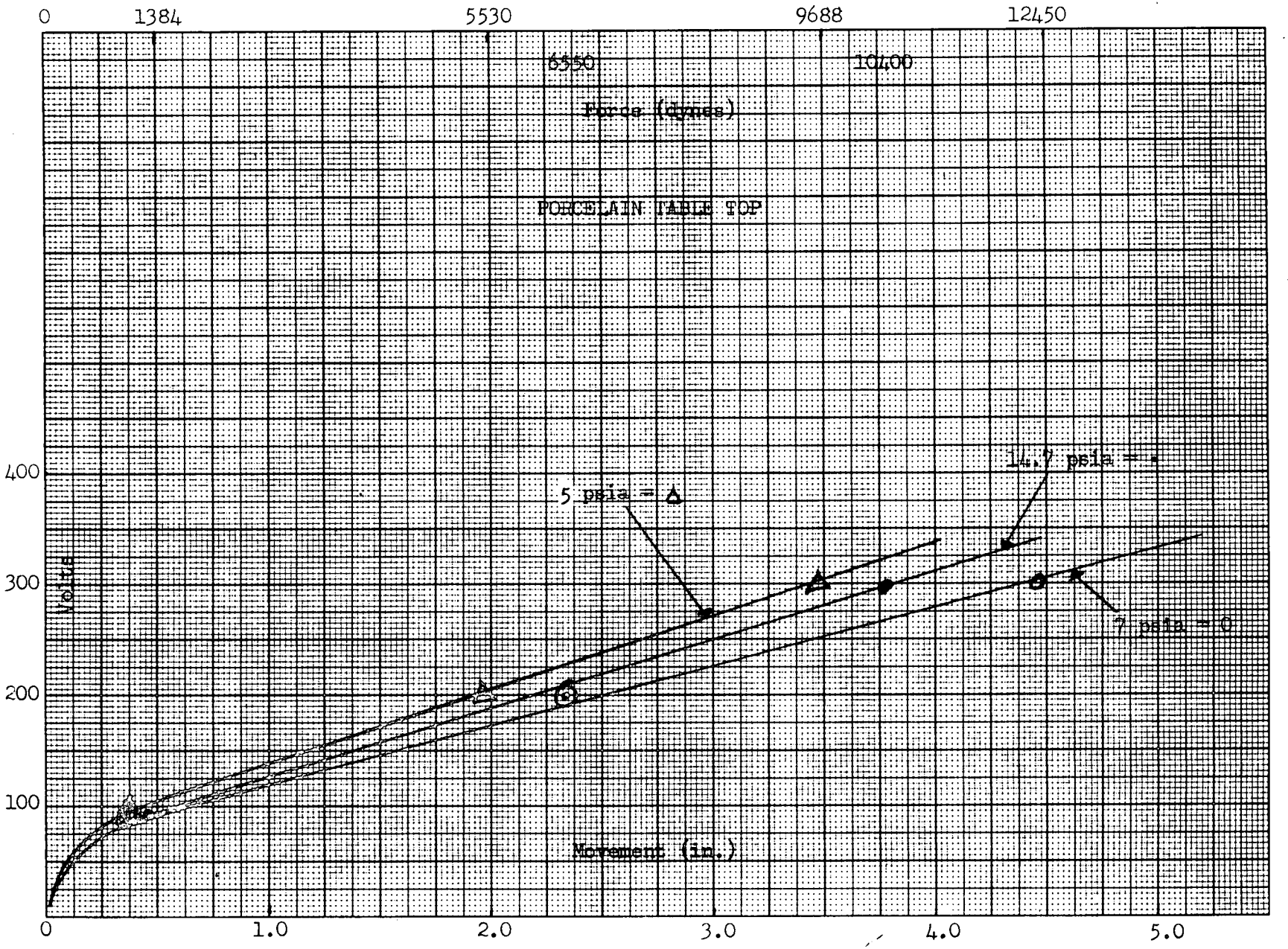
0
1384
5530
9688
12450
6550
10400
Force (dynes)
PORCELAIN TABLE TOP
400
300
200
100
Volts
5 psia = Δ
14.7 psia = •
7 psia = O
Movement (in.)
0
1.0
2.0
3.0
4.0
5.0

Figure 67

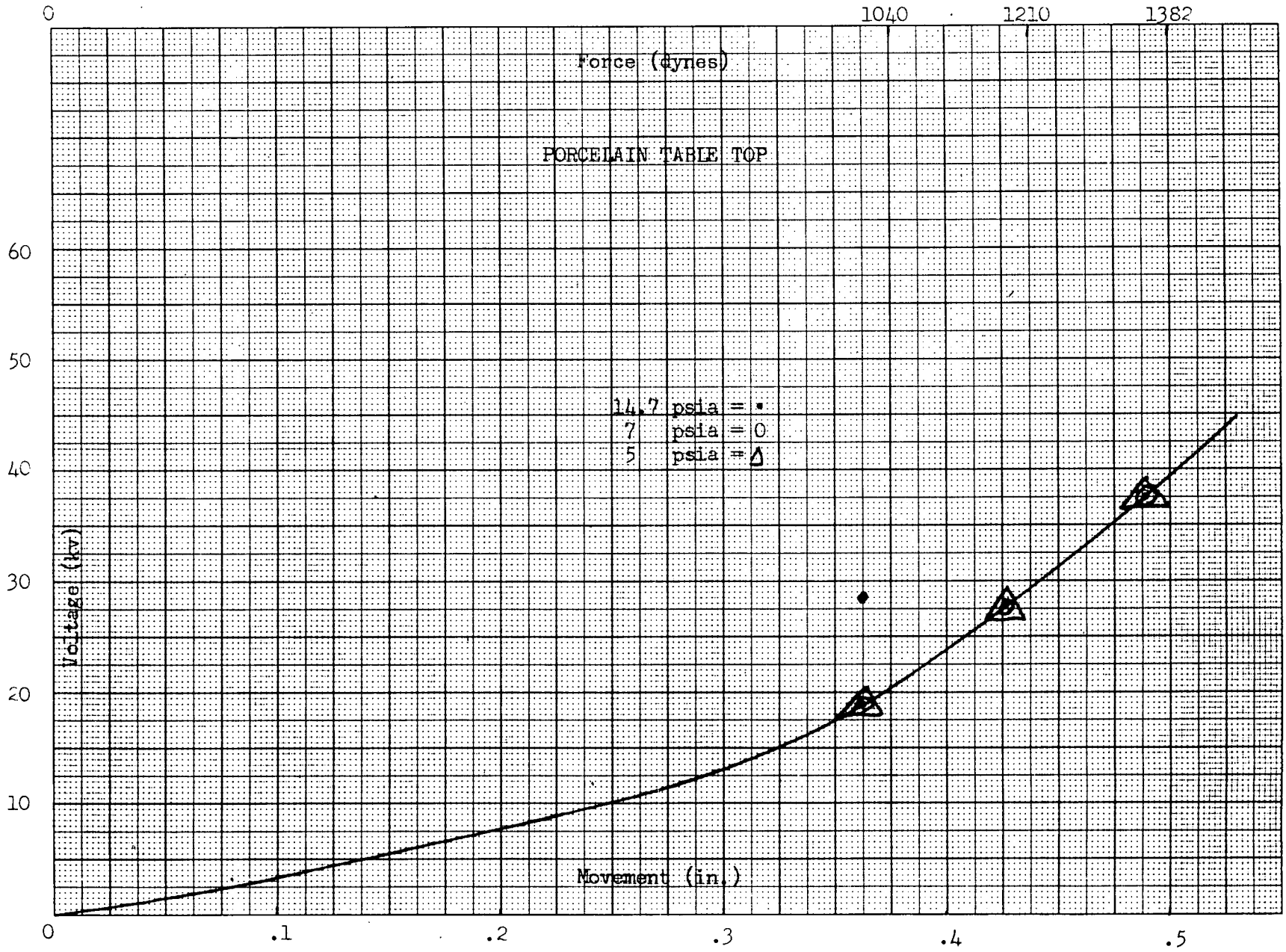
0
1040
1210
1382
Force (dynes)
PORCELAIN TABLE TOP
60
50
40
30
20
10
14.7 psia = •
7 psia = O
5 psia = Δ
Voltage (kv)
Movement (in.)
0
.1
.2
.3
.4
.5

Figure 68

ELECTRO-STATIC WORK TABLE Cont'd.

SHOCK TEST

By using different size metal objects and applying kilo volts of 5 to 60 TD the ion generator the following tests was conducted.

Metal Disc 1 1/8" in dia x 3/16" thick

KV	Shock	μAmps
5	no	.0
10	"	.0
15	"	.0
20	"	.0
25	"	.0
30	"	.0
35	"	.0
40	"	.0
45	"	.0
50	"	.00070
55	"	.00080
60	"	.00800

Toucking the metal object with one hand and grounding the other hand there were no shock at any of the above kilovolts.

(Signed) J. H. Hogan 1/7/69

Figure 69

INTER COMPANY CORRESPONDENCE

		FILE CODE	DATE 1/27/69
TO - NAME G. Hagen	DEPT. 2763	DIVISION Space	PLANT/OFFICE 7802/Michoud
FROM - NAME M. A. Berger	DEPT. 2742	DIVISION Space	PLANT/OFFICE 7802/Michoud

SUBJECT: DEVELOPMENTAL EMI TESTING RESULTS OF THE ELECTROSTATIC WORKBENCH (MF-24)

The prototype model of the Electrostatic Workbench was tested only to the radiated interference requirements of MIL-I-6181D in the screen room of the EMI/EMC laboratory on 1/20/69, 1/21/69 and 1/22/69.

Interference measurements were taken with Empire Devices Inc; Noise and Field Intensity Meters, NF-105, SN-2314 (Range - .15 - 1K MHz) and model NF-112, SN-373 (Range - 1. - 10K MHz).

The Ion Generator source voltage was adjusted for 30 KV, then 60 KV and tested under the following conditions:

1 - Line stabilization networks could not be used because of the high voltage (600 V AC/DC is considered maximum).

2 - The high voltage lead to the Ion Generator was isolated within physical limits from the ground plane and other test leads. (see photographs)

3 - Frequency spectrum was scanned from .15 - 10K MHz for C.W. and Broadband interference 15 minutes subsequent to the source voltage adjustment. The time lapse allowed for field and voltage stabilization.

Results: a) Ion Generator Source Voltage at 30KV

The radiated interference requirement of MIL-I-6181D was satisfied. No measureable interference from .15 - 10K MHz.

b) Ion Generator Source Voltage at 60KV

The radiated interference requirement of MIL-I-6181D were not satisfied. Extreme broadband interference was generated from .15 - 400 MHz. This static interference was probably due to the intense electrostatic field and high voltage leakage.

Photographs of the test arrangements were taken by Mason Rust and should be mailed approximately 1/29/69. The tests were conducted by the writer.

M. A. Berger
EMI/EMC Lab

Concurrence:
B. F. Heinrich - Manager
Instrumentation Section

MAB/db

cc: E. Lukawski
S. W. Paulson
File

84-110-7879 REV. 1-63

Figure 71